

UNIVERSIDAD DE OVIEDO

CENTRO INTERNACIONAL DE POSTGRADO

MÁSTER EN INGENIERÍA MECATRÓNICA

TRABAJO FIN DE MÁSTER

Construction and investigation of a roughness and shape measuring device with a rotating optoelectronic stray light sensor for use on ball studs

06/2021

Alumno	Tutor Universidad	Tutor Empresa
Ignacio Agustin Garcia Menendez	Miguel Angel Jose Prieto	Rainier Brodmann
[Firma]	[Firma]	[Firma]

INDEX

1.	ABSTRACT.....	5
2.	INTRODUCTION	6
	2.1.1. Introduction to ball studs	6
	2.1.2. Introduction to Optosurf GmbH	6
	2.1.3. Description of the project tasks	7
3.	SURFACE MEASUREMENT	8
3.1	Surface finish	8
3.2	Tactile measurement technology	10
3.3	Profile filter	11
3.4	Wavelengths.....	13
3.5	Profile parameters	15
3.6	Static identification functions	17
	3.6.1. The material proportion curve	17
3.7	Optical measurement technology.....	19
3.8	Scattered light method	21
3.9	Optosurf sensor	28
	3.9.1. Measuring the signal process	29
	3.9.2. Optosurf's Software	30
4.	FAMILIARIZATION WITH THE ALGORITHMS OF THE SPECIAL EVALUATION METHOD	32
4.1	Ball studs and evaluation project	32
	4.1.1. Ball joints and ball studs	32
	4.1.2. Ball stud process.....	34
	4.1.3. Stick and Slip method.....	36

4.2	Ball joints in the automotive industry	37
4.2.1.	Joint function: guiding the wheel	37
4.2.2.	Joint function: guiding the wheel as well as carrying the body	38
4.2.3.	Joint function: cross-axis joints	39
5.	CLIENT'S PROJECT	40
5.1	Evaluation of the Project.....	40
5.2	Degree of roughness of the ball stud.....	40
5.2.1.	Functional criterion: BqmF	40
5.2.2.	Wear criterion: BqV	41
5.3	Measurement of the ball studs with the sensor.....	42
5.4	Optical measurement of form deviation.....	43
5.4.1.	Optical measurement of eccentricity deviation	44
5.4.2.	Measuring ranges and drawing requirements for the ball stud.....	44
6.	CONSTRUCTION AND COMMISSIONING OF THE MEASURING DEVICE.....	46
6.1	OptoShaftTT	46
6.2	OptoShaft TT used for the project	47
6.3	Description of the rotary module for the sensor	49
6.4	Design to enable measurement of ball studs.....	50
6.5	Mounting the OptoShaft TT.....	54
6.5.1.	Optimization of the axes and assembly of the machine	54
6.5.2.	Mounting the measurement module with different angles	56
6.5.3.	Programming and tuning of the software of the different motors.....	56
7.	CREATION OF ALGORITHM MEASUREMENT AND VERIFICATION PROGRAMS WITH TEST PROFILES IN THE OPTOSHAFT TT	59
7.1	Setting up Optosurf's software	59

7.1.1.	Calibration of the sensor.....	60
7.1.2.	Activation of the motors and the reference position of the ball stud machine	60
7.2	Creation of measurement programs	61
7.3	Analysis of the first measurement and sensor function test.....	67
8.	VERIFICATION OF THE RESULTS IN PERFECT SPHERES AND IN OTHER COMPONENTS USED WITHIN THE AUTOMOTIVE INDUSTRY (BALL STUD) IN THE BALL STUD MACHINE	70
8.1	First tests on the ball stud machine with edge detection.....	71
8.2	Measurements with different angles of rotation	74
8.2.1.	BqV Analysis	75
8.2.2.	BqmF Analysis	75
8.3	Measurements carried out with programming	77
8.3.1.	Code description.....	77
8.4	Sensor consistency and error test measurements	79
8.5	Profile tests.....	81
9.	TECHNIQUES FOR CHECKING AND CONSISTENCY OF RESULTS	84
9.1	Messverfahren 2 method.....	84
9.2	Gage R&R method.....	84
10.	SUMMARY OF RESULTS OBTAINED AND CUSTOMER COMMENTS FOR FUTURE OBJECTIVES.....	86
11.	REFERENCES	87

1. ABSTRACT

The objective of the project is the determination of the measurement capacity and the analysis of a ball stud machine. This ball stud machine measures the roughness and profile of the ball studs. The technology used in ball stud measurement is the scattered light method. The scattered light method is a technique used to measure surfaces passively (reflection of emitted light). The project starts from the improvement of a real measuring machine from a well-known auto parts company.

The project carried out consists of the analysis and verification of the measurement values of this technology. It also includes the mechanical and electronic installation of the machine, as well as the programming and adjustment of the motors. These evaluations follow the standards of the German automotive industry to determine the consistency of measurements. As Optosurf does not have a ball stud machine model in its facilities, the first functional tests of the software and the new design are carried out on another machine called the OptoShaft TT. This machine has a multipurpose function within the company and achieves values very close to those of the real machine. This project also includes a construction design in Solidworks that allows the measurement of ball studs on standard Optosurf multipurpose machines.

Once the correct performance of the measurements on the OptoShaft TT had been verified, the new module was installed and assembled on the ball stud machine. During this development time the ball stud machine was on the customer's premises. The different measurements carried out on the machine included a technical analysis to determine which measurements to carry out and an optimization of the measurement of the results by programming. In addition, the consistency of measurement of the machine and the ease of use of the interface by the user have been improved.

The measurement values are evaluated by the customer, who determines whether the shape or roughness of the ball studs is adequate or not. Based on the values obtained, the client decides the type of measurement. The more accurate the result, the longer it takes to make the measurement.

The result includes a report from the client himself that specifies the great measurement consistency of the machine, the precision and the desire to purchase more models for measuring in other company facilities.

2. INTRODUCTION

2.1.1. Introduction to ball studs

Ball studs carry out an essential role in the assembly of automobiles. Ball studs are placed on the shafts and allow the rotation between parts at different angles of rotation. Being an important part for the control of the vehicle, their tolerance for correct operation is fundamental. A quick analysis of the shape and surface allows manufacturers to analyse as many ball studs as possible and determine the quality of the product. The measurement of the ball studs is carried out through an optical measurement based on the scattered light method. This technology is equipped in a specific machine for this use called the "kugelzapfen machine" (ball stud machine). This machine allows a greater automation of the measurement process and optimization of the quality determination process. The importance of this machine in terms of measurement stability and controllability is paramount. Not only the design of the machine with high-quality components is necessary, but the assembly and adjustment must be perfectly precise to carry out the measurements. In this project it will be proven that the machine measures correctly and is more efficient than other measurement methods used up to now.

2.1.2. Introduction to Optosurf GmbH

Optosurf GmbH is an innovative, international company in the field of optical production metrology, which was founded in 2004 by Dr. –Rer.nat. Rainer Brodmann. The company developed a unique optoelectronic technology for the surface measurement of components from various areas such as the automotive industry, mechanical engineering, or medical technology. The basis of the innovative measurement technology is the scattered light method. It is particularly characterized by its robustness, accuracy, and high measuring speed. The aim is to use Optosurf technology to optimize cost-intensive manufacturing processes, reduce tool costs, manufacture 100% tested parts, and examine the functional behaviour of surfaces. The company introduced scattered light measuring systems (Figure 1) for various applications in the market, including the first automatic measuring machine with scattered light for ball studs in 2017. In 2020, the customer of the ball stud machine requested an improvement from the Optosurf company to obtain new measurements related to the quality of the ball stud surface.

Figure 1. Optosurf's machine¹



2.1.3. Description of the project tasks



1. Deepening into the concepts of scattered light measurement technology (including the programming of the Melfa robot, Mitsubishi, for the measurement of different surfaces)
2. Familiarization with the algorithms of the ZF special evaluation method.
3. Creating a construction in Solidworks: to be able to measure the ball studs.
4. Mounting and commissioning of the measuring device.
5. Creation of measurement programs and algorithm verification with test profiles.
6. Verification of the results in perfect spheres and in other components used within the automotive industry (ball stud)
7. Test of the capacity of the measuring equipment following the standards of “Verfahren 1 (messtechnik)”.
8. Installation and tuning of the machine for presentation to customers.



3. SURFACE MEASUREMENT

3.1 Surface finish

The surface finish of every industrial part depends mainly on its manufacturing process. All surfaces have geometric as well as manufacturing marks defects and therefore cannot be considered completely smooth. The surfaces of these industrial parts often need to fulfil certain functions in technical applications. Depending on the function of the surface, certain parameters and tolerances must remain under certain limits. These parameters can include the media where they are going to work e.g., air, oil or other even other surfaces for which limits are more strongly required. Properties of the surface must be precisely defined so that the intended function is optimally fulfilled. Roughness and waviness are generally responsible for the surface functional behaviour and they can generate unwanted noises and directly minimize the operating life service. Figure 2 shows the different defects that can be found in machinery parts depending on its size.

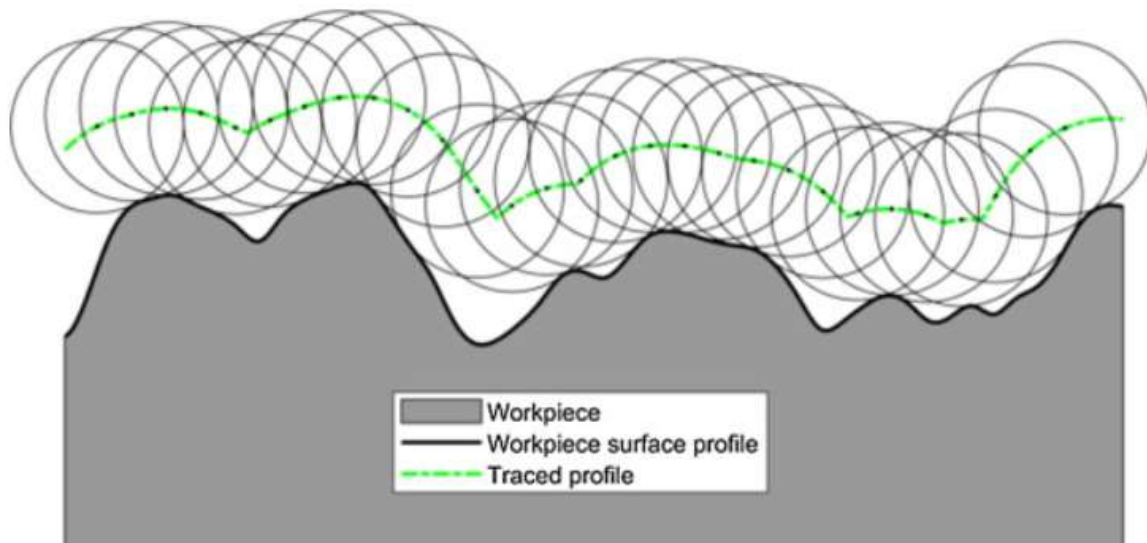
Figure 2. Types of shape deviation²

Shape deviation	Examples of the type of deviation	Examples for the cause
1 order: shape deviation 	Straightness, evenness, roundness, deviation	Defects in the machine tool guides, bending of the machine or workpiece, incorrect clamping of the workpiece, hardening distortion, wear
2 order: waviness 	waves	Eccentric clamping, form or running deviations of a milling cutter, vibrations of the machine tool or the tool

<p>3 order: roughness</p> 	<p>grooves</p>	<p>Shape of the tool cutting edge, feed or infeed of the tool</p>
<p>4 order: roughness</p> 	<p>Hovel Crests Marks</p>	<p>Process of chip formation (chipboard, shear chip, built-up edge), material deformation during blasting, bud formation during galvanic treatment</p>
<p>5 order: roughness</p> <p>Note: no longer easy to represent graphically</p>	<p>Microstructure</p>	<p>Crystallization processes</p> <p>Changes to the surface due to chemical effects, corrosion processes</p>
<p>6 order:</p> <p>Note: no longer easy to represent graphically</p>	<p>Lattice structure of the material</p>	

To determine surface deviations, two types of measurement methods are applied: tactile and optic. The main difference between each other is the contact with the surface. On the one hand tactile devices take their measurements directly on the surface. On the other hand, optical devices require a precise distance to the surface. The sensor must be also precisely maintained and remain stable throughout the measuring process. Measuring on the surface with a tactile device can lead into a loss of information about the surface. As tactile devices measures with a rounded tip, roughness smaller than the radius of the tip cannot be detected (figure 3). Measuring with optic devices allows an overlapping of the spots so it can create a continuous line that does not interfere with the surface and therefore can show a better representation of the surface. Tactile measuring systems are usually cheaper than optic sensors. As such, they are often the best choice for standard measuring tasks. But specific problems require special solutions. The speed of optical systems, the ability to retrofit them to existing machinery and the high level of integration and automation allow them to often make up for the higher initial costs.

Figure 3. Tactile measurement representation³

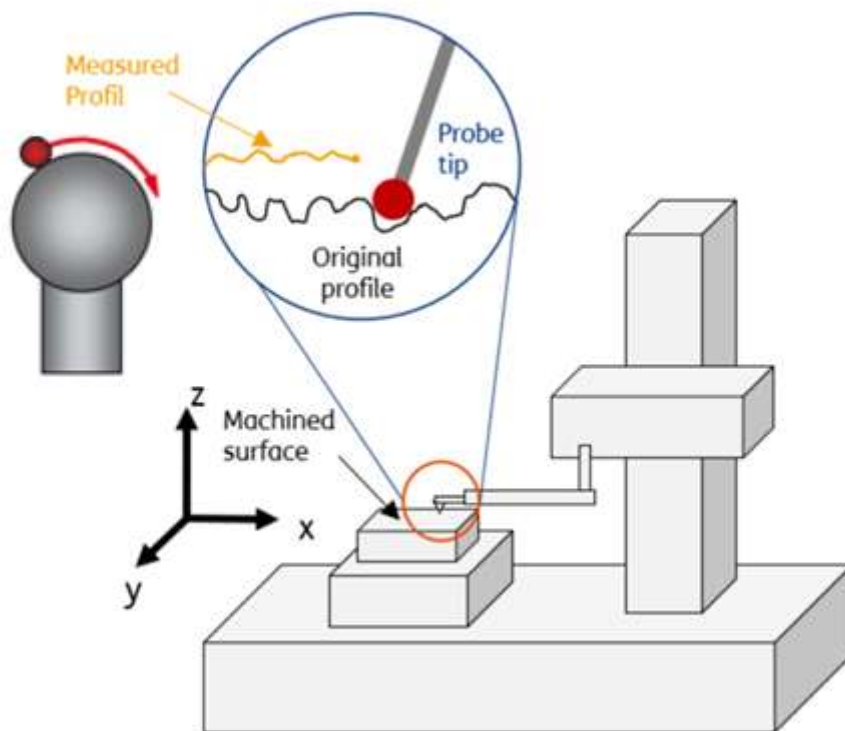


Regarding regulations applicable to both measure methodes, the tactile measurement technology, is standardized with DIN EN ISO standards. The optical measurement technology is not subject to any standard, although there are guidelines that are used as specifications. In the specific case of the optical scattered light sensor, the VDA guideline is used. (German Association of the Automotive Industry). The VDA is a German interest group of the German automobile industry, both automobile manufactures and automobile component suppliers. The specific parameters for the calculation of the sensor measures are shown in the “VDA 2009: Winkelaufgelöste Streulichtmesstechnik. Definition, Kenngrößen und Anwendung”

3.2 Tactile measurement technology

Tactile measurement technology is the standard measuring method for dimensional surface measurements of different parts of materials using a Stylus instrument. The method consists in driving a mechanical stylus device on the surface section that is going to be measured. The probe tip moves along the measuring path point by point, where contact-active sensors with a defined measuring pressure detect the movement and generate the measuring profile from it.

Figure 4. Tactile measurement machine⁴

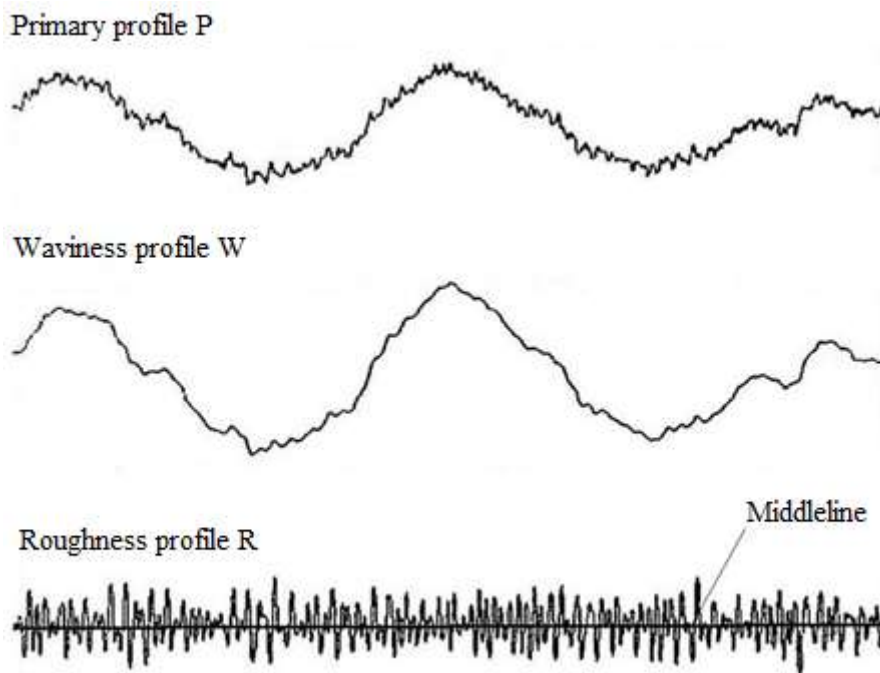


Because the stylus tip is in contact with the surface, the shape of the tip has a great influence on the measurement result. In the DIN EN ISO 3271 nominal properties of stylus devices, the point angle (cone shape) and the point radius r_{tip} are specified. The possible cone angles are 60° and 90° , however, the stylus tip can have other shapes such as cylindrical or round.

3.3 Profile filter

The recorded profile is divided into waves of different wavelengths. The wavelength decreases with the order of the deviations in shape. The limit at which the waviness changes into roughness is determined by the cut-off wavelength. Wavelengths and profiles are separated using a Gaussian filter. With the Gaussian filter, the distortion of the profile is reduced in the vertical direction due to the sudden change in the profile height. The phase shift in the horizontal direction is eliminated. This filter separates the primary profile(P-profile) into the roughness profile(R-profile) and the waviness profile(W-profile). This filter is standardized in DIN EN ISO 11562: Metrological properties of phase-correct filters.

Figure 5. Wavelength division of the profile⁵



Depending on the transmission behaviour, a distinction is made between long wave pass filter, short wave pass filter and band pass filters. The long-wave pass filter (low-pass filter) attenuates the amplitudes of the short-wave components of the surface according to the characteristic curve and the limit wave number. The short-wave pass filter (high-pass filter) transmits the short-wave components and attenuates the long-wave components. The profile filter with the cut-off wavelength λ_c is used as a short-wave pass filter for the roughness profile and as a long wave pass filter for determining the waviness. The filter profile is used to calculate the surface parameters and thus has a very large influence on the measurement result.

Figure 6. Long wave filter⁶

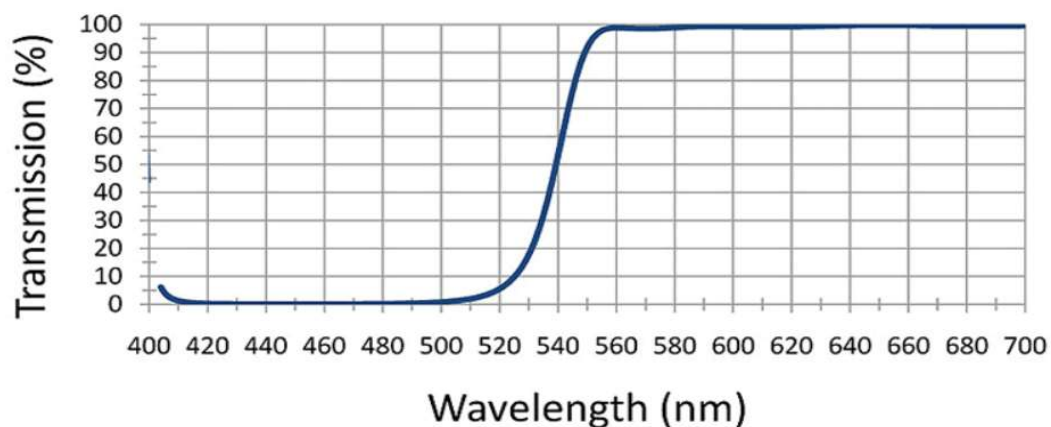
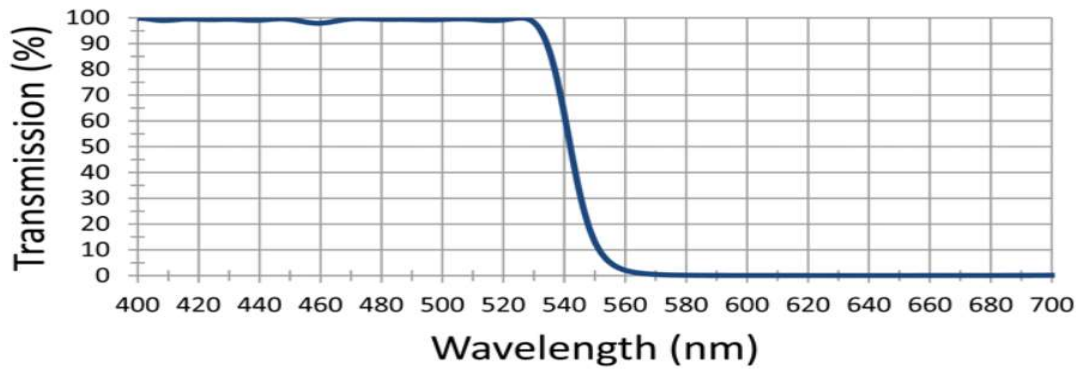


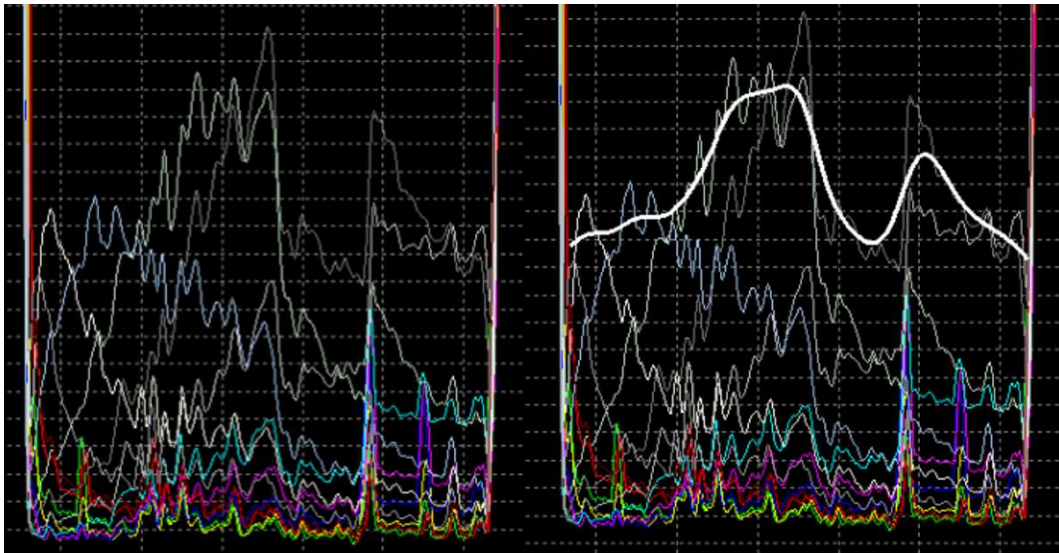
Figure 7. Short wave filter⁷



3.4 Wavelengths

The P-profile is divided into two limit wavelengths, λ_c for the R-profile and λ_s for the W-profile. The cut-off wavelength λ_c is the wavelength of the sinusoidal profile, 50% of the length which is transmitted through the profile filter. It defines the boundary between roughness and waviness.

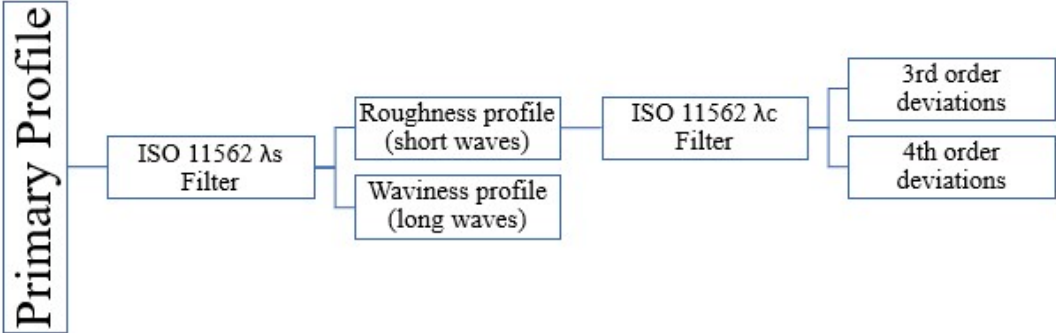
Figure 8. Comparison between non applying a filter and a λ_s filter



The cut-off wavelength λ_s defines the transition of the roughness to even shorter wavelengths. This separation into long-wave and short-wave components is made by calculating the centre line. The centre line is the long-wave profile component, which is determined for each point of the profile by a weighted average derived from neighbouring points. To make sure that the points at the beginning and at the end of the measuring section are correctly weighted, the

analysed section must be longer than the total measuring section for the filter to swing in and out. The leading and trailing sections each of half the limit wavelength λ_c are common.

Figure 9. Profile division⁸



The centre line is determined by the weight function, see Figure 10, which indicates the weight with which the neighbouring profile points are included in the calculation for each point of the centre line to be calculated. The transfer characteristic for the centre line is the Fourier transform of the weight function.

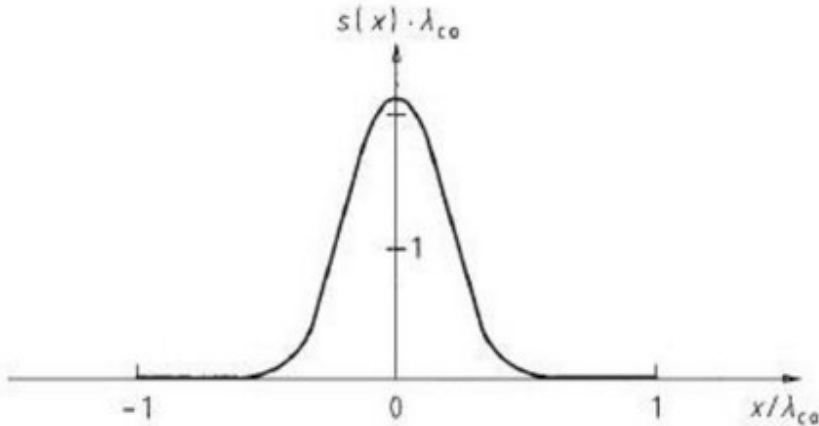
Figure 10. Wavelength calculation⁹

$$s(x) = \frac{1}{\alpha \cdot \lambda_{co}} \cdot e^{-\pi \left(\frac{x}{\alpha \cdot \lambda_{co}}\right)^2}$$

x the distance to the center of the weight function

λ_{co} The cutoff wavelength of the profile filter

$$\alpha = \sqrt{\frac{\ln 2}{\pi}}$$

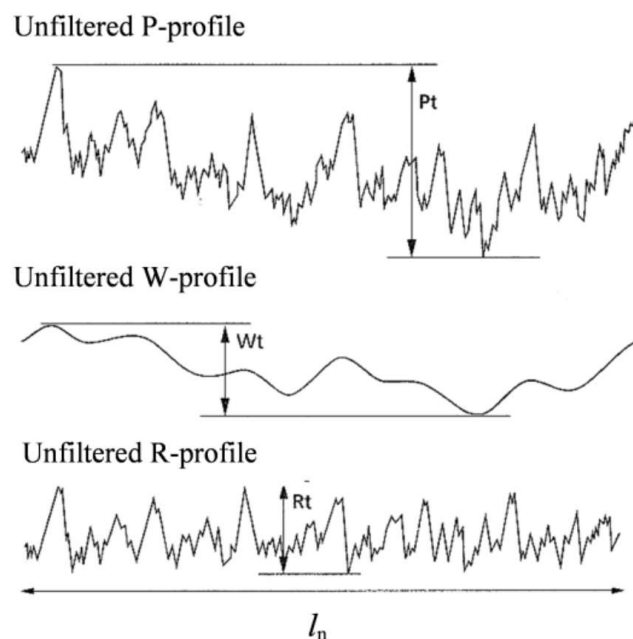


The standardized preferred values for the cut-off wavelengths λ_c of the profile filter are in the standard DIN EN ISO 3274: Nominal properties of stylus devices as follows: 0.08 mm; 0.25 mm; 0.8 mm; 2.5mm; 8.0 mm, unless otherwise stated.

3.5 Profile parameters

There are several parameters that can be used to define the profile of a surface. Therefore, surfaces are measured focusing only on the most relevant ones for its application. Parameters of the surfaces are differentiated according to the primary profile (P parameter), roughness profile (R parameter) and waviness profile (W parameter). Surface parameters are defined in accordance with DIN EN ISO 4287: designations, definitions, and parameters of the surface quality.

Figure 11. Types of profile¹⁰



There are 2 linearly independent properties that can be applied to obtain the profile parameters.

- Height properties

It is used to evaluate the roughness profile. There are several different values that can be used. The value R_z is a peak oriented parameter that calculates the average surface roughness. In the industry, the values R_a and R_q (which represent the arithmetic and the quadratic middle roughness respectively) are the ones most used to calculate the height, which is closely related to the dimensional tolerance. Moreover, there are other values collected in the ISO

(International Organization for Standardization) such as R_{max} (maximal middle roughness) and R (middle roughness height of motif) used in the German and French industry, respectively.

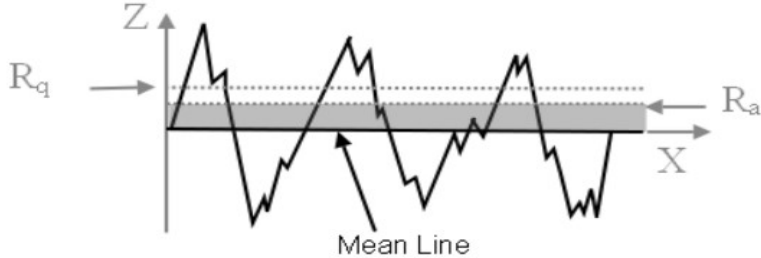
Equation 1

$$R_a = \frac{y_1 + y_2 + y_3 \dots + y_n}{n}$$

Equation 2

$$R_q = \sqrt{\frac{y_1^2 + y_2^2 + y_3^2 \dots + y_n^2}{n}}$$

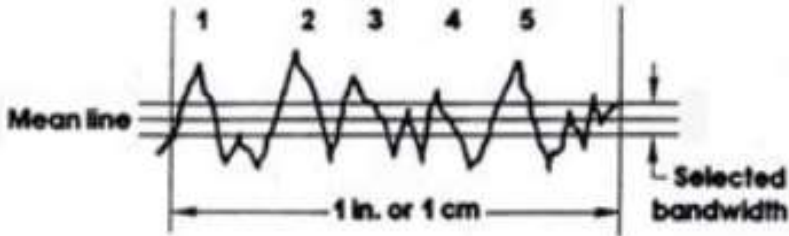
Figure 12. R_a and R_q evaluation¹¹



- Horizontal properties.

Horizontal properties are particularly valuable as additional information when the functional properties are also shaped by the structural properties of the roughness. When applying a coating to a surface, controlling the high-spot count in the process helps to ensure good finish aesthetics. Peak count (R_{Pc}) is defined as the number of roughness profile peaks per a unit length that rise above some predetermined line.

Figure 13. R_{Pc} evaluation¹²



Generally, just height properties are applied, however, surfaces whose quality characteristics require to be very precise, are measured both horizontally and vertically. When measuring a section, the following facts need to be considered:

The size of the peak oriented values increases monotonously with the length of the measuring distance; therefore, the measuring distance cannot be freely selected.

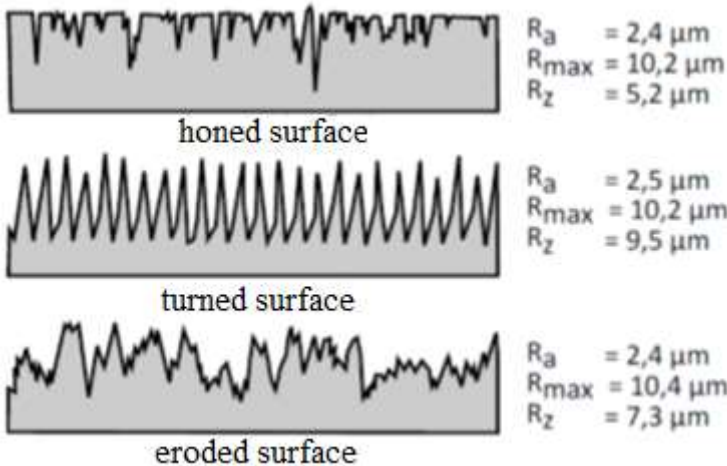
Mean values, on the other hand, converge towards the true value when increasing the measured distance and are statically more reliable through “Ensemble-averaging”.

3.6 Static identification functions

3.6.1. The material proportion curve

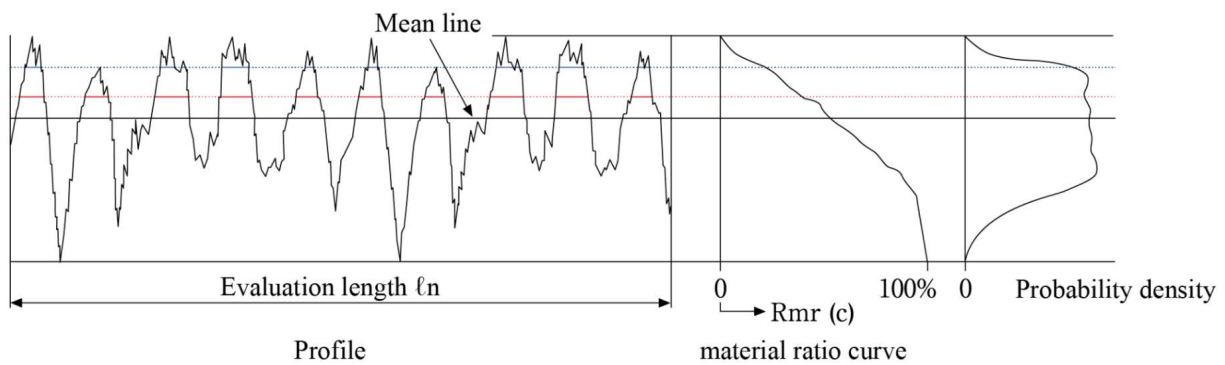
When measuring the peaks and the valleys parameters, there can be profiles that have similar values, however in the graphical representation look completely different.

Figure 14. Different roughness surfaces¹³



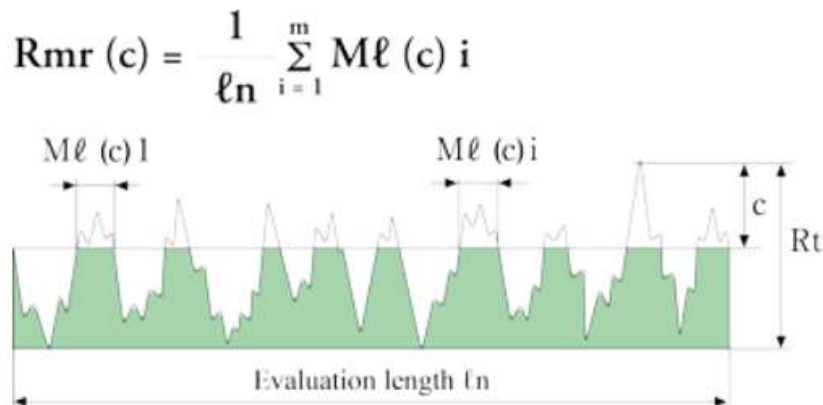
The Abbott–Firestone curves are currently used to characterize these surfaces. The Abbot curves give access to both size and proportion of the peaks and valleys of a given surface. It represents the increase in the material proportion of a surface with increasing depth of roughness. Probability density curves represent the probability of occurrence for height Z_x . The parameter is equivalent to the height distribution histogram.

Figure 15. Abbott–Firestone curve¹⁴



For calculating the material ratio, the profile is cut at a corresponding height and the material-cutting distances l_i are added up and set in relation to the total measurement distance ℓ_n . The material proportion curve is built with the $Rmr(c)$ parameter. This parameter indicates the ratio of the material length $Ml(c)$ of the profile element to the evaluation length for the section height level c .

Figure 16. The material ratio curve¹⁵



The most common use of engineering surfaces is to provide a bearing surface for another component to move relatively to it. The bearing ratio (t_p) provides the ratio of the profile bearing length to the evaluation length at a specified level. Contact between surfaces results in a friction and abrasion of the implicated parts and an overcontact between surfaces will cause a faster wear of the surfaces. The material proportion curve is carried out to determine whether the average friction and abrasion from the piece does not collapse the mechanism.

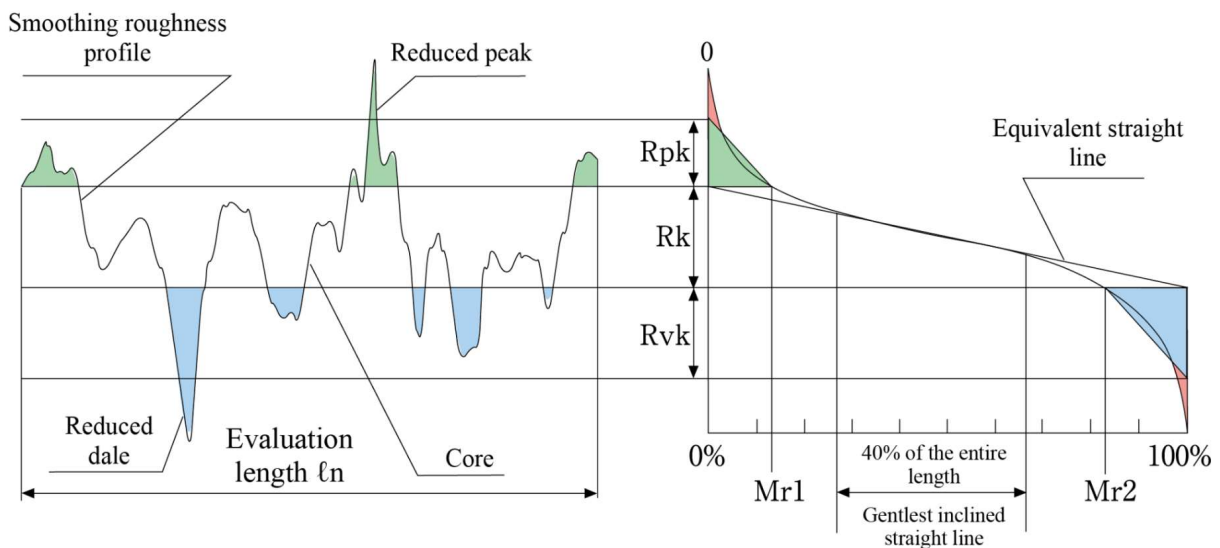
The characteristic values obtained are the following in the standard DIN EN ISO 13565: Surfaces with plateau-like, functionally relevant properties:

- Core roughness depth R_k : Depth of the roughness core profile.

- Material content $Mr1$: Material content, in percent, determined by the cutting line that separates the protruding peaks from the roughness core profile.
- Reduced peak height Rpk : Average height of the protruding peaks above the roughness profile.
- Reduced groove depth Rvk : Average depth of the profile valleys below the roughness profile.

Rk , $Mr1$, and $Mr2$ values are calculated from the linear curve (equivalent linear curve) minimizing the sectional inclination corresponding to 40% of the material ratio curve (The secant for $\Delta Mr = 40\%$ with the smallest increase forms the “central area” of the material proportion curve for calculating the regression line). A triangle with the area equivalent to the protrusion of the material ratio curve segmented by the breadth of the parameter Rk is drawn and parameters Rpk and Rvk are calculated.

Figure 17. Rpk and Rvk values¹⁶



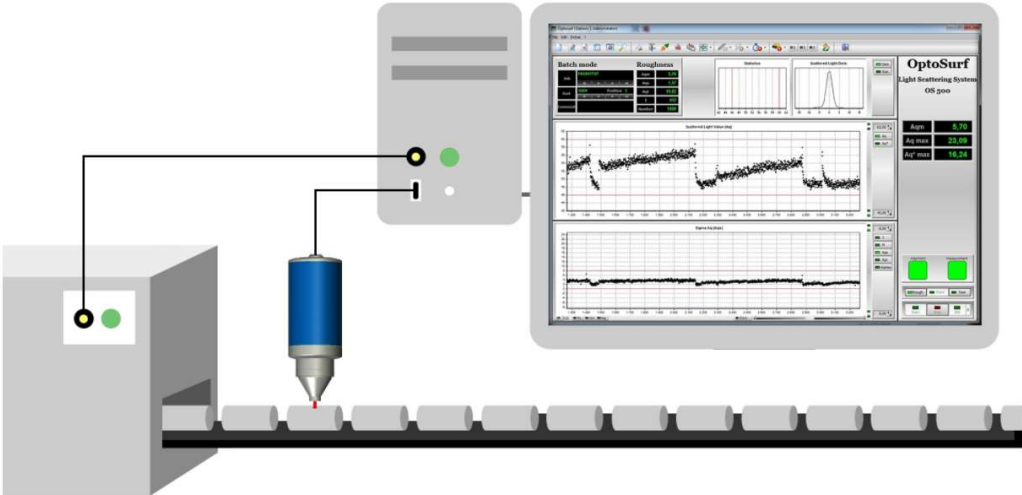
3.7 Optical measurement technology

Optical measurement refers to a noncontact measurement which uses various light sources. It usually requires at least one lens, a light source and a detector. It differs from other forms of inspection such as a tactile measurement method, in using either a point of reference (e.g. a crosshair) or a computer to calculate edge detection. Two of its greatest advantages are its capability to measure features too small or fragile to be measured by touch, and the fact that it is faster in comparison to other forms of measurement.

The medical, plastics, aerospace and automotive industries are where optical measurement has, and will continue to have, significant impact. Adopters of modern optical measurement devices are looking for easy-to-use technology that supports the acquisition of more accurate data in less time. As a result, there's a rising demand for in-line measurement and faster processing of acquired images. When deciding which optical measurement devices suits better the product, factors like the amount of pieces that need to be measured, precision, place of measurement and initial investment must be considered.

With optical devices, variable badge measurements can usually be evaluated, and devices can often be placed on the production line. Measurements that result from optical measurement systems are also usually presented in a clearer and easier way to understand with respect to tactile measurements, which rarely have a graphical representation. Such measurement techniques enable inline an immediate recording of process fluctuations and quality errors as well as a direct feedback of the measurement results into the process, as shown in figure 18. These results have a great potential for improving product quality and manufacturing efficiency. As an integral part of production, inline measurement technology becomes a value-adding factor in efficient and competitive production. This non-contact measuring method is also used on surfaces that are soft and or could be damaged by the probe tip.

Figure 18. Optosurf sensor device inline application¹⁷

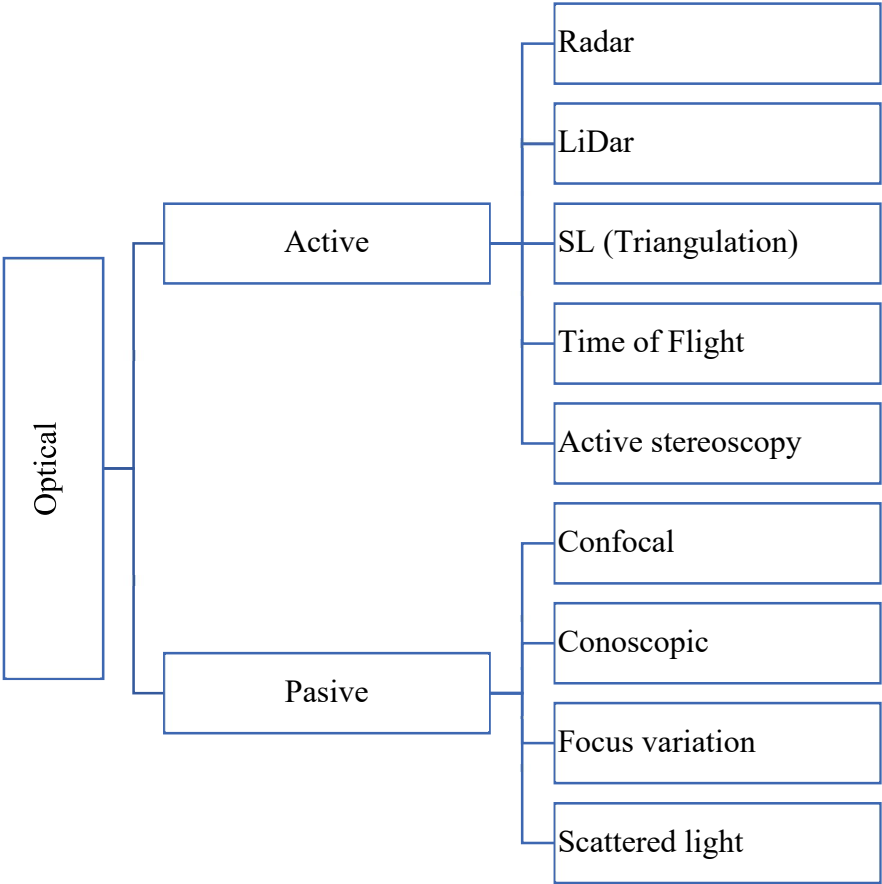


Optical metrology has a very high future and growth potential. Companies that use these technologies and thus invest in their own innovative projects will continue to be among the pioneers in their specific industry in the future. Optical measure can be divided into active or passive. Active sensors emit energy in order to scan objects and areas whereupon a sensor then detects and measures the radiation that is reflected or backscattered from the target. Passive

sensors gather radiation that is emitted or reflected by the object or surrounding areas. Reflected sunlight is the most common source of radiation measured by passive sensors.

There are a wide variety of measuring methods for optical roughness and shape measurement of surfaces (figure 19). In this master thesis the scattered light method is the optical measurement technology that will be used. In addition, other non-contact passive measurement techniques, such as optical confocal microscopes, white light interferometers, focus variation or conoscopic sensors are also used in surface measurements.

Figure 19. Types of optical technology



3.8 Scattered light method

The measure of a surface to obtain the roughness and waviness created in the machining process provides an information about the quality of the piece. Due to the automatization and the use of the CNC-Machines on the industry, faster, more precise and more controlled machining is carried out. However, the acute wear of the milling heads can cause a quality decrease in the machining finished.

With the scattered light measurement technology, the transverse and longitudinal roughness as well as the shape and waviness of reflective, finely machined surfaces can be checked quickly and close to production. Typical contact measure machines problems such as vibration effects can be neglected, and it can also be placed in the production process area due to its resistance to adverse working conditions. It can measure rapidly too (2000 times per second) which make it possible to measure many surfaces with a reliable measure.

Figure 20. Inline measure of the sensor¹⁸



The scattered light method is based on the angular deflection of rays that hit the measured surface almost perpendicularly. Figure 21 shows the scattered light on the rough surface, where the ray collides with the surface and reflexes. According to reflexion, in a completely smooth surface, the ray angle which collides with the surfaces must be the same as the one reflected. The reflection depends on the slope of the surface and the width of the ray. This ray is projected through a lens onto a photosensitive detector with a discrete number of photodiodes which collects the signal from the reflected angle. The received signal defines the intensity of the light absorbed which contains all the micro geometry information of measured surface.

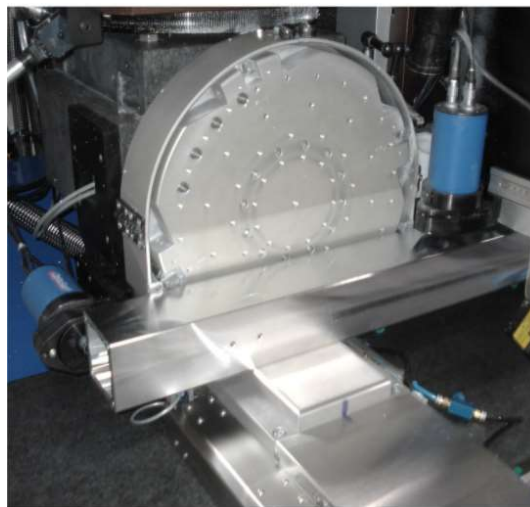
Figure 21. Surface reflection of the scattered light¹⁹



The measuring spot of the light beam has a certain diameter (from 0.03 to 7 mm) depending on the application and the surface of the product. For very fine structures a small diameter of e.g.,

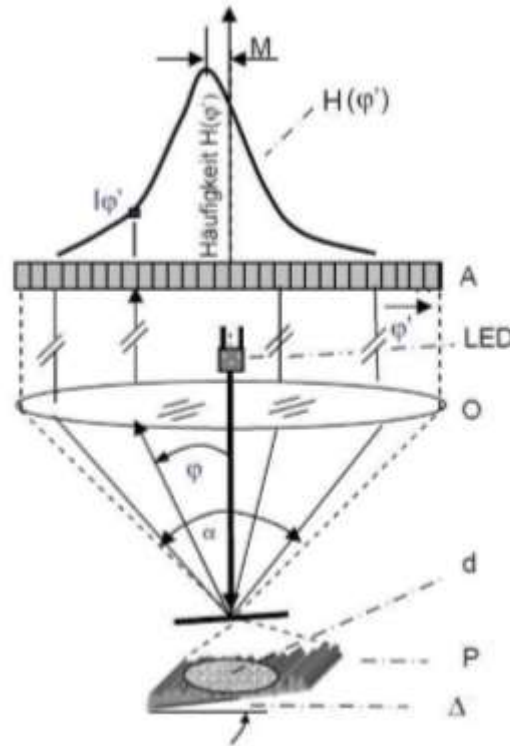
$d = 0.03$ mm is used and for rougher surfaces a diameter of 0.3, 0.9 or 7 mm is used. From this, the parameters of the measured surface are calculated, which are specified in VDA 2009: Angle-resolved scattered light measurement technology. The VDA is the largest automobile association in Germany and regulates certain guidelines regarding procedures carried out in the automobile industry. These guidelines are not ISO standards but are very important throughout German industry. Definition, parameters, and application are defined for the first time in this guideline. The VDA 2009 describes the basics, various statistical parameters and applications of scattered light measurement technology and gives recommendations for design drawings.

Figure 22. Measure for diamond miller cutters²⁰



The principle of scattered light measurement is shown in Figure 23. The surface P to be measured is illuminated vertically with the LED measuring spot of diameter d , the backscattered light within the maximum measurable scattering angle range α is captured by a measuring objective O and projected onto the linear detector. The number of photodiodes of the detector A are arranged in such a way that each diode supplies a corresponding intensity value $I(\varphi')$ of each discrete scattering angle value φ . This gives the linear scattering angle distribution $H(\varphi')$, which contains the information about the microstructure and the shape (angle Δ) of the evaluated surface.

Figure 23. Scattered light measurement principle²¹



The parameters of the scattered light method, which form the distribution curve, are determined from the scattering angle distribution. The most important parameters are A_q , M and I . The total intensity of the backscattered light is I . The value is formed from the sum of the intensity values I of all photo elements.

Equation 2

$$I = \Sigma I(\varphi')$$

M is the mean position of the scattering angle distribution. This is used when recording the macro-geometry and waviness of surfaces, since M can be calculated directly with the tilt angle of the macro-profile Δ via a simple relationship ($M = 2 \cdot \Delta$).

Equation 3

$$H(\varphi') = \frac{I(\varphi')}{\Sigma I(\varphi')}$$

Equation 4

$$M = \Sigma \varphi \times H(\varphi')$$

A_q is the variance of the scattered light distribution and the measure for the microstructure of the surface. It describes the standard deviation of the scattered light angle. This value is closely

related to the profile parameter Rdq, which is the measure of the statistical distribution of the surface profile angles. A correction factor (k) is used to calculate the Aq value, which considers, among other things, the distances between the photo elements. For given manufacturing processes, Aq correlates with the tactile roughness value Ra and the roughness depth Rz, as well as with the profile shape.

Equation 5

$$Aq = k \times \Sigma(\varphi' - M)^2 \times H(\varphi')$$

Aqm shows the mean value Aq of one measurement or multiple measurements.

Equation 6

$$Aqm = \frac{1}{n \times \Sigma Aq(i)}$$

Aqt is the measure of the greatest structural differences on the measured surface.

Equation 7

$$Aqt = Aq(\max) - Aq(\min)$$

The Aq can only be used for flat surfaces. In this case, as the measured surface is a sphere, the angle of the reflected light beam does not correspond to the real measurement angle Aq. This angle also includes the angle of the spherical surface itself. To eliminate this angle, the angle of the surface is calculated as a function of the diameter of the measurement point and the diameter of the sphere.

Equation 8

$$Bq = Aq - F \times \frac{D_{spot}}{D_{ball\ stud}}$$

From the Bq values, other parameters are analysed, such as BqmF for the mean values and BqV for the maximum values.

Equation 9

$$BqmF = \frac{\Sigma Bq(i)}{n}$$

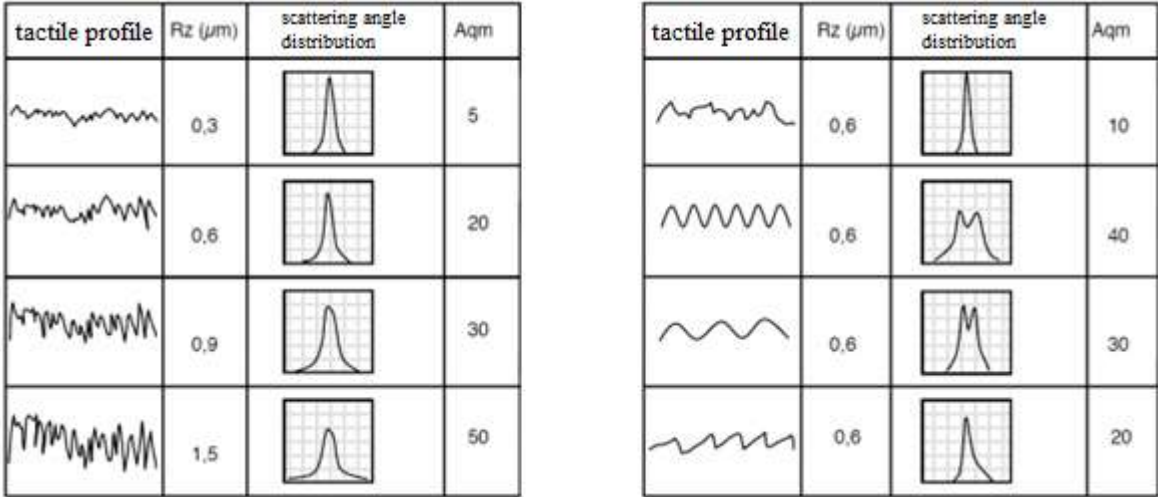
Equation 10

$$BqV = \max(Bq)$$

In many cases, scattered light parameters can provide additional information that tactile parameters do not provide. Figure 23 shows various surface profiles with the associated

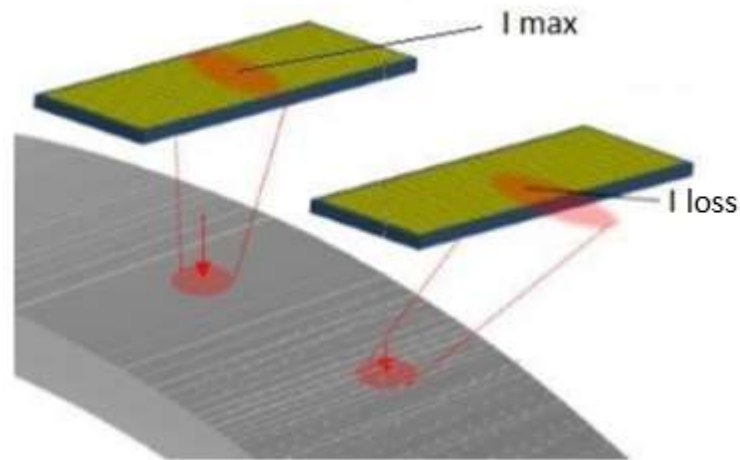
parameters R_z from the stylus method and A_{qm} from the scattered light method. A correlation of R_z with A_{qm} for the similar profiles can be seen in the table on the left. With the profiles in the table on the right the scattering angle distribution and A_{qm} value change with constant R_z.

Figure 24. Tactile vs scattered light measurement²²



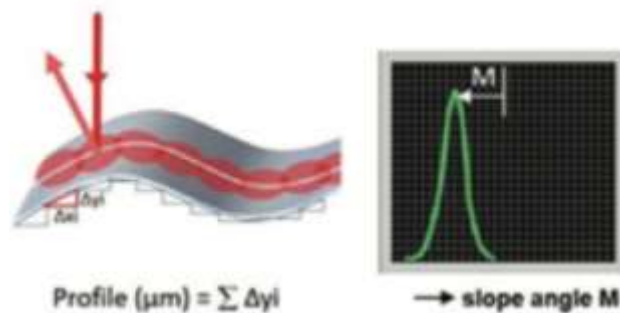
Due to the high accuracy of the scattered light measurement technology, the A_q value records differences in scattering angle, for example on polished surfaces. Since the A_q and M values are insensitive to small changes in distance and vibrations, scattered light is considered very robust. The macro profile calculation is also very precise and can be compared with high-precision tactile measuring devices. In this way, defects up to an amplitude of 0.01 μm can be reliably detected. The limit of the method arises with rough surfaces from Ra > 10 μm when the profile angles are too large and can therefore no longer be detected by the sensor. On the other hand, the sensitivity of the parameters brings with it certain restrictions in the manageability of the measuring head and requires the sensor to be set up correctly. Precise sensor adjustment is therefore essential for a suitable and reliable measurement. With an optimal alignment of the measuring head in the normal direction of the surface, the total intensity is maximum, and the position of the scattering angle distribution is in the middle area. Tilting the diode array in the longitudinal axis causes a decrease in the overall intensity. Tilting transversely to the longitudinal axis of the diode array results in an offset in the scattering angle distribution. Regarding the scatter value A_q, a change generally applies as a function of the tilt angles.

Figure 25. Intensity of the sensor²³



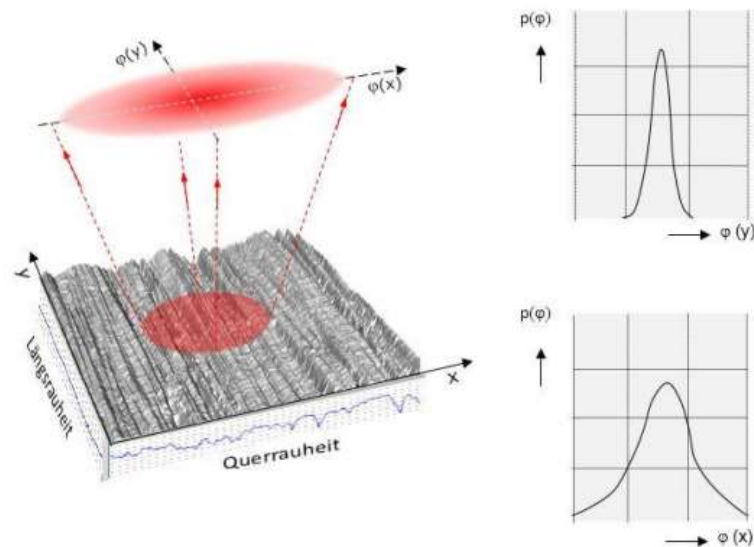
Due to the high accuracy of the sensor, it must be set up in such a way that the I value is maximum, and the M value is minimum in order to obtain all possible information about the surface. The tilt sensitivity of the scattered light distribution is shown in Figure 26, as well as the correct adjustment of the I value in Figure 25 and the M value in Figure 26.

Figure 26. M value of the sensor²⁴



The orientation of the scattered light sensor plays an important role in surface measurement. After the orientation, the sensor can detect the intensity distribution across or along the processing direction (figure 27). In the case of an anisotropic surface, this has a great influence on the distribution curve since the scattered light distribution is changed due to the tilt angle. One advantage of the optical measuring device is that by turning the sensor by 90 ° with the measuring head stationary, transverse and longitudinal roughness can be measured separately. In this way, additional information about the machining direction is obtained.

Figure 27. A_q value of the sensor²⁵



3.9 Optosurf sensor

The OS 500 (figure 28) is the sensor provided by Optosurf used to perform all the measurements. The sensor works on the measuring principle of the angle-resolved scattered light method in which the surface slope angle is measured. This makes it possible to record both the microstructure (roughness) and the macro shape (roundness, waviness). The sensor can be started and stopped via a trigger input. It can also be integrated into a machine control system via a Profibus. After setting up a batch, with the specified type of measurement (series measurement roughness, roundness, straightness), tolerances and parameters can be selected in the software menu and compared with the actual tolerances in the display. In contrast to traditional surface metrology methods, which determine roughness and shape by measuring distance, the angle measurement method has great advantages for physical reasons. Since the sensor is insensitive to small changes in distance and works without contact, the main area of application of the sensor is in harsh environments with existing vibrations. Also, the orientation of the detector allows transverse and longitudinal roughness measurements when the sensor is rotated.

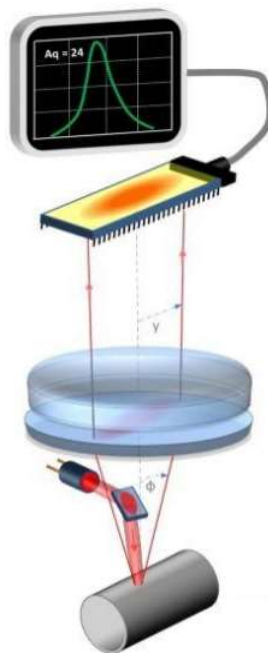
Figure 28. OS 500 sensor²⁶



3.9.1. Measuring the signal process

The sensor is formed by a hardware and a software (figure 29). On the one hand, the hardware includes the optics and electronics that make it possible to convert the light obtained from the light source into the values of A_q , I and M (roughness, intensity, shape) and record them. On the other hand, the software includes the programming to establish a connection with the receiving site. It also reads the sensor with the control of the respective components and evaluates the received raw data and calculates the characteristic values. The result from this combination of hardware and software enables the user to see the result of the measurement from the prepared interface.

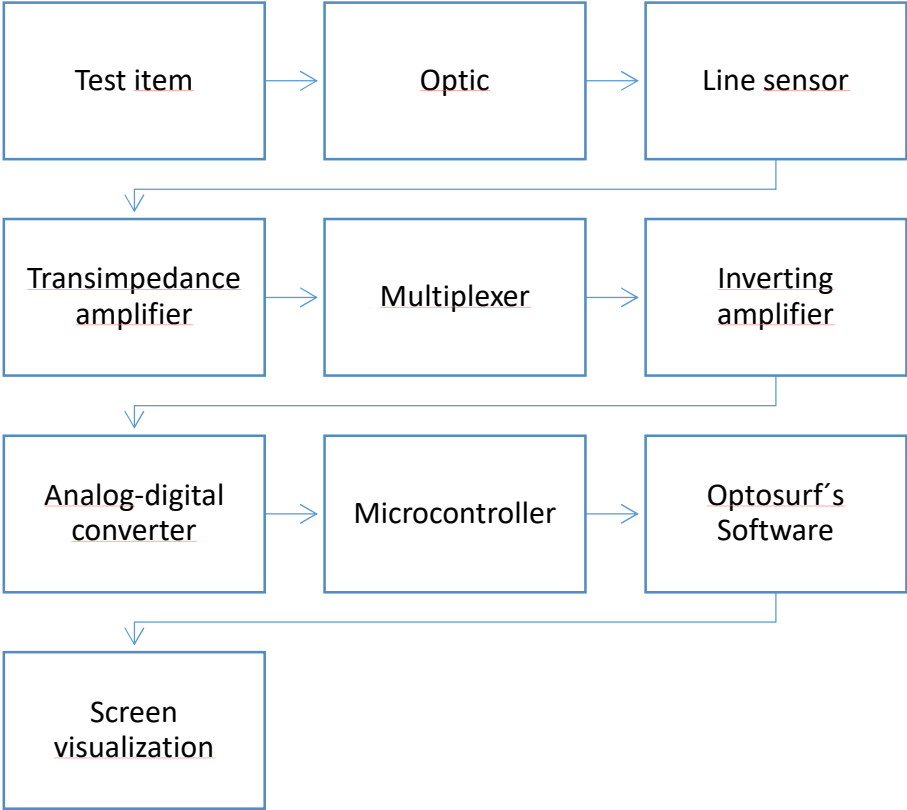
Figure 29. Process of signal visualization²⁷



The sensor measurement process is considered to range from the detection of the surface to the sample of the result programmed through the software. The measurement process starts when

the light from the light source passes through a collimator, which creates a parallel beam path. Then this light is absorbed and partially filtered through a photodiode array that just collects those wave lengths required for the beam. The currents from the array are converted into voltages by an operational amplifier circuit. Once the voltages are obtained, they are first multiplexed and adapted to the input voltage range of the AD converter with an inverting amplifier. Then the conversion from analog-to-digital takes place. After the conversion into a digital signal, the data is sent to the microcontroller, where it is processed. Last, the microcontroller evaluates the data, calculates the parameters and transfers the data through a USB interface. Figure 30 shows the representation of this measuring process.

Figure 30. Measuring process of the sensor



3.9.2. Optosurf's Software

The measured data from the sensor are transferred to the SW-500 software as data packets. This program oversees the reception of the sensor data and represents it through the screen. In addition, the program allows the development of a specific measure that allows us a better evaluation of the measures. Although the sensor measures the Aq, I and M values, the instant reading of these values is not practical when evaluating a surface. To solve this, the program software is responsible for saving the values measured by the sensor in a database and

representing them at the end of the measurement. It is also responsible for making calculations to obtain different parameters, such as shape deviation. This parameter is obtained from the roundness and waviness measurement via simple calculations. When assessing the roughness, statistical parameters from the angular distribution are used. The VDA 2009 guideline: Angle-resolved scattered light measurement technology is used for this evaluation. Definition, parameters and applications are specified there.

4. FAMILIARIZATION WITH THE ALGORITHMS OF THE SPECIAL EVALUATION METHOD

4.1 Ball studs and evaluation project

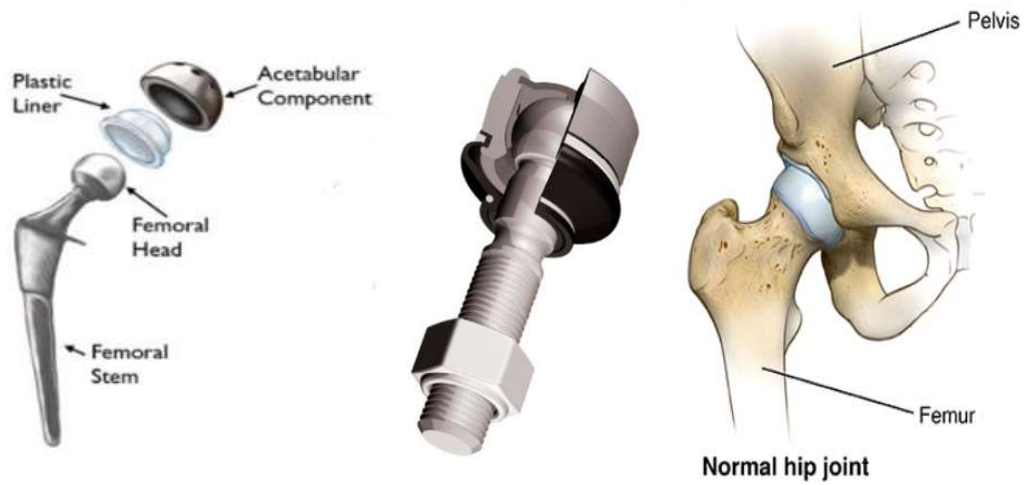
The evaluation of the ball studs corresponds to the measurement of the individual ball studs with the scattered light sensor and the subsequent evaluation of the measurements. Depending on the measured type of ball, a different algorithm is used to calculate the profile and surface finish of the piece in the most reliable way possible. This evaluation will determine if the quality of the product meets the expectations or if it is necessary to make any replacement in the production chain, such as changing the head that provides the machining of the ball studs.

The specific criteria to consider during the measurements are the roughness, by means of maximum and mean value, and the shape of the profile. The values to determine if the criteria are acceptable depends on the external company. The objective of the measurements carried out is to determine the quality and consistency of this process so that the ball stud machines can perform later a correct operation in the external company facilities. Other objectives such as the study of the ball studs are also implemented during these measurements.

4.1.1. Ball joints and ball studs

Ball joints are spherical bearings that connect the control arms to the steering knuckles and are used on virtually every automobile made. They biologically resemble the ball-and-socket joints found in most tetrapod animals. Ball joints are used in the biomedical industry, mostly represented in hip replacements. Figure 31 shows a representation of the human hip joint compared to the hip prosthesis and to a car ball joint.

Figure 31. Representation of a human hip ball joint w.r.t. a car ball joint^{28 and 29}



A ball joint is used for allowing free rotation in two planes at the same time while preventing translation in any direction, including rotating in those planes. Combining two such joints with control arms enables motion in all three planes (figure 32), allowing the front end of an automobile to be steered and a spring and shock (damper) suspension to make the ride comfortable. Figure 33 shows the common location of ball studs in automobiles.

Figure 32. Axis of rotation of the ball stud³⁰

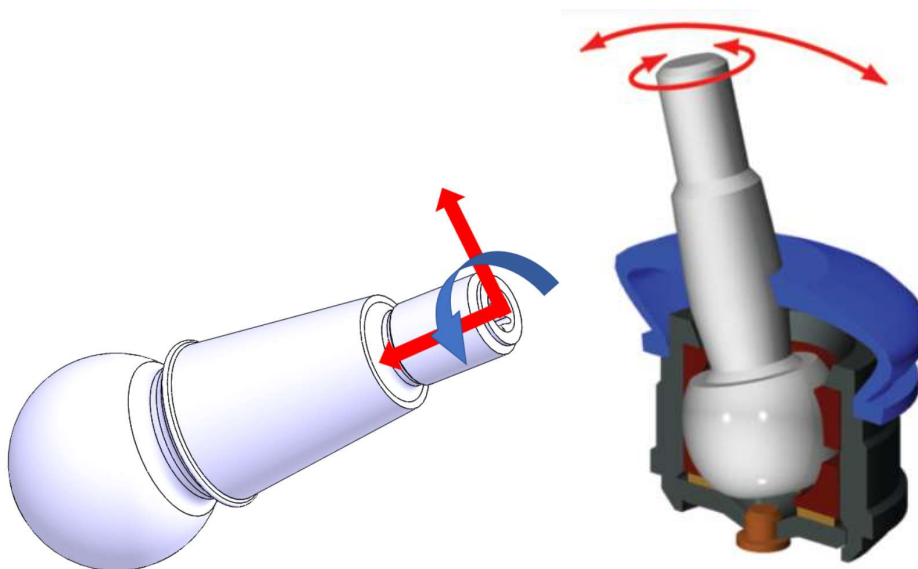
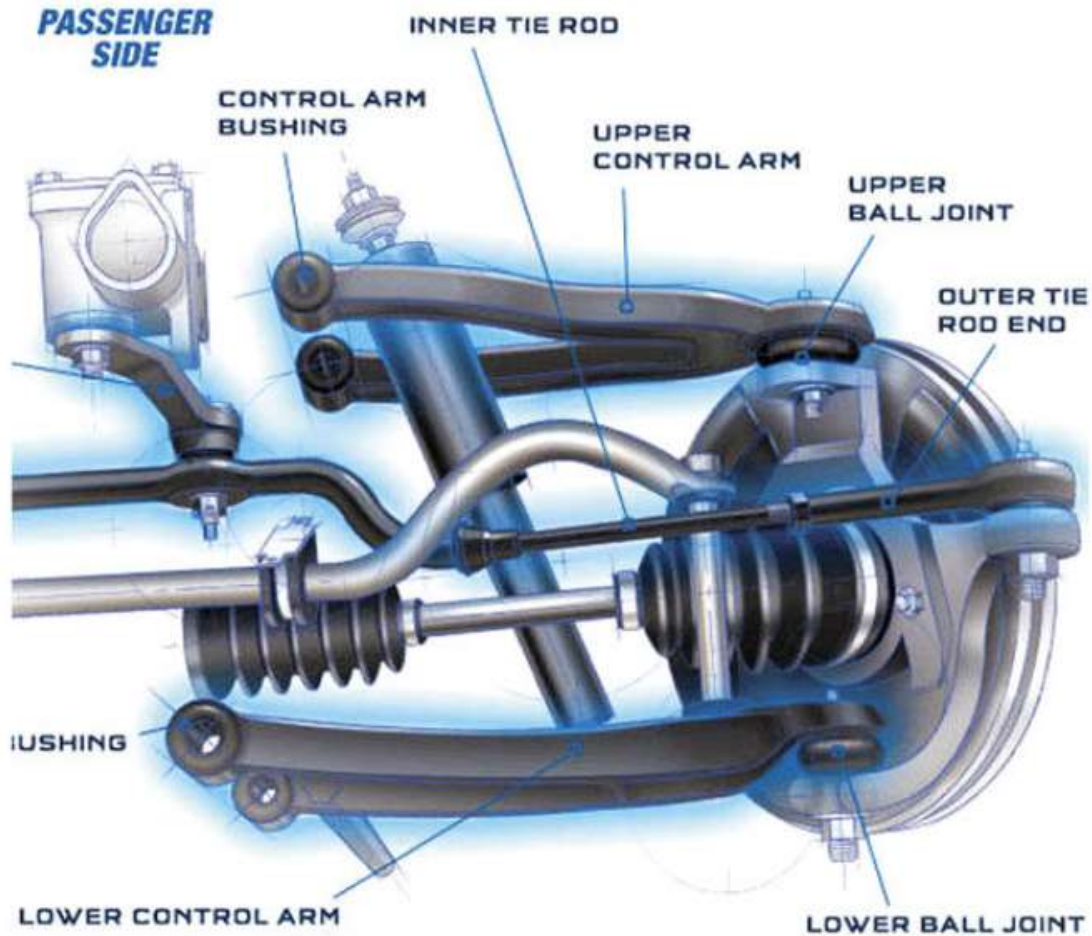


Figure 33. Representation of the ball joints in the car axles³¹



4.1.2. Ball stud process

The ball joint consists of a bearing stud and socket enclosed in a casing. Ball studs are made of steel and the typical material used to manufacture ball studs is 41Cr4. However, since 2005, the external company is using a conventionally rolled micro-alloyed ferritic-pearlitic steel called 35V1. The chemical composition of this steel is given in figure 34. The principal effect of the addition of vanadium is precipitation hardening.

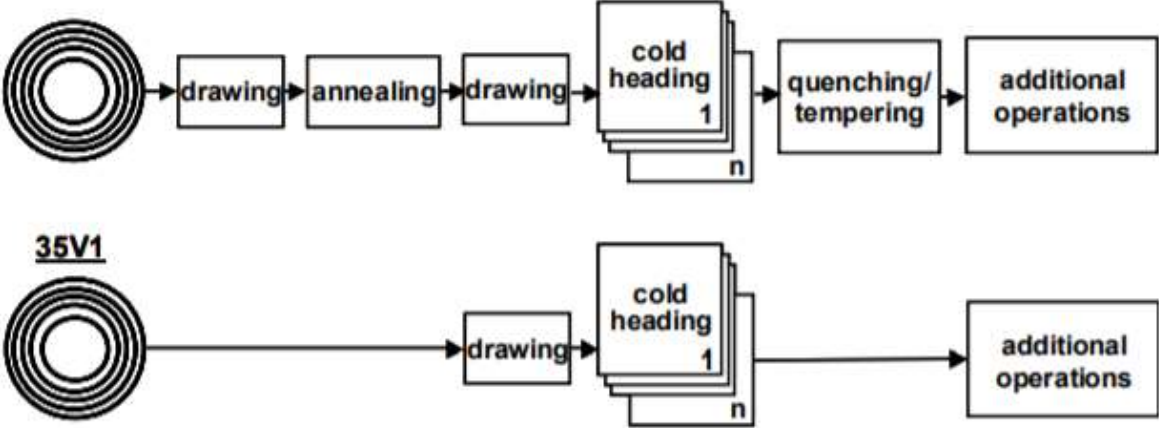
Figure 34. Composition of ball studs³²

	C	Si	Mn	P	S	Ni	Cr	Cu	Mo	V	Al	N
35 V 1	0,35	0,20	0,75	0,02	0,02	0,15	0,2	0,20	0,01	0,10	0,02	0,01

The most important criteria for material selection to obtain the requested strength level is the final strength of the product (880-1030 MPa for ball studs) and the strain hardening capacity of

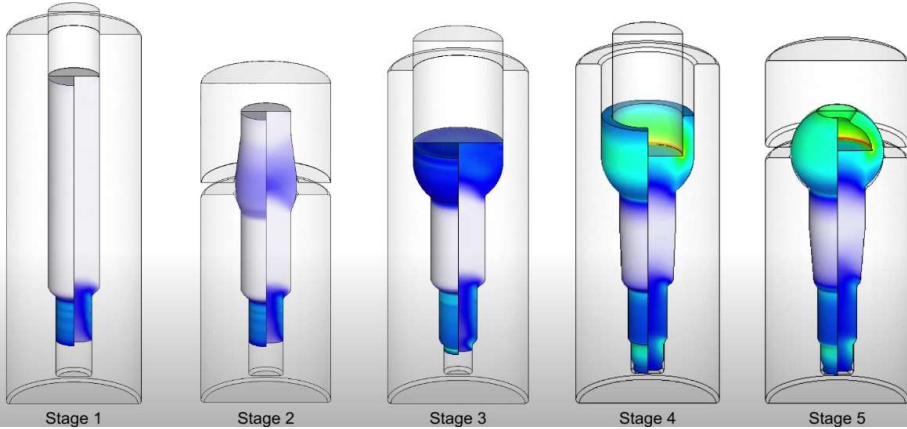
the material. After the selection of the material the production of ball studs takes place. This process varies depending on the chosen material composition (figure 35).

Figure 35. Ball stud process³³



Most materials require a spheroidal annealing before the cold heading process. However, with the 35V1 steel the production starts with the cold forming off the ball stud from the rod in a several step drawing process (figure 36). This cold forming assures giving a correct shape of the ball studs without changing the properties of the material. After the cold forming process threads are cold rolled and there is a machining process to reduce all the imperfections created in the cold forming process. This process will give ball studs its unique surface finish. To minimize the machining marks created by the machining process, the surface of the ball studs is burnished. This process creates a more uniform surface and therefore can prevent a fast wear of the ball stud as minimizing the stick-slip method of the ball.

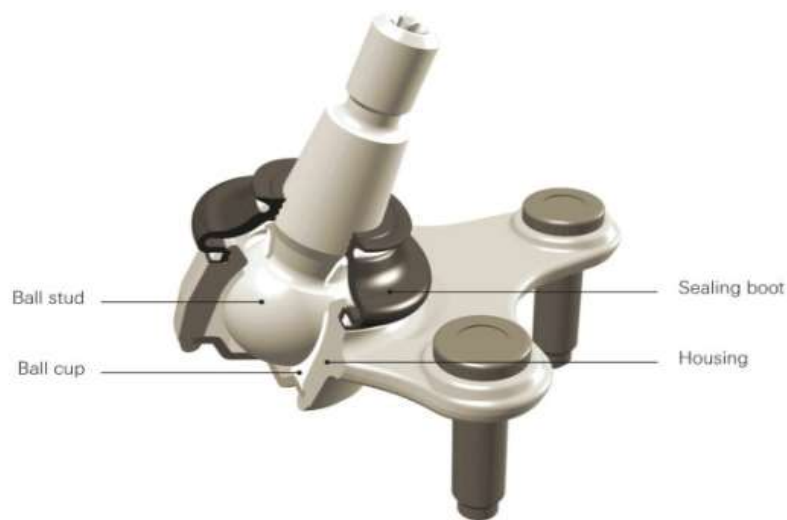
Figure 36. Ball stud cold forming process³⁴



4.1.3. Stick and Slip method

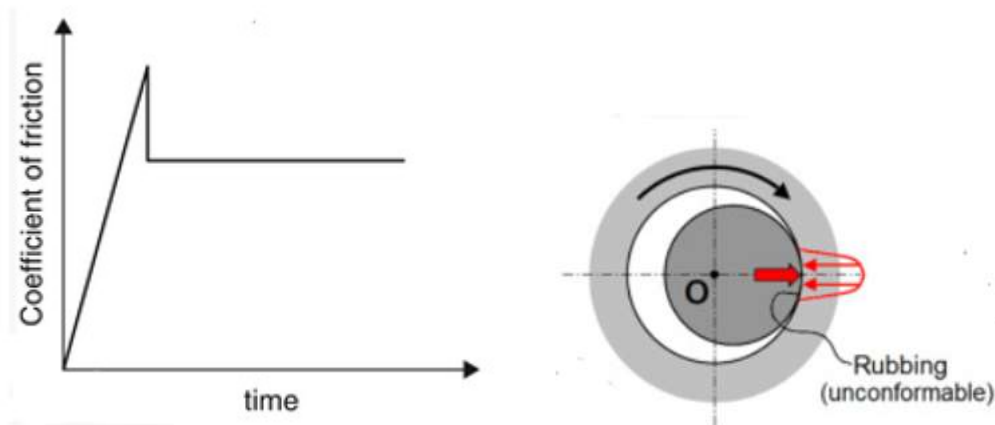
Ball joints used in passenger car chassis comprise a ball stud made from steel that sits backlash-free in a lubricated plastic bearing cup (figure 37). This bearing cup is also embedded in a steel housing. As the ball stud rotates inside the housing, this contact with the housing generates a friction which leads into the Stick-Slip method.

Figure 37. Ball joint representation³⁵



The stick-slip effect occurs if the static coefficient of friction is higher than the dynamic coefficient of friction as well if the slide velocity is low. Figure 38 shows how the coefficient of friction can change from a static to a dynamic position. Checking that ball studs are finished within the required parameters is critical. A defective ball stud finish will produce a greater stick-slip effect due to higher roughness. Ball studs are also located at the joints of the control arms and are connected to the steering of the vehicle. A ball stud with a poor finish may avoid making a smooth turn and then, suddenly, make a more aggressive turn. Such a deficiency can endanger people riding the vehicle. For this reason, measuring the average value of B_q in the working surface of the ball stud (B_{qmF}) is necessary to control the quality of the produced ball studs and prevent the production of high machined marked ball studs. Figure 38 shows how the local strain and stresses forces in-between the ball stud and the housing cause the stick-slip effect.

Figure 38. Slip-Stick effect³⁶



4.2 Ball joints in the automotive industry

Suspension joints are integrated into control arms, pressed-in or flange-mounted. Alternatively, they can be pressed or screwed into the wheel carrier. A distinction is made between guide and suspension joints for passenger cars and vans. While the guide joint generally transmits only longitudinal and lateral forces with a low proportion of vertical forces, the vehicle weight is additionally supported by the support joint. Moreover, there are cross-axis joints used for transferring extremely high dynamic forces.

4.2.1. Joint function: guiding the wheel

The wheel suspension ball joint establishes the connection and, consequently, the support between the front axle control arms and the axle body/carrier (steering knuckle). Its task is to guide the wheel carrier and wheel, to enable the spring deflection of the wheel and to permit the steering movement on the front axle. It is always installed at the triangle apex of the control arm. The height fixation is performed via the ball stud. The ball joint requires that it be easy to move, low in flexibility, maintenance-free and noise-insulating.

Figure 39. Guiding wheel joint³⁷



4.2.2. Joint function: guiding the wheel as well as carrying the body

In terms of design, the suspension ball joints and supporting joints are only marginally different from one to another. The supporting joint is located on the opposite side of the suspension ball joint, assembled in the steering knuckle. It absorbs forces in all directions and can be installed in a suspended or vertical manner. The ball joint housing is usually attached in the control arm and the ball stud is usually attached on the inside of the steering knuckle via its conical taper or a cylindrical dog point.

Figure 40. Guiding the wheel and carrying the body joint³⁸



4.2.3. Joint function: cross-axis joints

Apart from the joint function, there exists cross-axis joints. Cross-axis joints are primarily installed on the rear axle. They consist of a ball with cylindrical taper on both sides and a continuous bore in the middle. Although they are like the ball joint in terms of function and structure, their anchorage corresponds to that of rubber bearings. In contrast to rubber bearings, cross-axis joints can transfer extremely high dynamic forces and have no aligning torque. Cross-axis joints are preferably used if a stiff control arm connection is desired like in sports cars or light commercial vehicles.

Figure 41. Cross-axis joints³⁹



5. CLIENT'S PROJECT

5.1 Evaluation of the Project

The project design is intended to measure the ball studs of the guiding wheel to obtain reliable results that can be repeatable in the client's company facilities. The project is not about evaluating the product but how to ensure a stable and accurate measurement. The assessment is only focused on demonstrating the sensor's measurement capacity and its comparison with other measurement instruments such as the tactile ones. The measurements carried out in this project include optical measurement of form deviation as well as a degree of roughness of the ball stud surface.

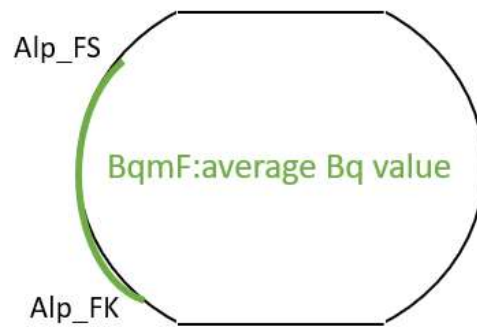
5.2 Degree of roughness of the ball stud

With the scattered light method from Optosurf, in accordance with VDA 2009, the ball stud's roughness can be measured (Bq). For this purpose, a measuring spot of 0.9 mm of diameter is illuminated and the frequency of the angular distribution is measured. From this, parameter Aq is obtained and knowing the radius of the ball stud, the scattered light Bq value is calculated through the software. Measuring the Bq's perimeter of the ball stud fulfils two functional criteria:

5.2.1. Functional criterion: BqmF

BqmF is specified for uniform and reproducible torques. It represents the mean value for the functional area. The values of Bq are measured in the length shown in the figure 42 and represents the average quality of the surface finish. The length which needs to be measured is specified by the client and depends on the ball stud. The client also requires naming the top up (alp_FS) and the top bottom (alp_FK) of the measurement by its specific company name. These names will be shown in most of the software programs when measuring ball studs.

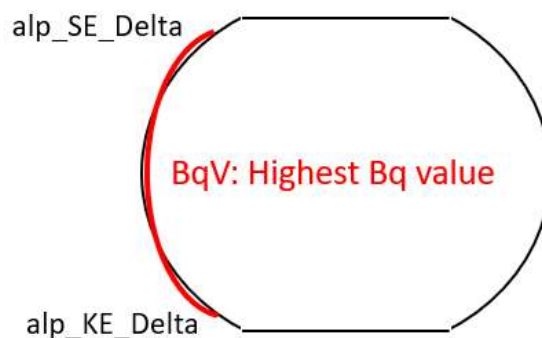
Figure 42. $BqmF$ representation in the ball stud



5.2.2. Wear criterion: BqV

A high roughness in a car ball stud can cause a stick-slip effect and therefore an instable control of the vehicle. The BqV value is calculated, by choosing the highest value of Bq in the analysed length (figure 43). The size of the measured length for calculating BqV depends on the type of ball stud and it is chosen by the client. Also, the naming of the top (alp_SE_Delta) and the bottom (alp_KE_Delta) of the length are chosen by the client following their production guidelines. Being the value of BqV the highest among all the Bq values and having a longer measurement distance, BqV is expected always to be higher than $BqmF$. The stick-slip effect can happen in any area of the ball stud with a deficient surface finish. It is just needed one defect point for the stick-slip effect to happen. The highest value of Bq is always chosen to assure the maximal roughness defect of the ball and determine whether it is acceptable or not.

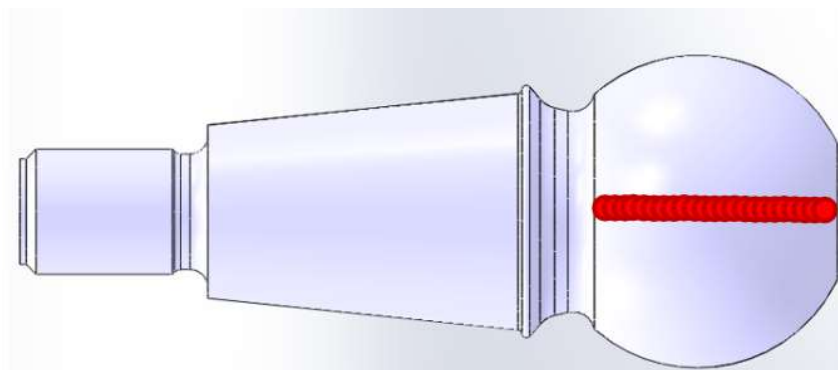
Figure 43. BqV representation in the ball stud



5.3 Measurement of the ball studs with the sensor

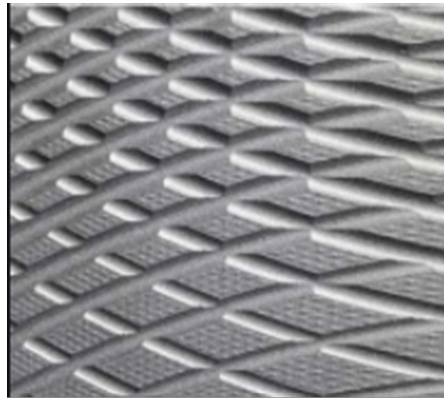
For measuring the roughness, the orientation of the sensor must always be perpendicular to the surface structures (machining marks). The roughness and the proportion of scattered light are the worst in this orientation and therefore the correct values to determine whether the ball stud is acceptable or not. For this project, pre-machined and burnished ball studs are evaluated. A measurement sensor with one spot of 0.9 mm is used to evaluate the surface. To obtain a better representation of the ball stud roughness, the sensor is programmed to make 1024 measures along the perimeter of the ball stud. For this process, the ball is placed in a rotating Z-axis table. When the ball stud rotates, the sensor starts measuring the surface of the ball. 1024 measurements along the perimeter considering that the diameter of the spot is 0,9 mm and the diameter of the ball stud being 25-40 mm causes an overlapping on the spots. This overlapping transforms the initial spot measure into a straight-line measurement through the perimeter (figure 44)

Figure 44. Representation of of the sensor measuring through the ball stud



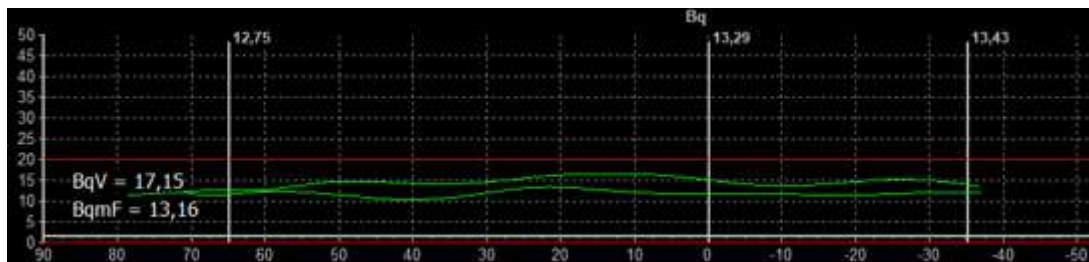
Ball stud's surface structure makes it impossible to determine the surface quality with one measurement around its perimeter. Due to the peculiar machining of the ball stud (cross structure), the sensor cannot measure perpendicular to the machining marks. As the measures are not perpendicular to the machine, the highest values for the roughness cannot be obtained with just one measurement. Therefore, the client initially determined that ball stud's roughness should be calculated with at least 6 different sensor angles measurements to obtain a representation of the actual ball stud surface. The measures with different sensor angles are carried out by rotating the sensor itself in the X-plane. These 6 measurements will vary in 30° from one to another. With this purpose, spanning an amplitude of 150 °, the sensor ensures that it finds an approximation to the perpendicular to the machining marks.

Figure 45. Surface of the ball stud⁴⁰



The determination to make 6 measurements was a theoretical idea agreed in-between Optosurf and the client. This idea is based in achieving the most realistic representation possible within the minimum amount of time to determine that result. The final representation of these measurements corresponds to just one measurement with the highest values of Bq of the 6 measurements (figure 46). These values coincide with the most perpendicular point from all the different angle measurements.

Figure 46. Representation of the roughness of the ball stud



5.4 Optical measurement of form deviation

The form deviation is measured to calculate the roundness of the ball stud profile. As the ball stud is encapsulated in a casing, the profile's form and repeatability are crucial for the ball stud. A deficient roundness can lead to an interference with the casing, as well as an unbalanced wear of the ball. In addition, when ball studs need to be replaced in vehicles, both profiles need to be identical to allow the joint to perform under the same conditions.

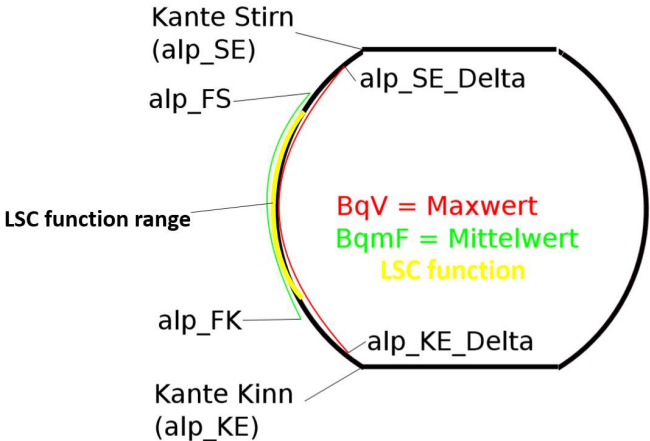
To calculate the shape of the profile, the M value is calculated at every measured point. As the M represents the slope between two consecutive measured points, a line between these 2 points is traced. The sum of every line measured creates the profile of the ball stud.

This development model is meant to be compared with the tactile measuring method installed in the machine.

5.4.1. Optical measurement of eccentricity deviation

Ball stud position cannot be fully centred. Mechanical tolerances position the ball off the real centre. As profile design calculations require a good centring to be accurate, this deviation must be compensated. By calculating the eccentricity of the ball, a circle compensation function (Least Square Reference Circle “LSC”) can be used to centre the ball when calculating the M values. For calculating the LSC function, the angles of measurement are chosen in the program. The values chosen for the LSC function are chosen by the client to be the lengths with an arch smaller than BqmF (figure 47).

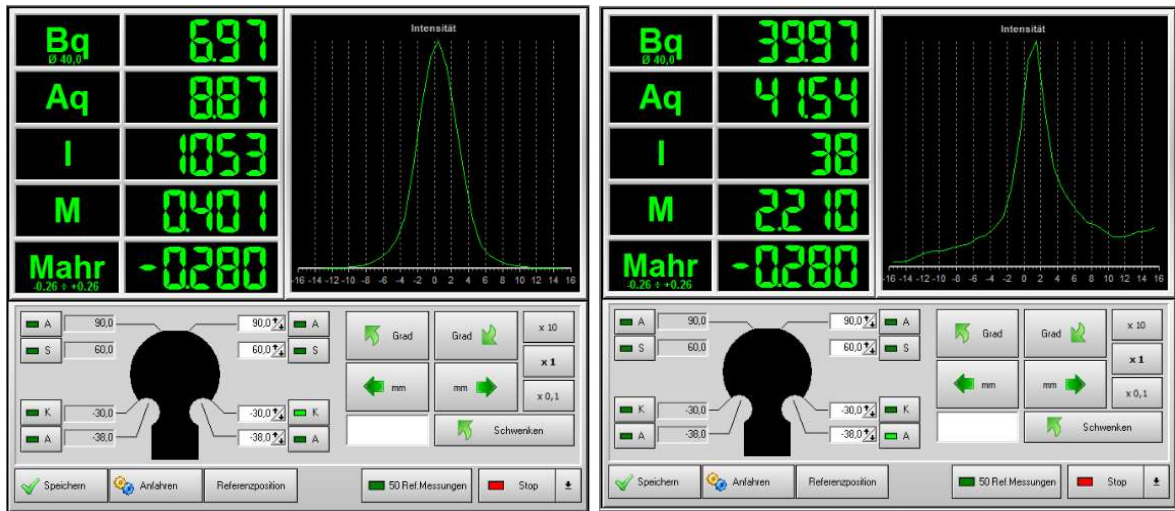
Figure 47. Ball stud ranges to be analysed



5.4.2. Measuring ranges and drawing requirements for the ball stud

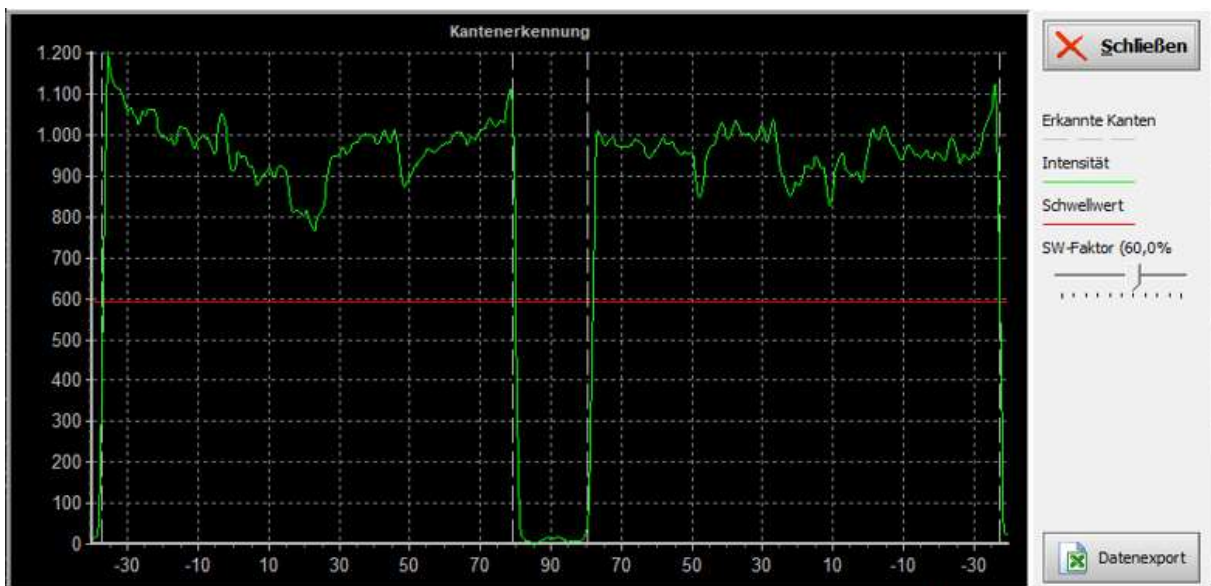
Ball stud optical measures are received and saved in the software after the measurement. This data measured by the sensor is collected into a specialised program for ball studs which is focused on detecting the edges of the ball based on the intensity I received by the sensor. The drop of the intensity is considered as an edge for the program and determines where the sensor starts measuring the ball (figure 48).

Figure 48. Comparison of I before and after reaching the edge



The determination of the edge is achieved through a function of the program, the measurement threshold. This function allows locating the exact position of the edge from the maximum percentage of intensity (figure 49). This percentage varies depending on the type of ball stud or its composition. For polished surfaces, higher thresholds are used (over 80%), whereas for darker surfaces, such as ZnNi coated ball studs, lower thresholds (60%) are used.

Figure 49. Representation of the edge detection



6. CONSTRUCTION AND COMMISSIONING OF THE MEASURING DEVICE

6.1 OptoShaftTT

The complexity, uniqueness and the low scalability of Optosurf's machines, focus them on a very specific market niche. The development of Optosurf technology over the years allows updating and improving existing machines to continue offering an avant-garde measurement service. Sometimes, these upgrades can be simply software updates that can be changed in the client's facilities. However, other times, the upgrade can be much more complex, can take up to several weeks and it is not possible to make those changes in the facility where the machine is held. Taking the machine from the client through the complete process of developing a new upgrade (which can take up to a year) would incur in the loss of a large amount of money for that company. The incapability of the company to continue measuring its products concurs in a big loss of opportunity cost.

Optosurf has developed a polyvalent tabletop measuring station, the OptoShaft TT (figure 50), which can provide similar measurements to the ones obtained in the "real machine". Achieving similar results means that it is no longer required to bring the machine (from the client's facilities) through the developing process. The OptoShaft TT can be defined as a compact, universal measuring device used in R&D, quality engineering or for quality assurance as an SPC (statistical process control) device. Alongside a scattered light sensor, it is fitted with a high-precision rotary table and a motorized z-axis. Both axes are positioned by a CNC control to enable even full scans of different machined parts such as gear shafts or to measure inside the flanks of EPS-worms or spindles. The sensor can be also rotated vertically and fitted with an optical adapter to measure inside boreholes.

Figure 50. OptoShaft TT⁴¹



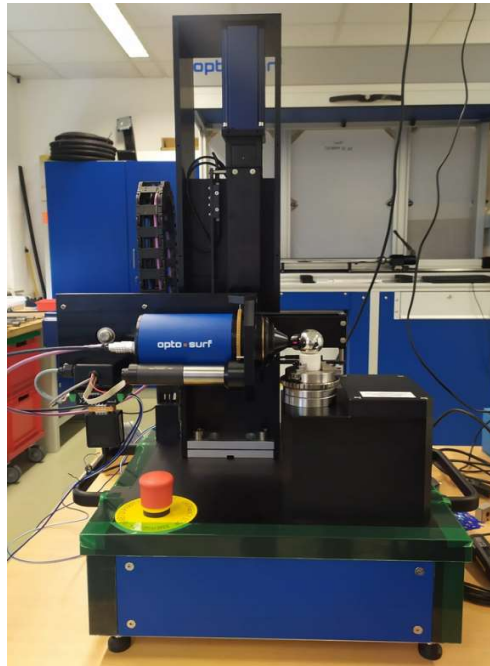
6.2 OptoShaft TT used for the project

In addition to these 2 axes of rotation, the OptoShaft TT has 3 more axes. These 3 axes can be manual or motorized (depending on the measurement needs and the client's budget). The 3 axes consist of: X-axis of the machine, where the sensor is attached, the rotation of the sensor's Y-axis (tilt axis) and the sensor's X-axis of rotation. For the design of this unit, motorized axes have been used both in the X axis of the machine and in the rotation of the X axis of the sensor. As measurements will always be measured with the sensor positioned horizontally to the ball studs, it is not necessary to use the sensor's Y-axis. Figure 52 shows the design of this OptoShaft TT.

Figure 51. OptoShaft TT Axles

Axis	Position
1	high-precision rotary table (Z-Axis)
2	motorized z-axis for the sensor displacement
3	motorized x-axis for the sensor displacement
4	Rotation x-axis for the sensor
5	Tilt y-axis for the sensor

Figure 52. OptoShaft used for the project



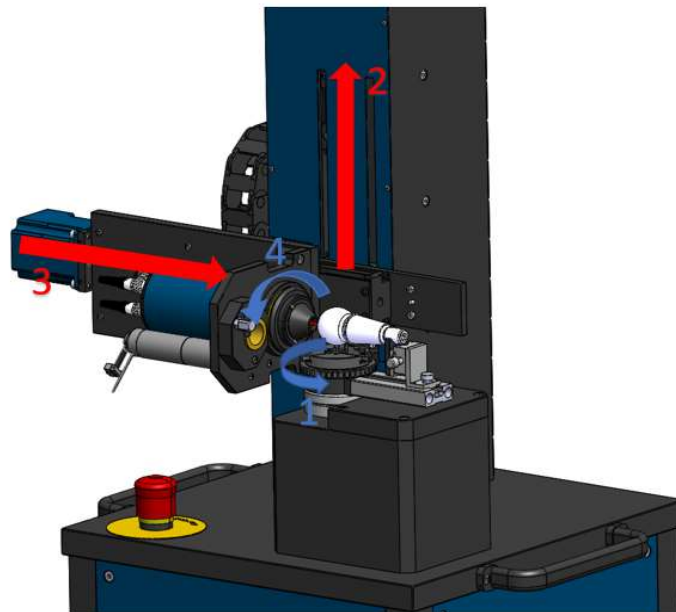
All axes from this OptoShaft TT are represented in Figure 53.

- Axis 1 determines the rotation of the table where the ball stud is located. This axis will rotate during the measurement while the sensor remains immobile but measuring the ball stud. The ball stud is placed in the support provided, which is fixed to the shaft. Thus, when the rotation table rotates, the ball stud also rotates with the shaft.
- Axis 2 determines the height at which the sensor should be positioned. This height is controlled by the Z-axis motor. The objective of this axis is to place the sensor at a height which corresponds to the middle of the ball stud. At this position, the reception of the light beam is the greatest.
- Axis 3 determines the distance between the sensor and the ball stud. The sensor has been developed so that the exact measurement between the lens of the sensor and the object is 43 mm. In this case, the sensor has a protective cap with a length of 33mm so the distance between the border of the cap and the ball stud must be 10mm. To achieve this, the motor is programmed to be positioned at this corresponding distance.
- Axis 4 is used to rotate the sensor between measurement and measurement. Since the sensor cannot measure the surface structure of the ball studs perpendicularly, it needs to be rotated. With this rotation of the sensor, a greater number of points perpendicular to the structure of the ball studs can be obtained. For the rotation of the sensor, the

number of rotations and the angles of these rotations in the motor can be programmed directly through the software.

- Axis 5 determines the inclination of the angle to measure with the sensor. This axis is very useful for measuring vertical objects or those that, due to their shape, need to be measured with a certain inclination. For ball studs it is not necessary to use this axis as they will always be measured horizontally.

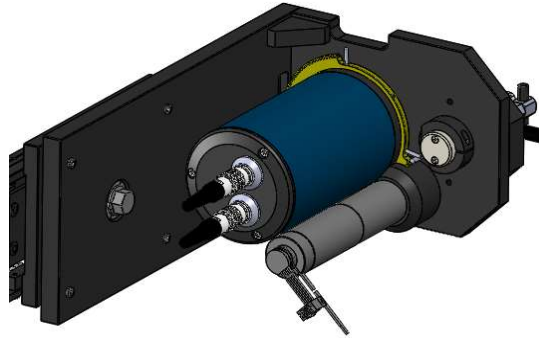
Figure 53. OptoShaft TT axes



6.3 Description of the rotary module for the sensor

The rotary module for the sensor shown in figure 54 has been designed to measure ball studs from different angles. The module consists of a stand which supports the sensor and the rotation mechanism. This mechanism consists of a straight toothed gear between the motor and a gear wheel attached to the sensor. Moreover, there is a tactile sensor also attached to the mechanism which allows the machine to measure with both methods without changing the stand module.

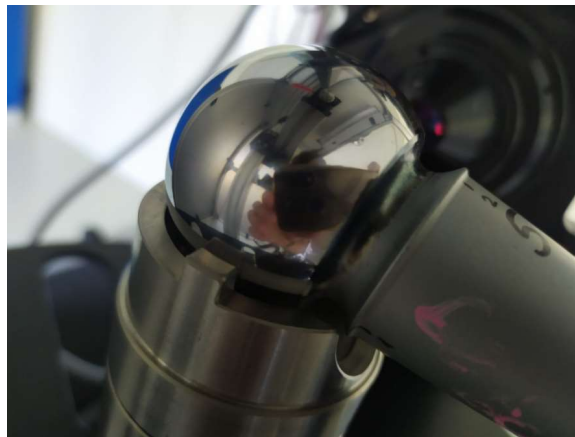
Figure 54. Rotation module of the sensor



6.4 Design to enable measurement of ball studs

The design of a support for the ball stud is necessary to hold the piece. The weight distribution of the ball studs is uneven, and the ball must be in the measuring position of the machine (middle of the shaft) (figure 55). In order to support the ball stud, a support has been designed to support any model of ball stud to be analyzed. Ball studs vary in both diameter of the ball and length of the shank. Therefore, ball stud supports design must include both length and height adjustment.

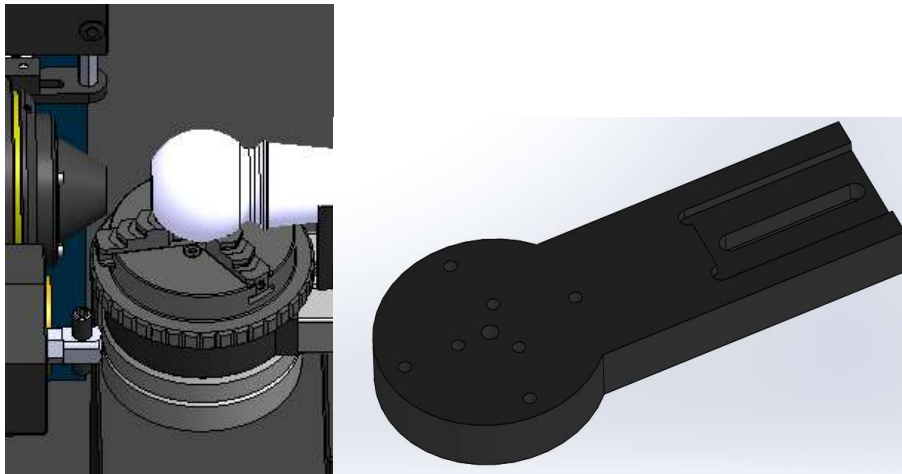
Figure 55. Measuring position of the ball



For the realization of the design, existing components in the company or those that the official Optosurf distributors had in stock were used in order to reduce costs. Likewise, the designs created have gone through the review of the designer of the company. During the design process, 2 models were made, a first design model and the final model. The different pieces that make the first support are the following:

A clamping piece has been designed between the motor shaft of the rotary table and the three-jaw chuck where the ball stud is placed. A rounded machined part with similar measures to the rotary shift has been designed. The elongated part corresponds to the one in charge of the ball stud support. A long hole and a knurled screw are used to adjust the length. To ensure longitudinal movement, a guide has been designed (figure 56). The material chosen for this piece is anodized aluminum. Black anodization prevents the light beam from the sensor from reflecting on the different parts of the machine.

Figure 56. Design used for clamping the structure to the OptoShaft TT



For the height adjustment, a MISUMI mechanism has been chosen. The ZFG25 model (figure 58) allows horizontal movement of up to 25mm. Ball bolt diameters vary between 25-40mm (figure 57) so the stroke of the MISUMI is sufficient for all ball stud measurements.

Figure 57. 40- and 25-mm ball stud

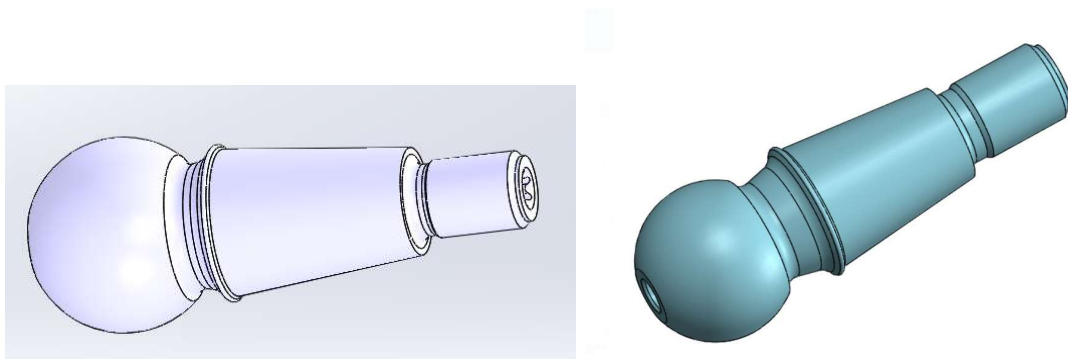
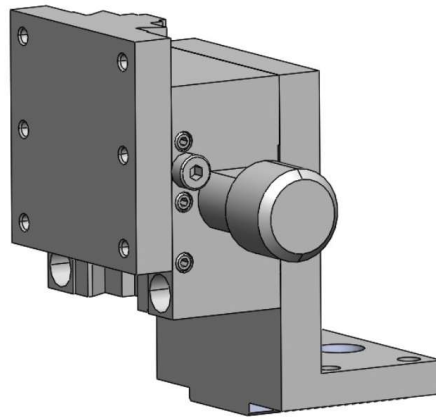
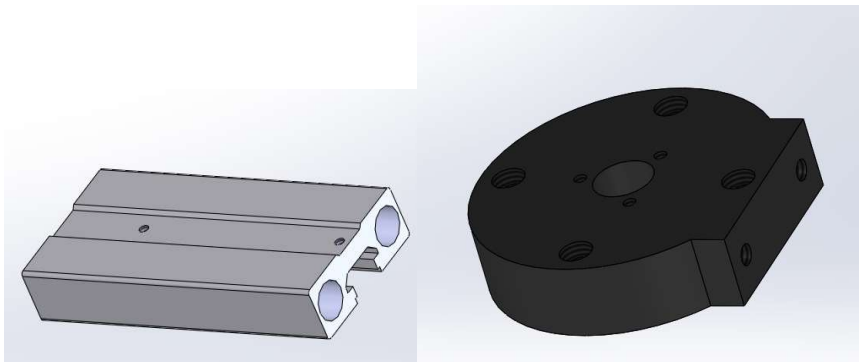


Figure 58. Misumi mechanism



At the design presentation, the design team suggested an improvement in the design of the base part in order to simplify machining and save costs. The new proposed design consists of dividing the base piece into 2 parts. One part would be formed by machining and would fulfil the function of fastening between shaft and mandrel (figure 59). To support the MISUMI mechanism, a 15x40 Rose-Krieger profile has been included (figure 59). This profile is screwed to the machined base. In addition, the profile has two holes including two screws that will serve as the beginning and end of the horizontal axis stroke.

Figure 59. Rose Krieger profile and machining clamping piece



The MISUMI mechanism is intended to move along the horizontal axis. To achieve a linear movement, a milling process has been done to adjust it to the profile as seen in figure 60. In addition, a hole has been made in the base of the MISUMI mechanism where the knurled screw is placed. With this screw position can be adjusted depending on the ball stud that is measured. To hold the ball stud a prism support is used. The idea of designing a prism support comes from the type of supported piece (cylinder), for which prisms are the best supports. The prism support is screwed to the moving part of the MISUMI mechanism so that it can be displaced with the same stroke as the mechanism.

Figure 60. Mechanism to regulate the height

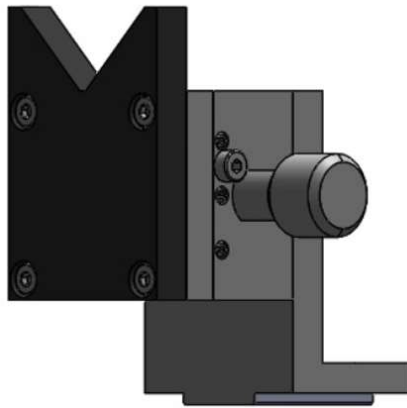


Figure 61 and 62 shows the similarities and differences between the two designed models. On the upper side is the first model proposed, and on the lower the final model designed.

Figure 61. First designed model

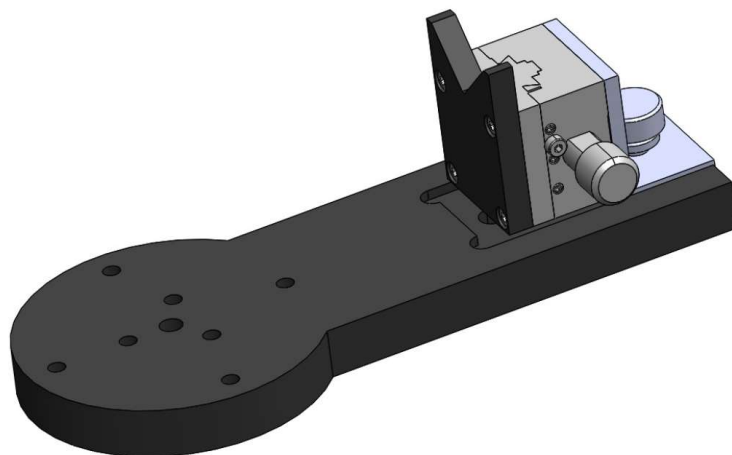


Figure 62. Final model

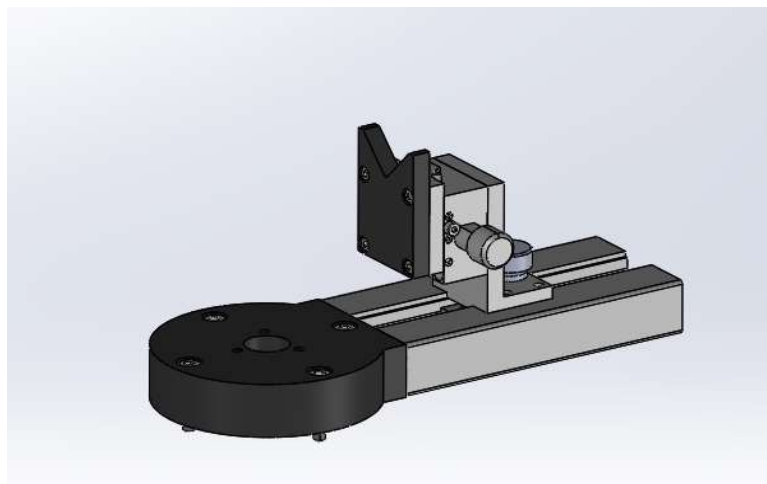
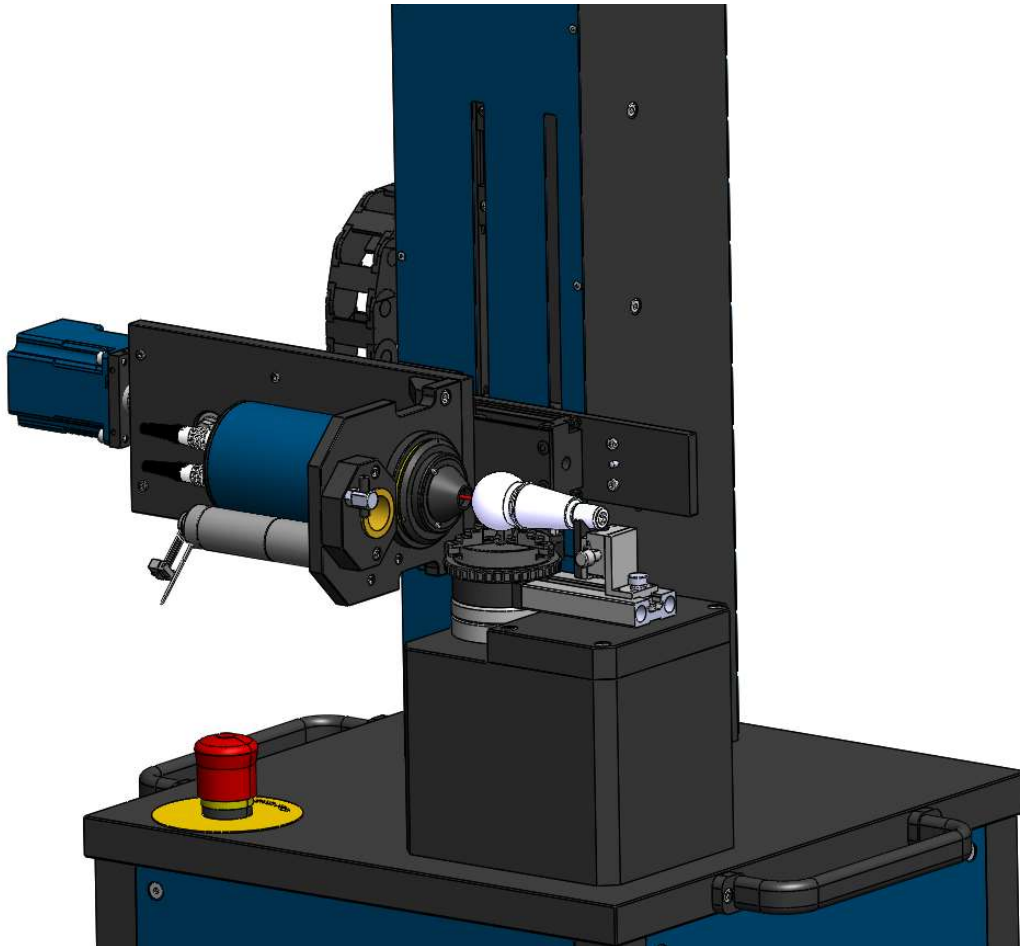


Figure 63 shows the construction design mounted in the ball stud machine in Solidworks. Once the designed model has been verified in the machine, the drawings for its production are created. Only machined parts are drawn. These drawings are sent to an external workshop where the pieces are produced. The description of the drawings can be found in the annexes.

Figure 63. Design installed in the OptoShaft TT



6.5 Mounting the OptoShaft TT

6.5.1. Optimization of the axes and assembly of the machine

The adjustment of the axes in the assembly of the machine is a fundamental process for a correct measurement. In the case of this OptoShaft TT model, two different motorized axes had to be fitted. One axis for vertical movement and the other one for horizontal movement. These shafts were formed by a base with a spindle coupled to a motor (figure 64). On the spindle there is a stand that moves along its stroke. To maintain the linearity of the movement, the stand is on

track to the base. For a correct operation and reduction in friction, both the spindle and the support must be correctly greased.

Figure 64. Horizontal axis of the OptoShaft TT



In addition, the base has two limit switches attached to it. These sensors make it possible to electronically limit the stroke of the mechanism if necessary. It also works as a safety element since it prevents the support from colliding with the beginning or end of the stroke.

The motor is connected to the spindle by a metal bellows coupling. The use of this coupling reduces the shear stress created in coupling the motor with the spindle. This shear stress is generated by the impossibility of assembling both parts of the coupling completely straight. The spring absorbs these constant stresses that would otherwise be distributed by the mechanism, damaging the useful life and possibly causing it to break. In the case of the design of manual axes, this type of coupling is not necessary because the axle is rotated directly.

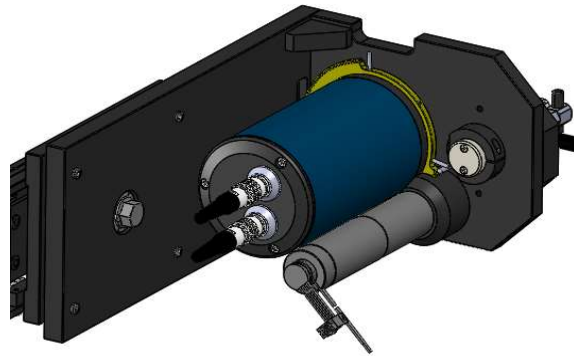
Figure 65. Bellow couplings in the axle



6.5.2. Mounting the measurement module with different angles

In the assembly of the measurement module, all the fastening parts of the sensor, the motor and the touch meter were screwed. When screwing, adjustment plays an important role, all surfaces must be as orthogonal as possible.

Figure 66. Bellow couplings in the axle



6.5.3. Programming and tuning of the software of the different motors

The programming is different for each of the motors. On the one hand, the Nanotec motors of the axes (figure 67) are programmed through an IMS terminal for its initial configuration (figure 68). Nanotec motors are used for controlling the vertical and horizontal position of the OptoShaft TT machine. Both motors are initially configured apart to test them manually before including them in the automatized software.

Figure 67. Nanotec motor st5918



Most motor manufacturers have an instruction manual where the variables necessary for motor control are declared. Parameters such as an initial “safe” position, a reference position, initial

velocity, work operating velocity, acceleration are set up in the program. All these values need to be probed and manually checked before automatizing the process. In the terminal the initial position is declared, as well as the speed and acceleration of the motors. Adjusting the motor to its optimal speed and acceleration improves the efficiency of the measurement.

Figure 68. Declaration of Nanotec values

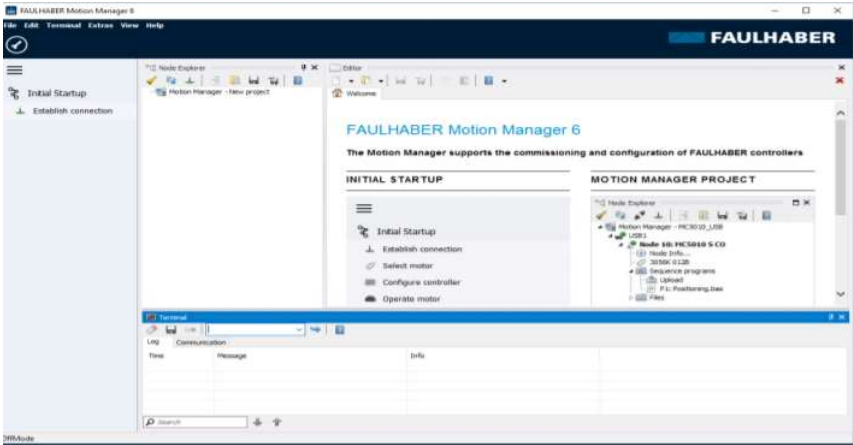
```

MC_MFORCE_Micro_Partymode_ST5918L3008-...
[PROGRAMS]
PG 1
LB Su
Dn = "C"
Py = 1
Hc = 50
Rc = 65
Ms = 180
Vm = 10000
Vi = 500
A = 20000
D = 20000
S1 = 1, 0, 1
D1 = 1
S
E

```

In addition to the Nanotec motors, there is a Faulhaber motor which controls the rotation of the sensor and it is also programmed through its own control program, called Motion 6 (figure 69). In the same way as with the Nanotec motors, the different parameters were firstly checked manually in the program before including them in the automatized ball stud machine. Parameters such as a safe position, reference position, position limiting (maximal angle measurement), velocity of measurement and acceleration are included in the motor. These parameters can be configured manually through the motor’s program.

Figure 69. Motion 6 program



The motor has its own variables for different functions which has been probed in the Motion 6. All the motor variables can be found in the function manual offered by Faulhaber. These variables are necessary to run the motor and to later automatize the program. After the manual probe they must be included in the program to control the motor. One of these functions would be calling different routines from the RS232 interface. This would be the case of the “JMP2”

function. This function moves the motor to a limit switch and then to the Hall sensor zero point, in order to obtain the most precise reference point possible. In addition to allow the rotation in the desired positions, other variables have been determined that ensure the sensor's rotation path. Despite having some mechanical limits and a torque limit on the part of the motor, some functions have been added to determine the maximum rotation of the motor. This avoids the contact of the mechanism with other parts and a possible misalignment. Other functions were implemented when combining with the Optosurf's software. This is the case of the "DIERI" (Disable Error Interrupt). These functions improved the performance of the whole software. All necessary values used in the program are shown in figure 70.

Figure 70. Declaration of the Faulhaber motor values

```

A1          ; Marke1
SP5000     ; Maximaldrehzahl
AC100      ; Beschleunigung
DEC100     ; Bremsrampe
LPC200     ; Spitzenstrom auf einen geringen Wert stellen
LCC180     ; Dauerstrom auf einen geringen Wert stellen
LL-272000  ; negatives Positionslimit
LL2000     ; positives Positionslimit
APL0       ; Positionslimits deaktiviert
ERI3       ; Sprunge im Fehlerfall zur Marke3
V600       ; Drehe mit 20rpm. Wert und Vorzeichen, Drehrichtung wählen
A2         ; Marke2
JMP2       ; Sprung Halteschleife
A3         ; Marke3
V0         ; Stop Bewegung
DIERI      ; Disable Fehlersprung
LR-2200    ; Fahre 2200 Incremente zurück Wert und Vorzeichen wählen
NP         ; Notify Position
M          ; Move
HO         ; Setzte Zählerstand auf null
APL1       ; Positionslimits aktiviert

```

7. CREATION OF ALGORITHM MEASUREMENT AND VERIFICATION PROGRAMS WITH TEST PROFILES IN THE OPTOSHAFT TT

The creation of the programs is done through Optosurf's software. This software varies depending on each project, although for scalability terms, there exists some default versions. These versions also include new specific functions required for the project. In this case, the software version used is the default one for measuring spherical surfaces (figure 71). A section has been added to this version that allows visualizing the structure of the ball studs surface in each of the angles measured with the sensor. It also includes specific values calculated by the software for this application such as BqV or BqmF.

Figure 71. Optosurf's program⁴²



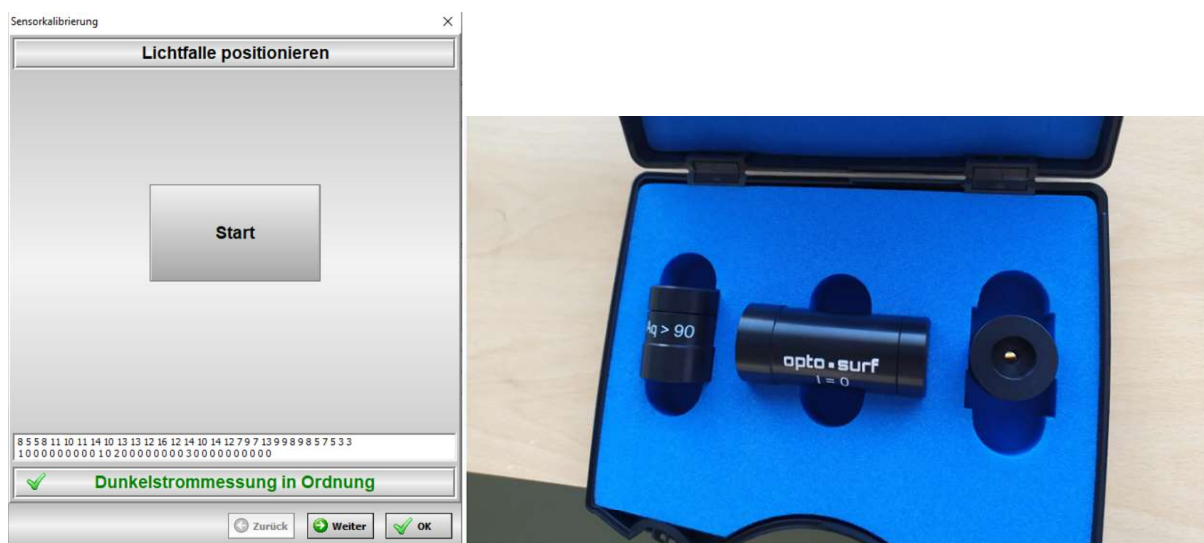
7.1 Setting up Optosurf's software

Before creating programs, it is necessary to set some parameters and correctly activate the sensor and motors. These functions are only necessary to perform them in the set-up of the machine or after a revision of the sensor or the motors.

7.1.1. Calibration of the sensor

The intensity of the sensor depends on the light it receives. Before the adjustment in the intensity parameters, a sensor calibration process is carried out. The calibration of the sensor enables the standardization of the measuring process. This sensor's calibration consists of adjusting the maximum and minimum values of A_q of the sensor with Optosurf's own equipment (figure 72). A silicon mirror is used to calibrate the minimum value of A_q and a dark current is used to calibrate the maximum value. By doing this, the sensor is adjusted to measure in the A_q range from 2-100 (2 corresponding to the silicon mirror and 100 corresponding to the dark current). The reason to use a silicon mirror as the minimum value corresponds to its surface reflecting properties. It is considered the most perfect mirror. On the opposite site, the reason to use a dark current is to obtain the minimum amount of reflected light which will correspond to an A_q value of 100.

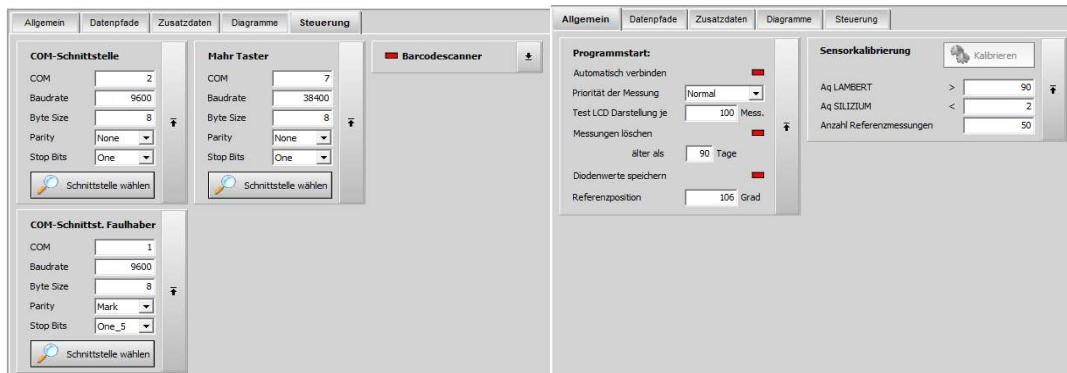
Figure 72. Optosurf's calibration equipment



7.1.2. Activation of the motors and the reference position of the ball stud machine

Motors must be assigned with the corresponding serial port to which they are connected for their use in the program (as shown in figure 73). The reference position refers to the starting position of the rotary table. With these settings, the measurements always start from the same position and the motors can operate. This process is automatic if the motor ports are not changed, or the rotary table shaft is not removed.

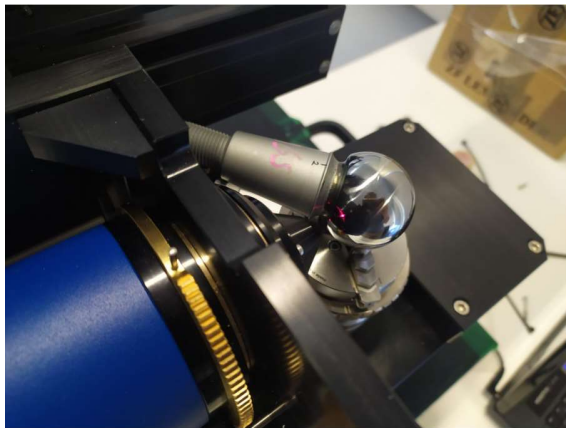
Figure 73. Activation of the motors



7.2 Creation of measurement programs

The first measurements are focused on determining the consistency of the sensor in the new design. To do this, the same ball studs were measured in different positions by turning them (the ball studs) manually (figure 74). By measuring the ball studs in different positions, the overall homogeneity of the surface roughness can be determined.

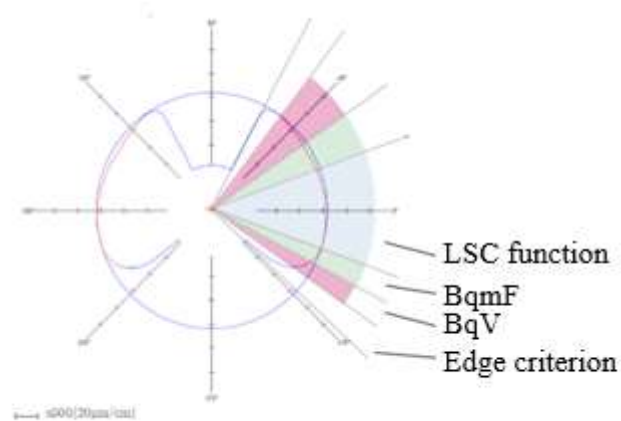
Figure 74. Location and position of the ball stud in the Opto-Shaft TT machine



The measurements have been made in a program that allows the sensor to measure with six different angles. These measurements cover a sensor rotation angle of 150° with 30° difference in each measurement. The measuring angle must cover the useful area of the ball stud as specified in figure 75. This means that the measurement must go from border to border of the BqV angle. The measurement angle of BqV depends on each ball stud. For this case, the length

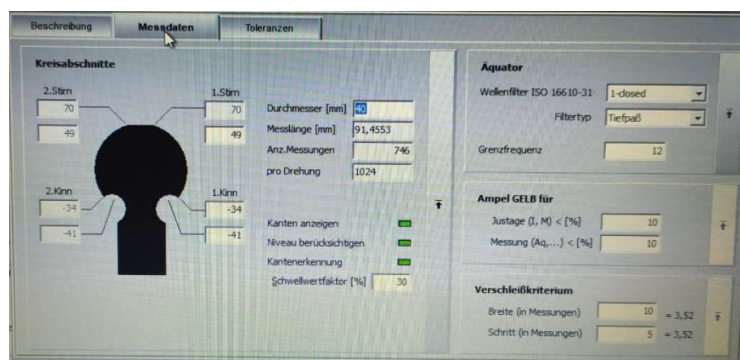
of BqV up to 8 ° from the edge of the ball stud has been determined for this test. This 8° angle comes as a first guess from the theoretical interpretation from the client.

Figure 75. Ball stud edge criterium⁴³



The determination of the amplitude of the measurement area is set in the program. Figure 76 shows the ball stud parameters that need to be filled. It is necessary to determine the edges. To know the position of the edges, edges have been found empirically. It is necessary to make a program for each type of ball stud as the position of the edge varies from one type of ball stud to another.

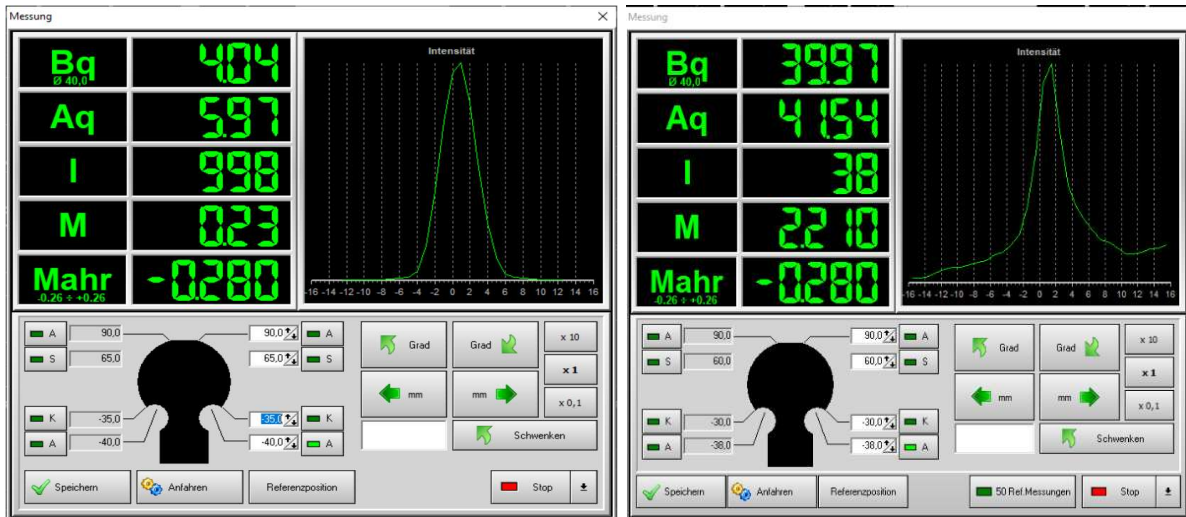
Figure 76. Ball stud configurator



The software test window is used to determine the edge in first place. In this window the position of the motors can be manually adjusted. The edge determination occurs when turning the Z axis table. The ball stud rotates with the table and it is measured by the sensor. When the sensor reaches the edge the value of Aq increases and the intensity value of the sensor decreases. A decrease in the Aq values means that the measured surface is not regular anymore and therefore the light distribution is no longer concentrated in one point but distributed along the row of diodes. As this distribution occurs, it also means that a part of the reflected light will not be

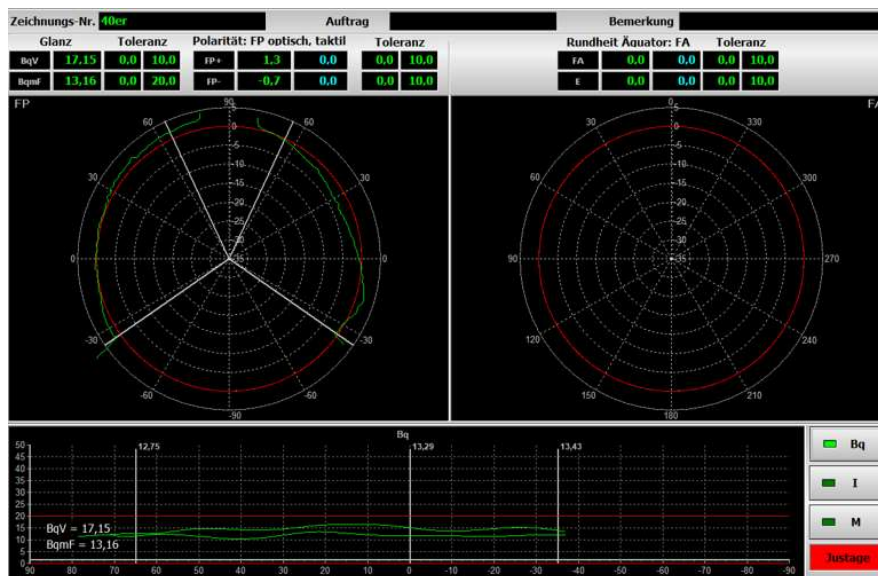
detected by the row of diodes. The intensity will then decrease as the sensor goes over the edge (figure 77).

Figure 77. Loss of intensity at the edge



The diameter must also be specified in every program. Depending on the selected diameter, the sensor moves along the y-axis in order to position itself 10 mm away from the surface of the ball stud. The number of sensor measurements is preprogrammed and specified for a complete scope (1024 measurements). Therefore, depending on the angle selected in the edge detection, more or fewer points are used for the measurement.

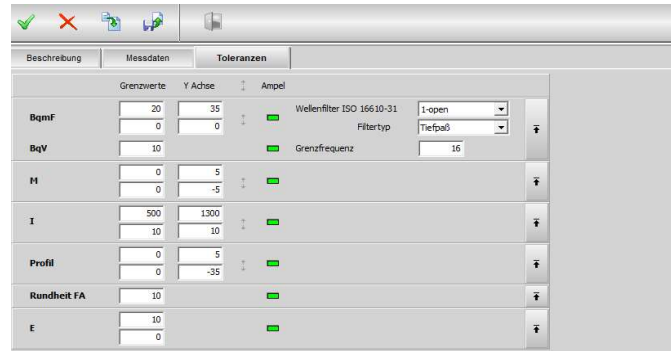
Figure 78. Main window for the graphical representation of the ball studs



The results obtained in the measurement program can be shown through three different graphic representations (figure 78). The parameters of these graphs can be adjusted to obtain a more representative visualization of the result (figure 79). The sizes of the measurement axes can be

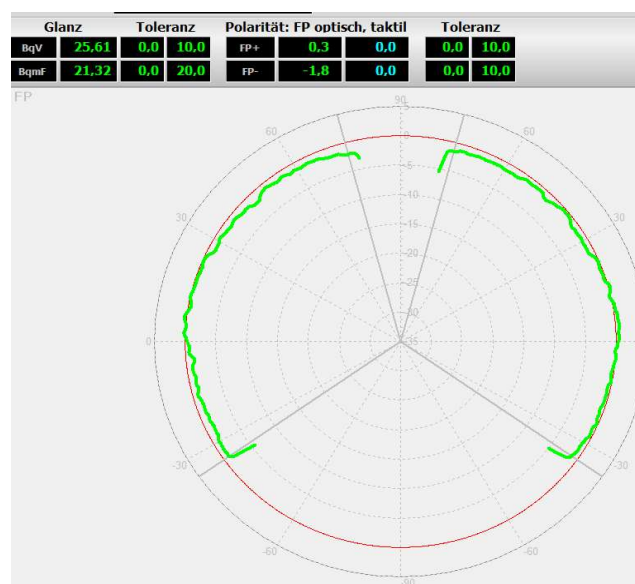
designed, as well as parameterize which values are acceptable, and which are not. Limits on values like Bq, I or M can be set up to help the evaluation of the surface. In addition, there is a parameter that enables the filtering of irrelevant noise in the measurement.

Figure 79. Boundaries for the graphic representation of the obtained results



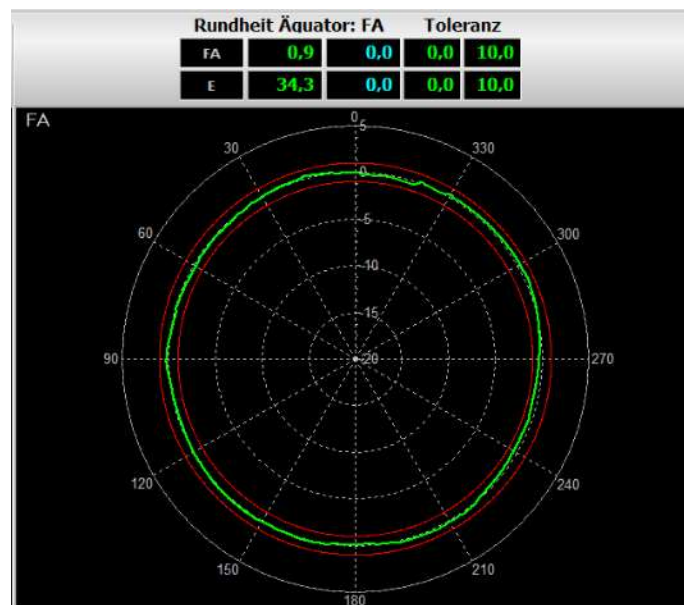
The top left graphic (figure 78) indicates the profile of the ball stud in the optical position. This graph determines the contour and how circular the ball stud is. **To calculate it, only one sensor rotation measurement is made, in which its angle is chosen by the person making the measurements.** The light beam sensor determines the perimeter of the circumference while the ball stud rotates on the rotary table axis. The representation of the perimeter is shown in figure 80. In the upper part of the figure, the values of FP (Formpolarität) are shown. The values of FP + and FP - represent the maximum value and the minimum value of deviation of the diameter with respect to the initial point of measurement. These values are measured in micrometres (μm). The possibility of making these measurements with the tactile device permits a comparison to the FP calculated with the sensor.

Figure 80. Profile of the ball stud measured with the sensor



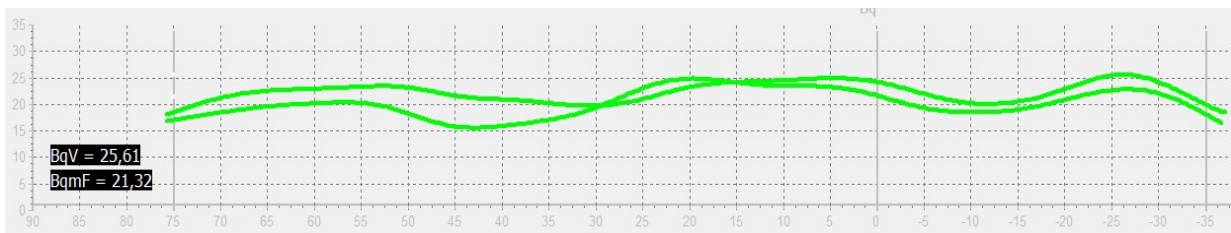
The graph on the right (figure 78) represents the measure of the contour at the equator. By measuring the equator, a different and more precise contour of the ball is obtained. **To calculate it, only one sensor rotation measurement is used, the angle of which is chosen by the person who performs the measurements.** With this measurement, the perimeter of the ball stud can be measured completely without detecting edges or without colliding with the ball stud itself. This option allows to obtain another representation of the contour than the one made in the optical measurement mentioned above. In this case, the maximum deviation of the circumference FA (Formabweichung) is calculated (figure 81). In addition, the eccentricity E of the ball stud is also calculated. To compare and check the results of the sensor, it is also possible to compare it with the tactile measurement in the same way as in the optical measurements.

Figure 81. Graphical representation at the equator



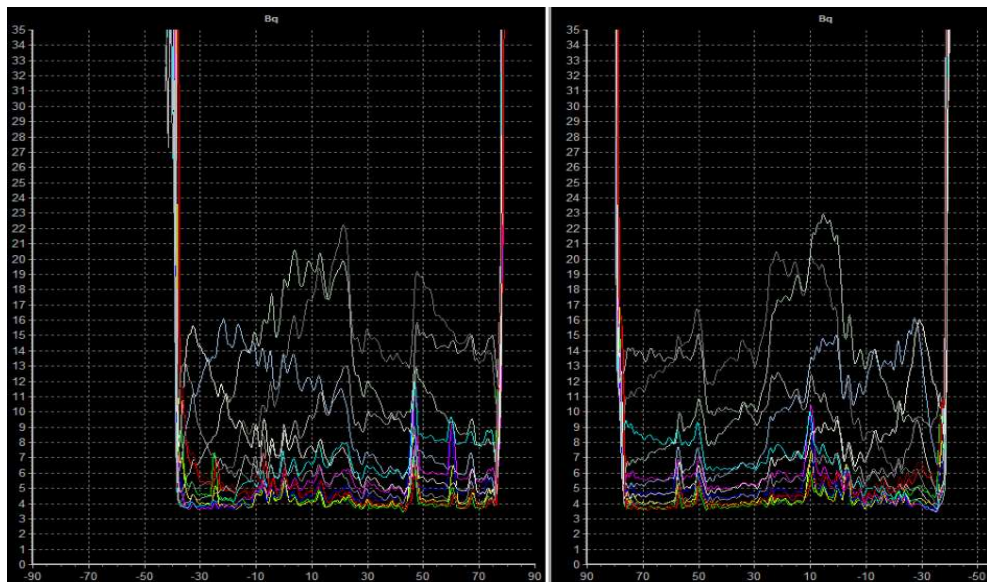
The bottom diagram (figure 78) represents the Bq values along the measured length. **To calculate them, all the sensor rotation measurements that have been programmed are used.** The lines represent the highest values of Bq at each of the measurement points of the different angles with which it has been measured. Figure 82 shows two lines corresponding to a single measure. Each line represents the length measured between two of the edges of the ball. The values of BqV and Bqmf are also represented in the graph. In addition to the Bq values, the software also allows the visualization other values of interest such as intensity (I) and slope (M).

Figure 82. Roughness representation through Bq



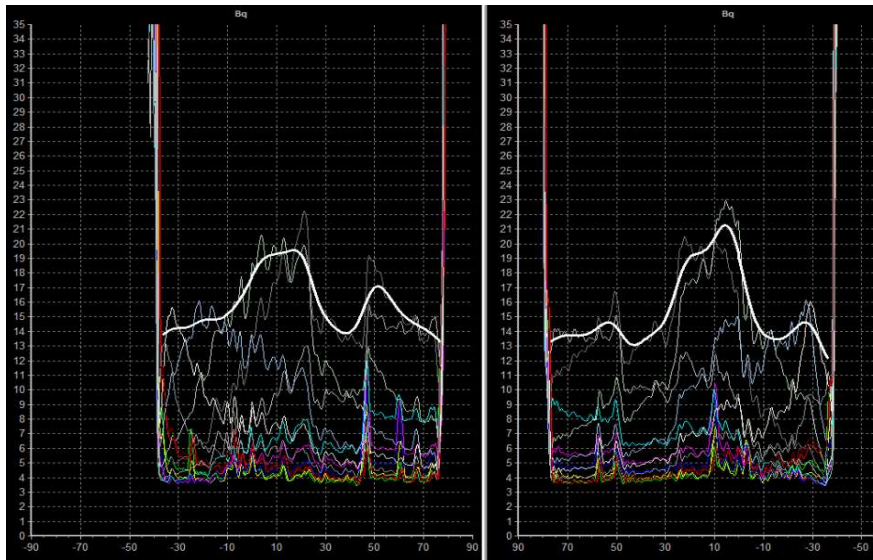
In addition, there is the possibility of viewing the measurements of each of the angles separately. Figure 83 represents the values of these measurements. The graph on the left shows the values of a measurement line from one edge to the other, while the other line shows the measurement values between the other two edges.

Figure 83. Bq representation along the different measures



There are occasions in which the obtained values present many peaks and irregularities that complicate their evaluation. For these cases, there is the possibility of smoothing the results obtained by means of a filter. This filter is activated during the design of the tolerances of the program described above. In this case, a high-pass filter will be used that eliminates all small imperfections in the measurement. In the choice of filter, the number of waves to be used is determined. The number depends on the result of the measurements, although generally values between 8 and 16 waves are taken. Figure 84 shows significant differences of this new filtered measure with respect to the previous graph.

Figure 84. Filter in the graphical representation



7.3 Analysis of the first measurement and sensor function test

The first measurement test consists of checking the measurements, the operation of the rotary axis of the sensor and the possibility of exporting the data through a csv file for a later analysis.

The data obtained is exported and analysed in excel. Tables are created to determine the value of Bq at each of the measured angles. In this case, figure 85 shows how the measure of an angle does not remain as the highest Bq value. These values were expected due to the cross structure of the ball stud. It confirms the theory of need to measure at different angles to get a more realistic representation of the surface. The diagram also shows the detection of edges at the ends (increase in Bq). Analysing the Bq diagram, local irregularities can be also found in the ball stud. In used or not new ball studs, there might be irregularities that do not represent a machining defect. These irregularities can be shown as a darkening or an external defect to the machining (a fall that can deform the ball). By only measuring the perimeter of the ball, it is not possible to determine these types of defects. **Therefore, the measurements carried out for ball studs only allows to correctly detect machining marks.**

Figure 85. Representation of the Bq values through the software

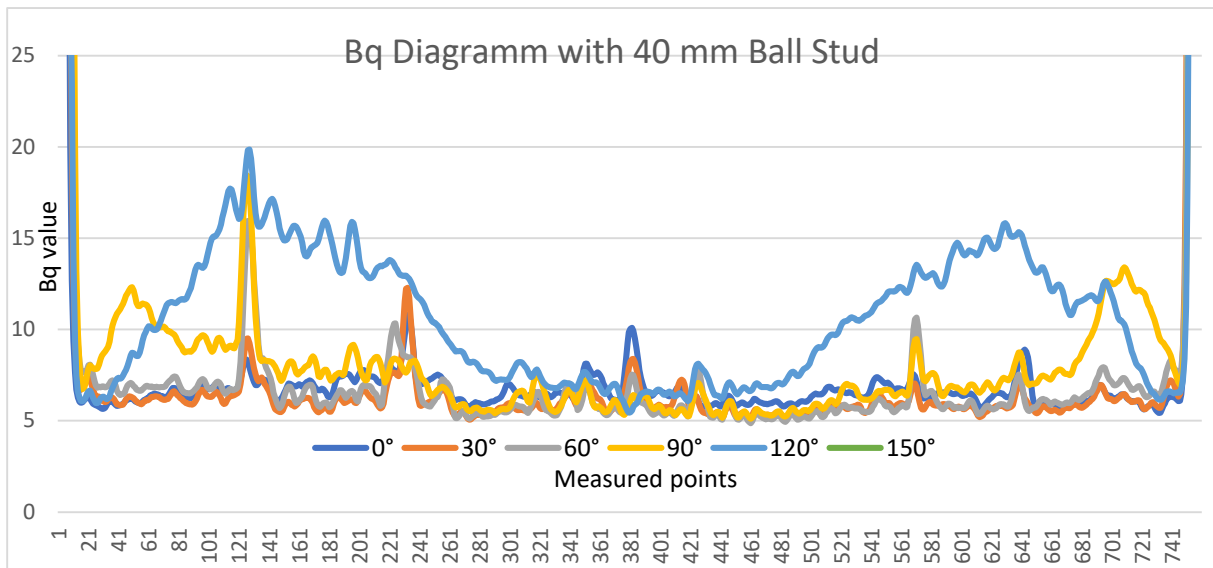
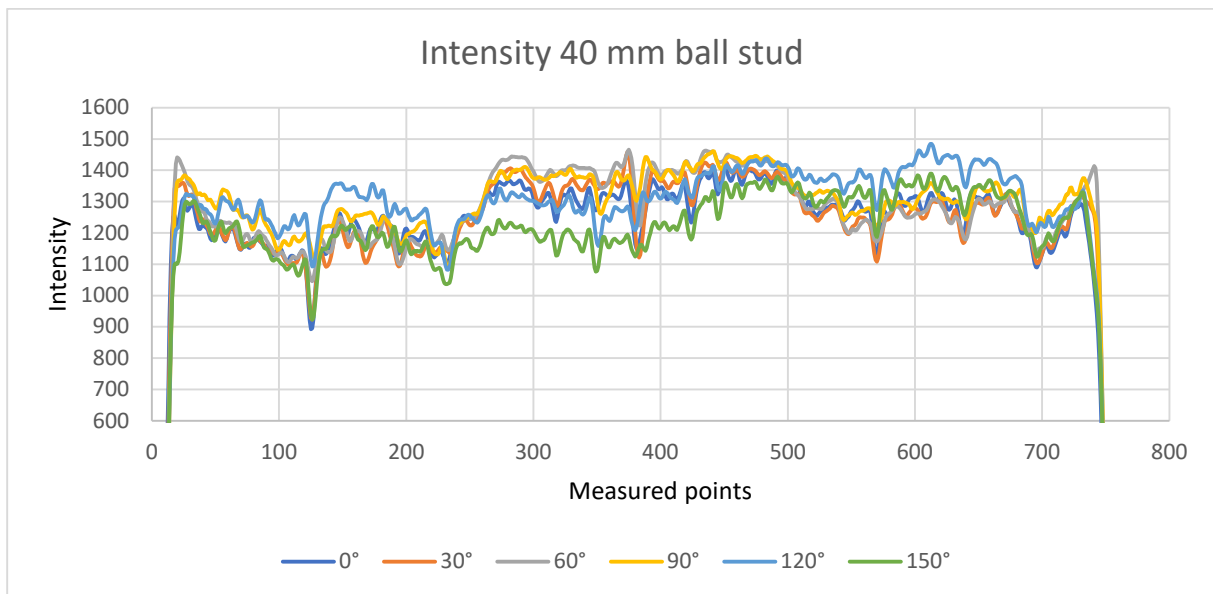


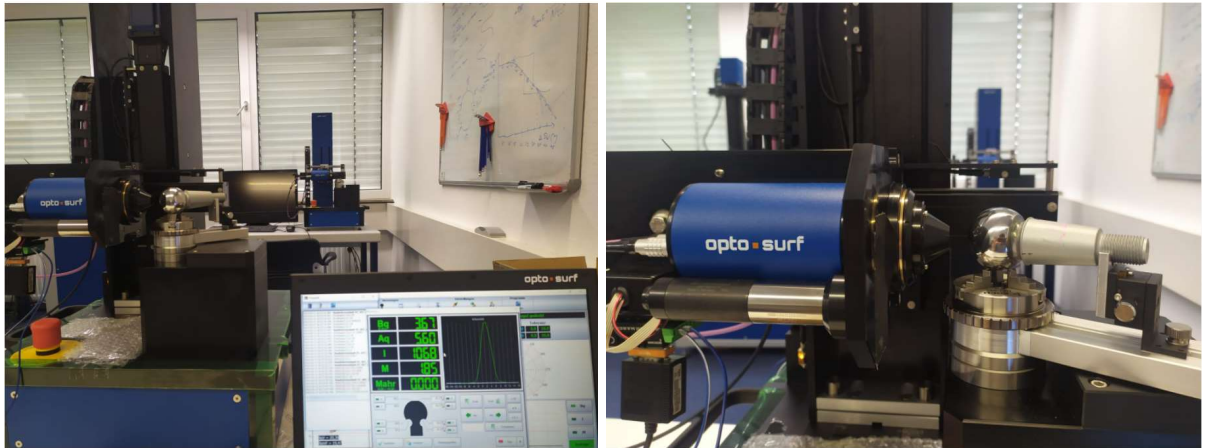
Figure 86 shows the intensity of the measurement for each of the measurement angles used. The intensity is reduced when reaching the edges. It is also possible to distinguish the decrease in intensity at the same point of decrease in the Bq value. A significant decrease of intensity in some specific measured angles confirms the existence of a local defect (figure 86).

Figure 86. Ball stud intensity representation for 6 different angles



Several ball studs were measured in order to probe the rotation sensor of the machine with a positive feedback. Results showed a good design, programming and consistency of the rotation motor. From this part of the project, we can confirm that the supporting design works in the reality and the motors were properly programmed to obtain the desired measurements.

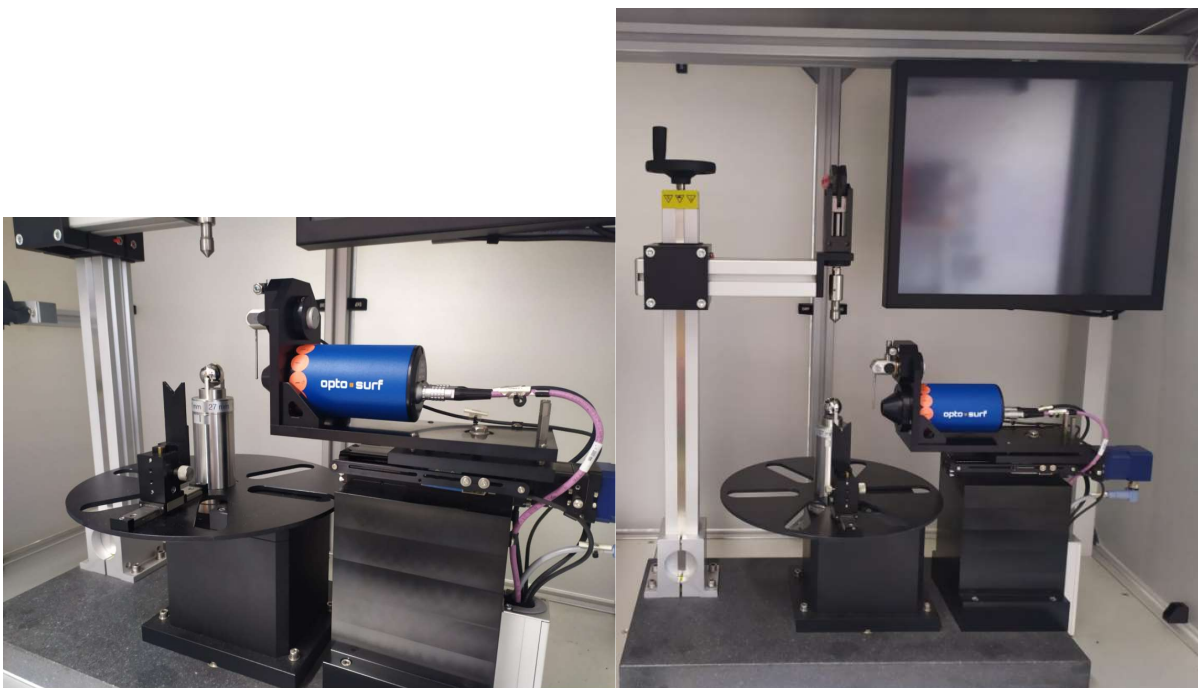
Figure 87. Representation of the measurements in the reality



8. VERIFICATION OF THE RESULTS IN PERFECT SPHERES AND IN OTHER COMPONENTS USED WITHIN THE AUTOMOTIVE INDUSTRY (BALL STUD) IN THE BALL STUD MACHINE

Once satisfactory results have been obtained by measuring the different ball studs on the Opto-Shaft TT, it is possible to mount the rotary module on the ball stud machine. As they are modular machines, it is only necessary to replace the sensor holding module with the new rotation module (figure 88).

Figure 88. Ball stud machine before installing the new module



The ball stud machine has fewer degrees of freedom than the OptoShaft TT. As shown in the previous figure, the ball stud machine does not have a longitudinal movement in the Z axis. Despite measuring ball studs of different diameters, each ball stud has its own support that equalizes the height of all ball studs. The rotation module must be correctly aligned with respect to a height that will remain static. In addition to regulating the height, it is necessary to adjust the module parallel to the measurement table so that the sensor does not measure with any inclination and therefore the value of A_q is kept as high as possible. The adjustment of this

measurement is done by positioning measurement standards in the areas of screw connection of the rotation module with the base of the machine (figure 89).

Figure 89. Measurement standards



The rotary table must also be adjusted so that it is aligned with the sensor. In case of being misaligned, the M values of the structure would be affected. To adjust it, the rotary table has long holes in the base that allow movement transverse to the position of the sensor (figure 90).

Figure 90. Long holes for positioning the ball stud machine



8.1 First tests on the ball stud machine with edge detection

The design of the ball stud machine allows to calculate the position of the ball edges. Ball edge measurement is necessary to calculate the optical ball stud profile. Furthermore, Bq values close to the edges and their specific behaviour can be also calculated and evaluated.

Checking the homogeneity of the surface of the ball studs is essential to study their roughness. Ball stud measurements are made by drawing lines on their perimeter. By being able to draw infinite different lines on the perimeter, infinite different results can be obtained. The objective of these measurements is to demonstrate the homogeneity of Bq by measuring the perimeter of the ball stud in different positions. For this we will use the previously mentioned method of measuring with six different angles and creating the line with the highest Bq values.

To measure this surface homogeneity, six ball studs of the same diameter (40 mm) with eight different positions marked in each one were used. The choice of these measurements was determined by the number of samples of this ball stud model and the number of positions measured was chosen by the client.

Figures 91,92 and 93 show the measurement of ball studs in different positions and angles and show that the value of Bq is similar in all ball studs. Small point peaks stand out, for example in the right zone of position 0 (pos 0). These peaks do not have a real influence since their Bq values fall within the normal parameters of the ball stud. The Bq values varies depending on the angle of the sensor that is being measured, however, all values between positions are correlated. **With these results we can affirm that the value of Bq in the ball studs is homogeneous throughout its structure.**

Figure 91. Bq representation of the pos 0

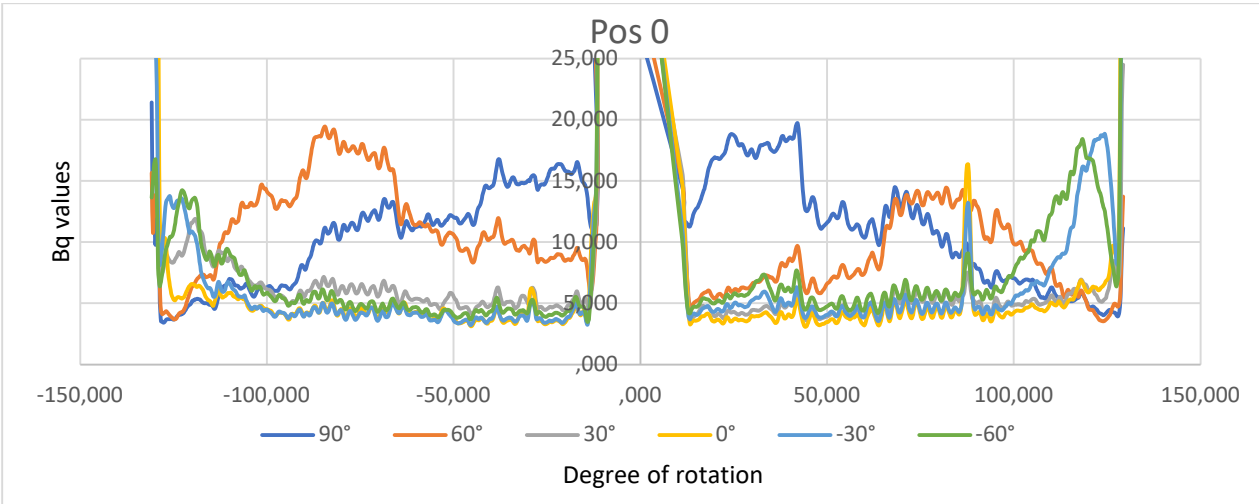


Figure 92. Bq representation of the pos 1

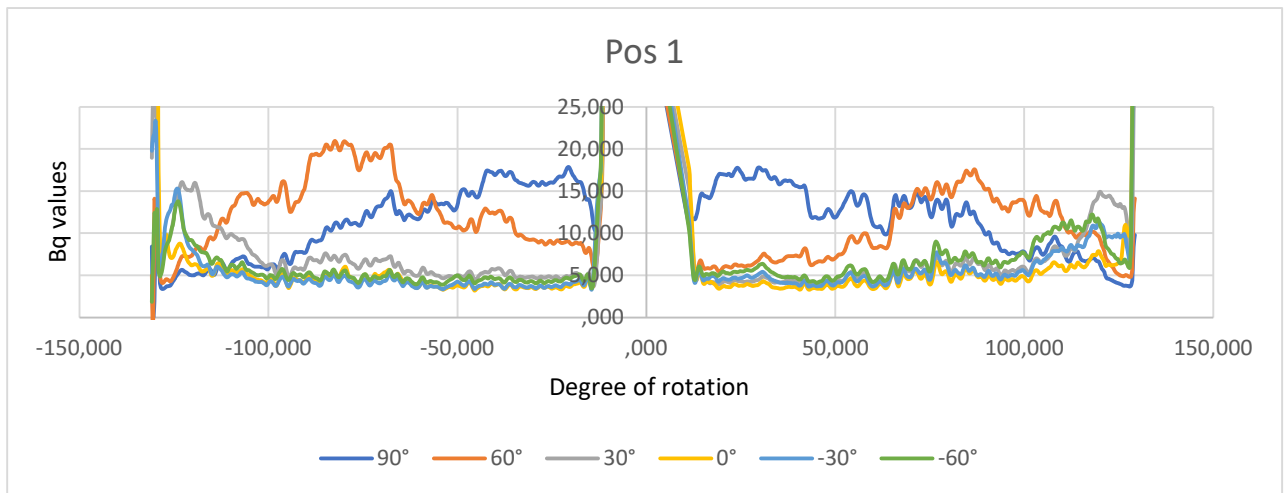
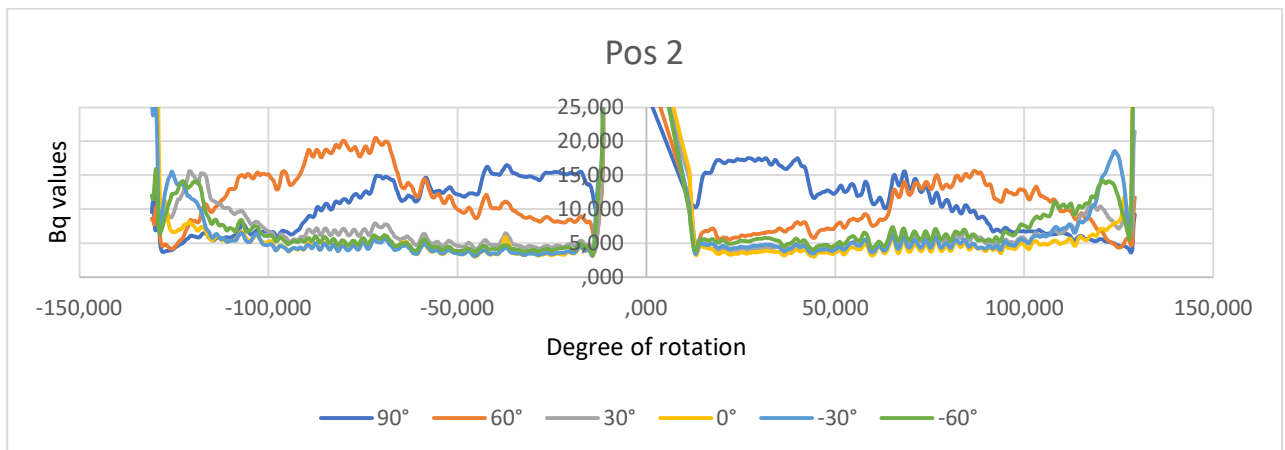


Figure 93. Bq representation of the pos 2



The repeatability of values in the measurements is essential to obtain a consistent measurement. To determine if the measurements are consistent, the measurement must be repeated several times. In this case, the measurements of the different ball studs were determined, and their measurements were repeated alternating both the positions and the different ball studs. Figures 94 and 95 show small differences between a measurement and the repetition. The values change slightly due to the impossibility of measuring exactly in the same position, but even so, the values are practically identical. **With this result we confirm that the consistency of the sensor and its repeatability works correctly.**

Figure 94. Bq representation in Optosurf's program

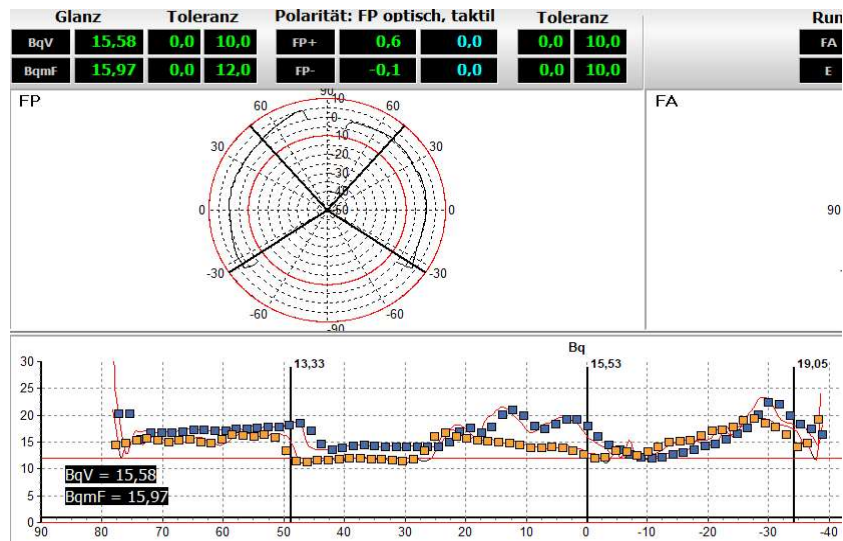
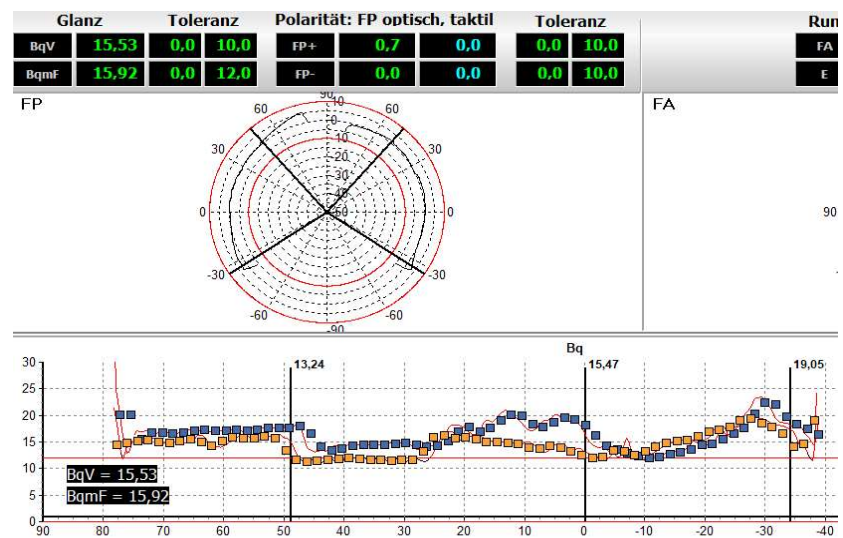


Figure 95. Repetition of Bq representation in Optosurf's program



8.2 Measurements with different angles of rotation

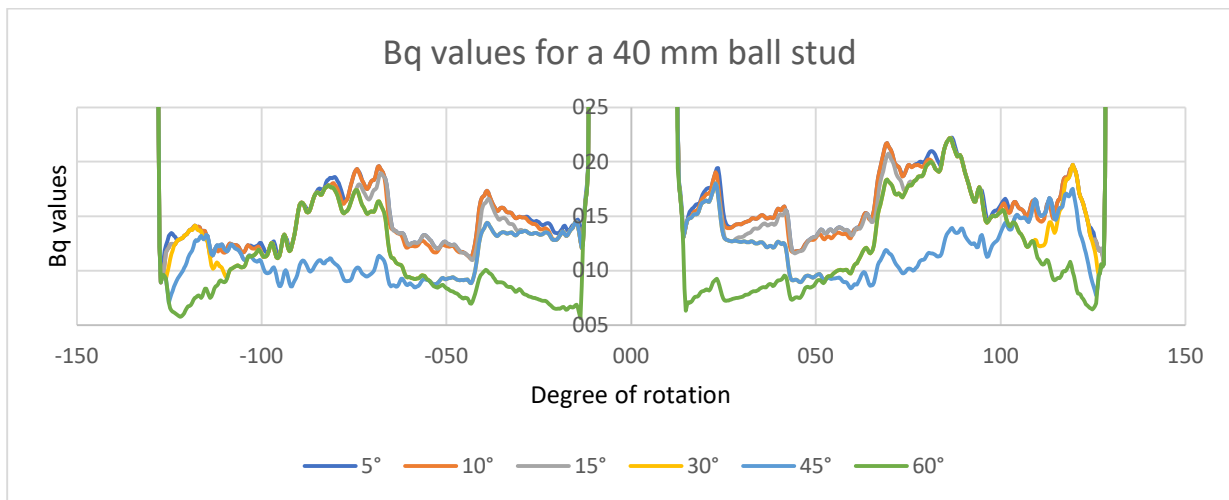
The measurement of Bq with six different angles gives us six different measurements of the structure of the ball stud. These first six measurements were determined in order to have the most accurate structure possible in a reasonable amount of time. The objective in this experiment is to obtain the value Bq of the real measurement and compare it with the results measured with different a variety of ranged angles.

8.2.1. BqV Analysis

For the first experiment, the BqV value was determined with measurements every 5 ° with a 180 ° rotation of the sensor. These results were compared with the measurements that would have been obtained every 10 °, 15 °, 30 °, 45 ° and 60 °. With these data it is possible to analyse how great the loss of information is as it is measured with a larger angle. The results obtained are represented in figure 96. In this figure it can be seen how in the 45 ° and 60 ° measurements the loss of information is important since the BqV values are much lower than the rest of the values. In the 30 ° measurement line there is a loss of information on the BqV value, although not so prominent.

This test was determined for five ball studs of equal diameter with similar results on all balls. **The conclusion therefore of this test is that the value of BqV is significantly influenced by the number of measurements that are made.**

Figure 96. BqV analysis for 6 different angles of rotation



8.2.2. BqmF Analysis

The determination of the loss of information to be measured with a few turns of the sensor has also been studied for BqmF values. For this, the values of the same experiments as for BqV have been considered and they have been analysed according to the BqmF. To calculate the BqmF, the values between 25 ° and 125 ° have been measured. These values have been taken by choosing an amplitude of BqmF of 10 ° less than the position of the edges. The values obtained are shown in figure 97 and figure 98. It can be seen how as the angle with which the measurements are made decreases, the value of BqmF decreases. The reason why it seems that

the BqmF value increases slightly between 45 ° and 60 ° is that the chosen measurement lines are different as one is not a multiple of the other.

Figure 97. BqmF analysis for six different angles of rotation (left edge)

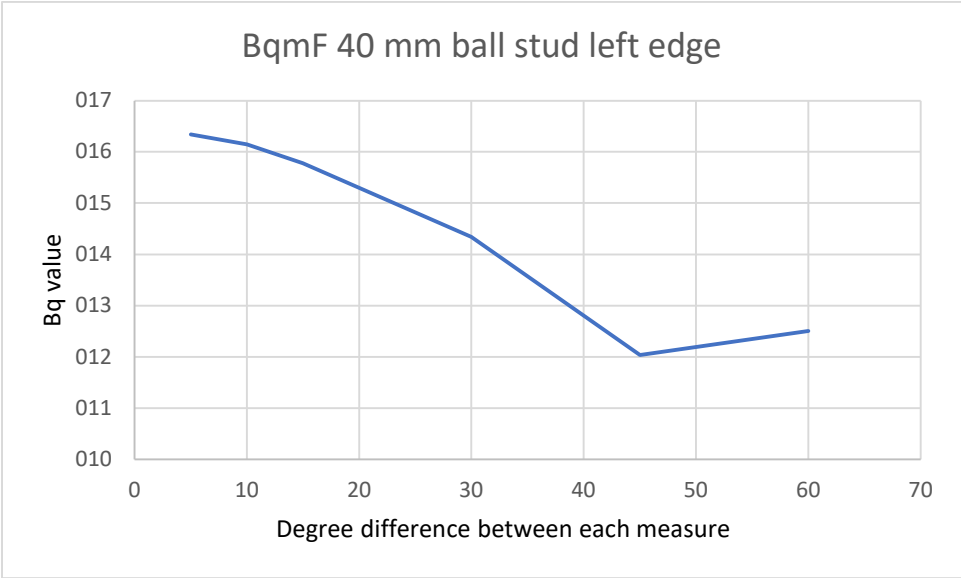
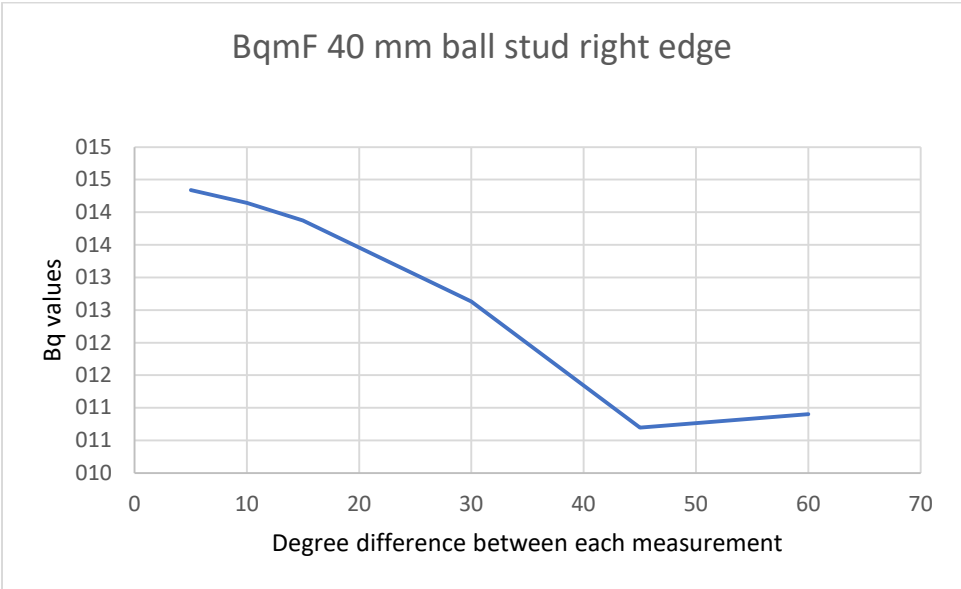


Figure 98. BqmF analysis for six different angles of rotation (right edge)



The conclusion of the BqV and BqmF measurement tests is that the value of both decreases as the angles of the sensor measurements are greater. Determining whether these values are acceptable is up to the customer. In this case, after the sample of the experiments carried out on the client, it was determined that for the following experiments the BqV and BqmF values should be measured with an amplitude of 15 ° between measurement and measurement.

8.3 Measurements carried out with programming

In addition to the change in the amplitude of measurements, the client also specified the interest in knowing the second highest value of BqV with the idea of studying its structure in depth. Due to the volume of measurements carried out for this study and the low speed with which diagrams can be designed in Excel, a Python program was designed that would allow the results obtained from a csv file to be measured. This program allows the creation of graphs from the grouped values in Excel.

8.3.1. Code description

In this code diagrams, numbers and letters will be used. Some functions must be imported so that they can be programmed: pylab and pyplot for the diagrams, numpy and pandas for the letters and numbers).

In order to make the tables we need to read the Excel so we must create a function that reads the file. Then, the workspace must be defined in terms of how big it will be. The interesting values are chosen through the “sort” function, in which the highest values are taken. Then two separate cycles are created, one for the values of Bq and another to obtain the position of the angle where it is being measured. Another cycle will be also necessary to calculate the measurements with a different position (in this case 30° which would be six times greater than 5° which is the value of the data obtained). The measured angles are increasing and decreasing through the same measurement. This precludes the direct representation of the figure. Therefore, another cycle has been created to approximate the angles of the measurements to the ones in our desired figure.

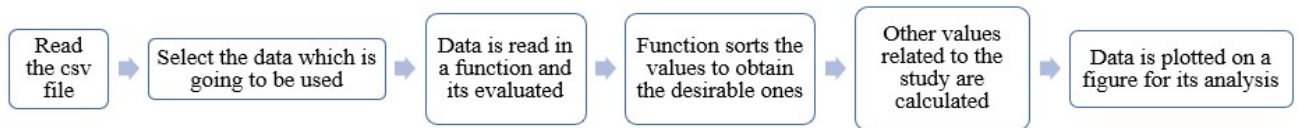
After all the cycles and the calculations for Bq, the values of BqV and BqmF can be obtained. Both will be obtained for all measured angles (in this case 5° and 30°). The client was also interested in analysing the second highest value of Bq to determine if there is a substantial difference with respect to the highest value. Thus, in the graphical representation there were four different lines representing the two different angles with the two different Bq values.

The last part of the coding was the visualization of the values through a diagram. This diagram included the representation of the four different measures clearly differentiated plus their labeling. The Bq and angle axis are named and represented in the diagram. The title of the diagram

is also specified and includes the name of the ball stud measured plus the BqmF of both measured angles.

Figure 99 shows the flowchart of the program. The specific code will be also included in the annexes.

Figure 99. Flowchart of the program



The values obtained in these measurements are reflected in the following figures. The first idea of the programming was thought to compare the highest and second highest value of Bq (figure 100). However, Optosurf found useful the idea of fast analysing through Python and requested for a comparison between angles (figure 101 and 102).

Figure 100. Comparison between highest Bq values

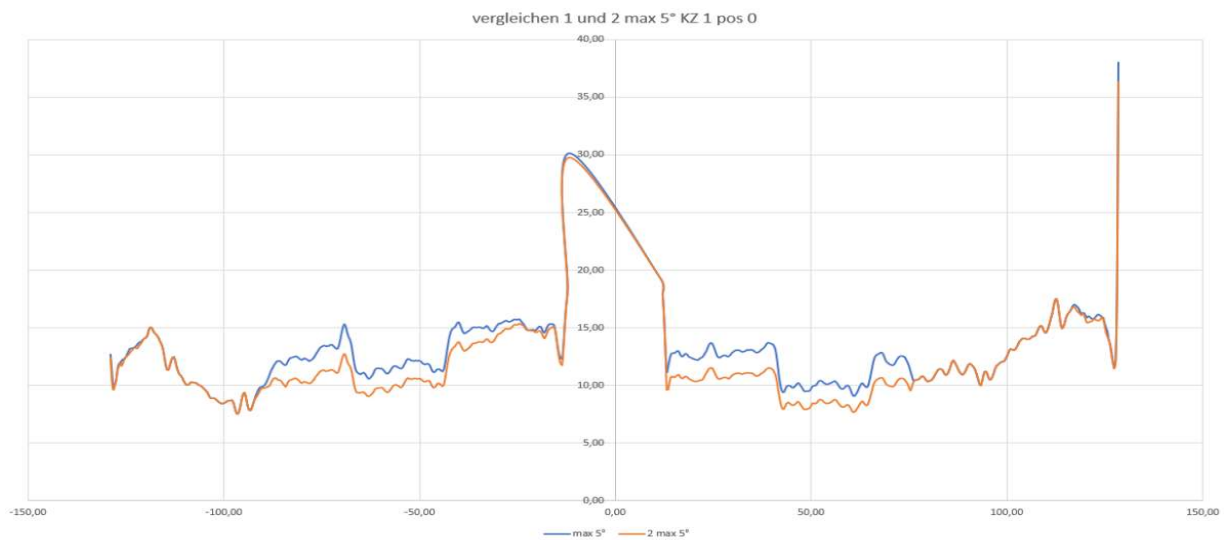


Figure 101. Comparison between highest Bq values in between angles KZ3

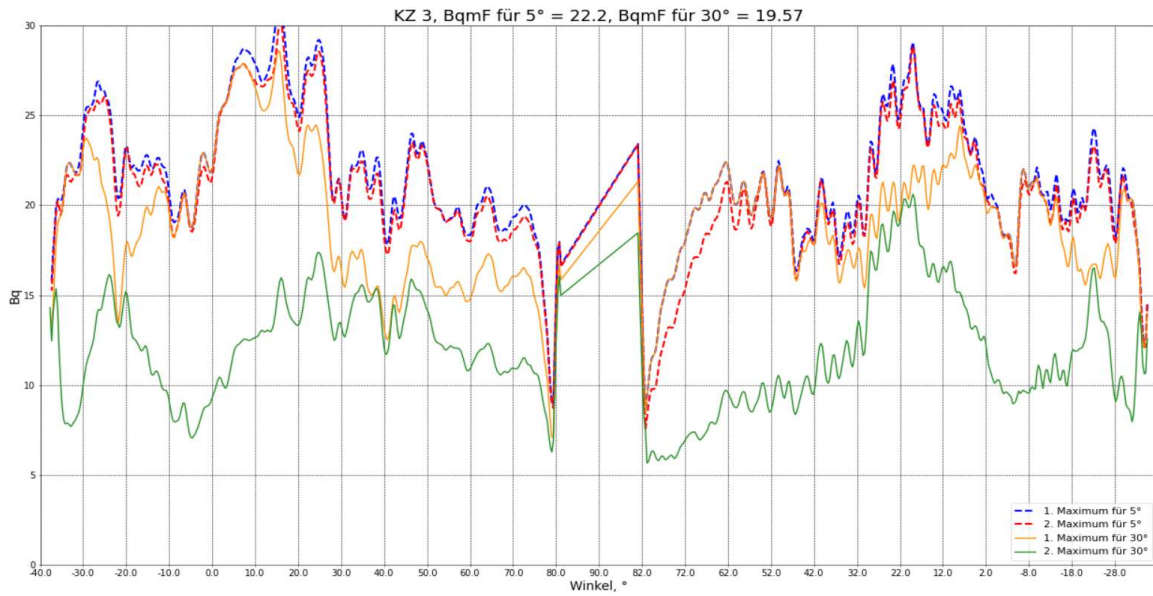
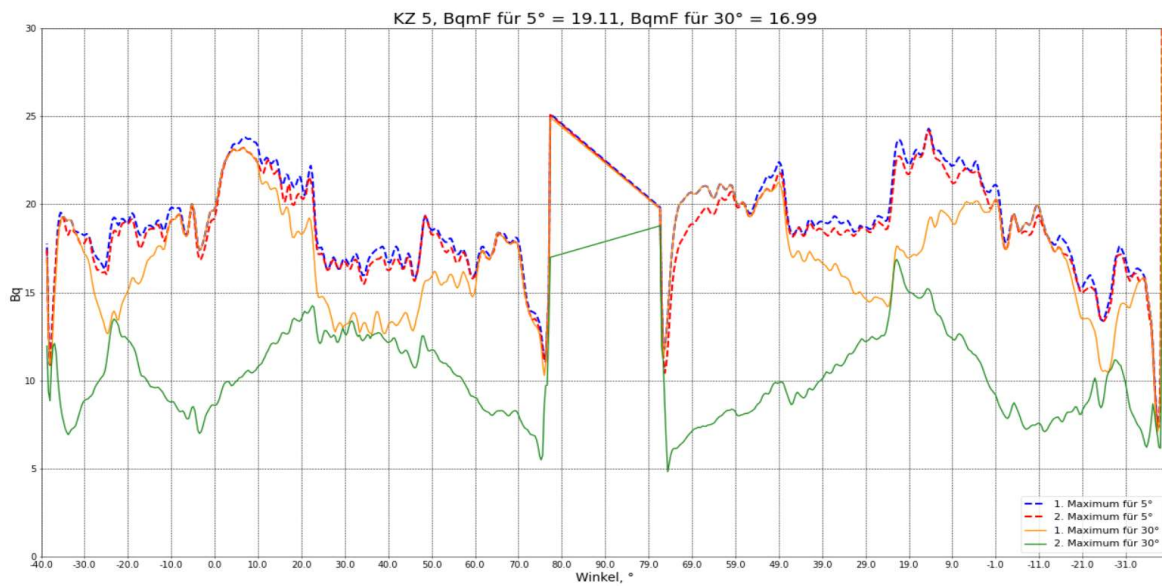


Figure 102. Comparison between highest Bq values in between angles KZ5

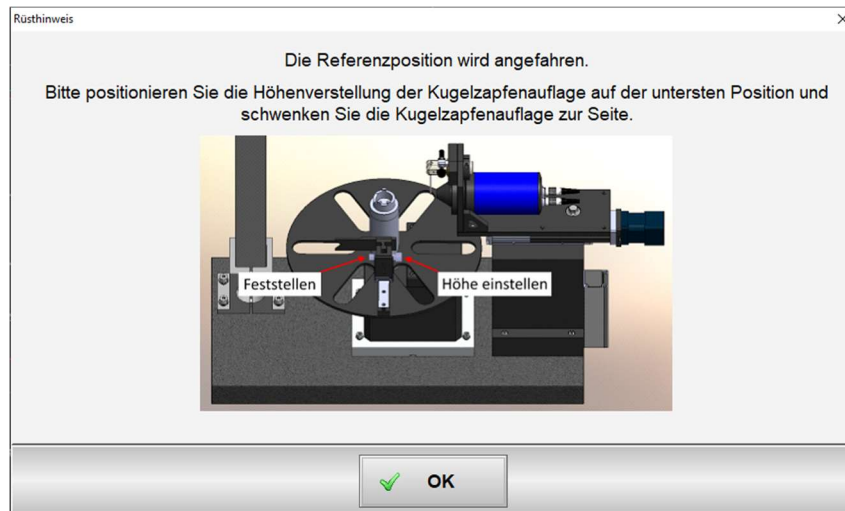


8.4 Sensor consistency and error test measurements

The person who assembles the machine and measures every day on that machine knows how it works. However, the use given by people who are not used to working with this machine is different. Software that is designed from scratch is not always perfect. There are times when the program works perfectly, but when it comes to putting it into practice it is different. In this

experiment, a trial-and-error improvement of the software was carried out. With this, what is intended is to improve the interface with the user and that he can make sporadic measurements without problems (figure 103). Users of this type of machine will not be working on it all the time but will be on the assembly line and when they need to measure, they will use the machine.

Figure 103. Description of the operating position of the ball stud machine



In these measurements the different ball stud diameters are used and ball studs are measured in different positions and without a defined order of measurement. The desired goal is to find as many interface errors as possible while still testing the sensor for consistency with different diameter ball studs.

The resolution of interface errors is not part of this project, but it is documented through an Optosurf's internal application. The computer team oversees solving and improving software problems in a coordinated manner with engineers. Some examples of errors found in measurements can be seen in the following figures 104 and 105.

Figure 104. Description of the errors and recommendations of the ball stud machine

```

Berichtet von:      B.Brodmann
Zugewiesen an:    garcia
=====
Projekt:          ZF Lemförder TK (Gräber)
Eintrag-ID:       932
Kategorie:        Software
Reproduzierbarkeit: immer
Auswirkung:       schwerer Fehler
Priorität:        normal
Status:           testbereit
Ansprechpartner beim Kunden:
Kunde:
Standort der Maschine:
Ticket-ID:
Lösung:           erledigt
Behoben in Version:
=====
Erstellt am:      2021-04-13 10:24 CEST
Zuletzt geändert: 2021-04-14 08:16 CEST
=====
Zusammenfassung: Diagramm lässt sich nicht bearbeiten
Beschreibung:
Unter Einstellungen - Diagramme besteht nicht die Möglichkeit dasselbe anzupassen. Alle Schalt und Eingabeflächen sind inaktiv

```

Figure 105. Description of the errors and recommendations of the ball stud machine

```

Berichtet von:      Schnabel
Zugewiesen an:    garcia
=====
Projekt:          ZF Lemförder TK (Gräber)
Eintrag-ID:       931
Kategorie:        Software
Reproduzierbarkeit: nicht getestet
Auswirkung:       schwerer Fehler
Priorität:        hoch
Status:           testbereit
Ansprechpartner beim Kunden:
Kunde:
Standort der Maschine:
Ticket-ID:
Lösung:           erledigt
Behoben in Version:
=====
Erstellt am:      2021-04-06 15:52 CEST
Zuletzt geändert: 2021-04-14 08:16 CEST
=====
Zusammenfassung: Die Messergebnisse (Rauheit) sind nicht plausibel
Beschreibung:
-Bq am Äquator wird mit 11,52 ausgewiesen, liegt tatsächlich zwischen 5 und 6.
-BqmF sollte zwischen 5 und 6 liegen, angezeigt wird aber 7,21.

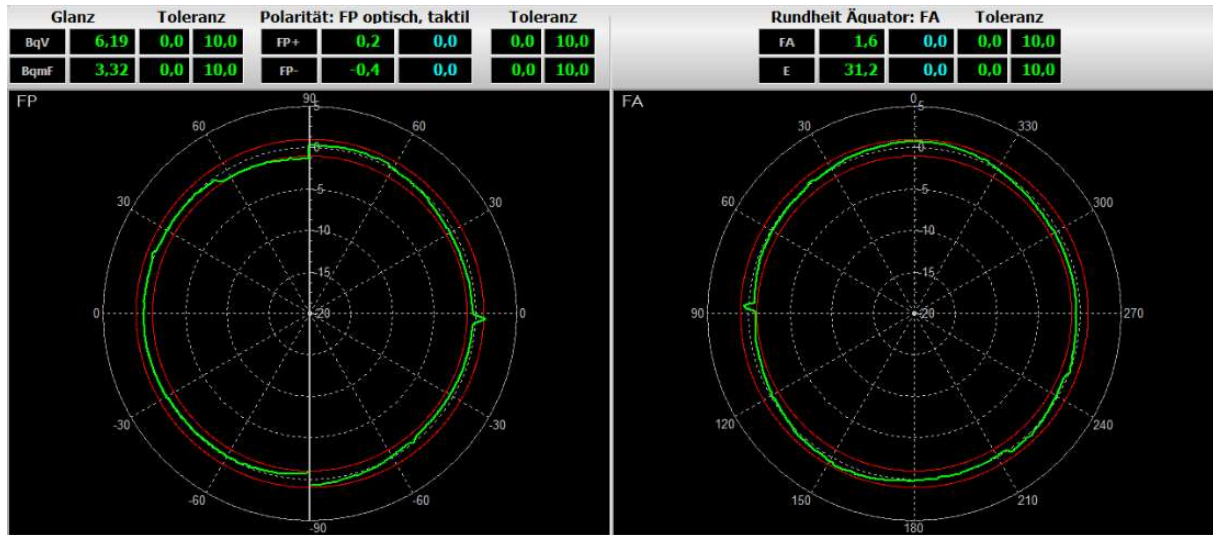
```

8.5 Profile tests

In addition to the roughness tests, consistency tests of the sensor profile were also carried out. The sensor was first measured to check if the shape of the profile was correct. The way the profile is calculated has a high complexity due to the number of parameters used. This generates certain errors that can be corrected by the client in combination with the Optosurf company.

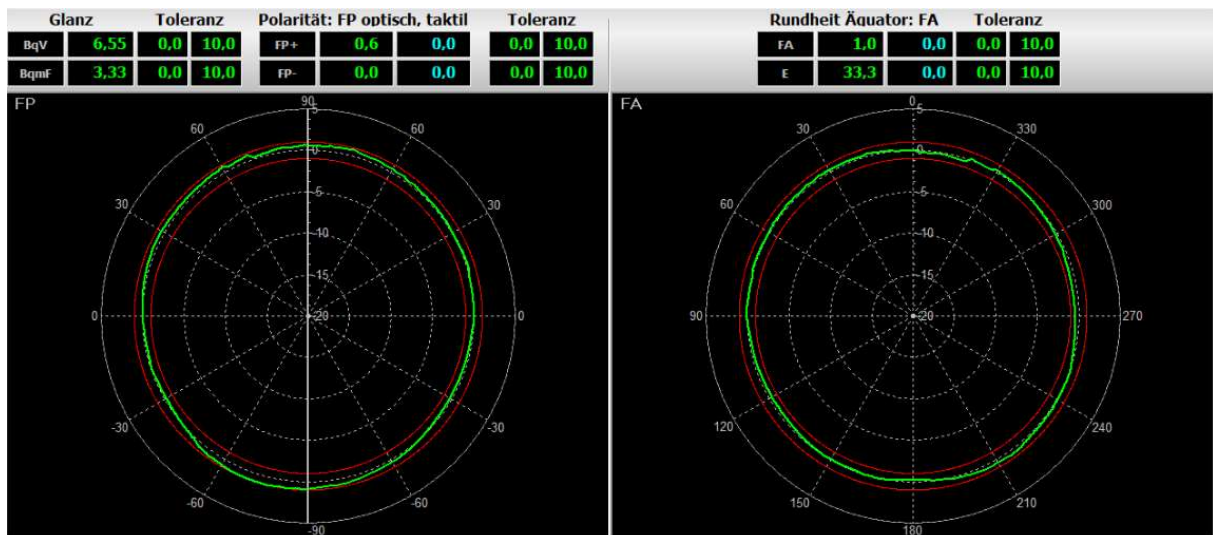
One of these errors consisted in the union of the different profiles calculated to obtain the final profile (figure 106).

Figure 106. Comparison between optic and equator measures



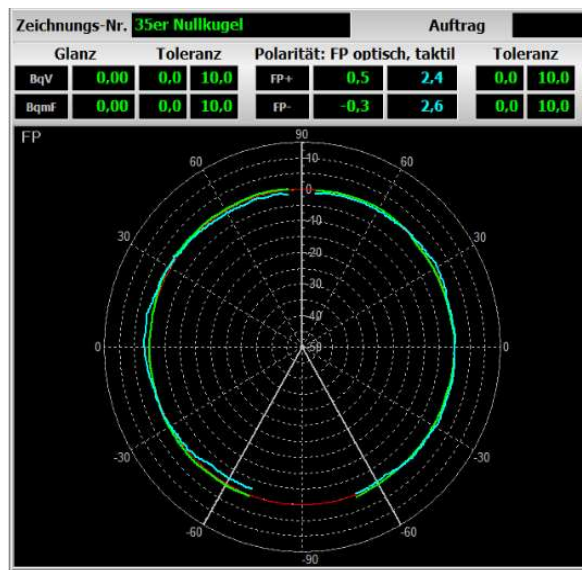
These errors are part of the product development process and locating them is essential. In figure 107 the correction of the measurement error between the two profiles have been solved and both measures are practically identical.

Figure 107. Comparison between optic and equator measures



The objective of the sensor is the replacement of the touch profile in most measurements where the roughness of the profile is small. In this test the use of the profile was compared with the different ball studs. In Figure 108 both measuring technologies are compared. The green lines represent the values obtained by the sensor and the blue ones by the touch profile. As expected, the values obtained by the sensor are much more precise.

Figure 108. Comparison between the sensor and the touch meter



The ball stud machine allows the measurement of the profile both on the optical axis and the axis of the equator. The calculation to determine the profile of each one is different. While on the axis of the equator the full circumference can be measured, on the optical axis this measurement is not possible due to the stick of the ball stud colliding with the machine. By comparing the axis of the equator with the optical axis we can determine if the equations applied to calculate the shape of the axis are correct. For this experiment, a hip ball replacement has been used. Figure 109 shows that the values between both measurements are very similar. With these results it is confirmed that the theoretically calculated shape of the profile is correct.

Figure 949. Comparison between optic and equator measures



9. TECHNIQUES FOR CHECKING AND CONSISTENCY OF RESULTS

9.1 Messverfahren 2 method

This procedure examines the repeatability and reproducibility of a measuring device (English repeatability and reproducibility, hence R&R, also Gauge R&R or Gage R&R) and is only used when the measuring device, in accordance with the procedure 1 has been classified as capable. Here, ten parts, which should cover the entire scatter range of the measured feature as far as possible, are measured two or three times by three different operators (or at three different locations or with three different devices of the same type). None of the operators can see the results of the other operators. The parts should also be measured on each run in a randomized order so that the operator can never remember the measurement result from the previous run.

When the measurements are complete, an overall mean and an average span value (based on the differences between the largest and smallest measurement the operator determined for each part) are calculated for each operator. The difference between the largest and the smallest operator mean value allows a statement to be made about the comparative precision; the overall mean value of the average range values calculated for the individual operators is used to make a statement about the repeatability. Based on the repeatability and comparative precision, the total scatter of the measuring equipment is then calculated and related to the characteristic scatter or tolerance.

9.2 Gage R&R method

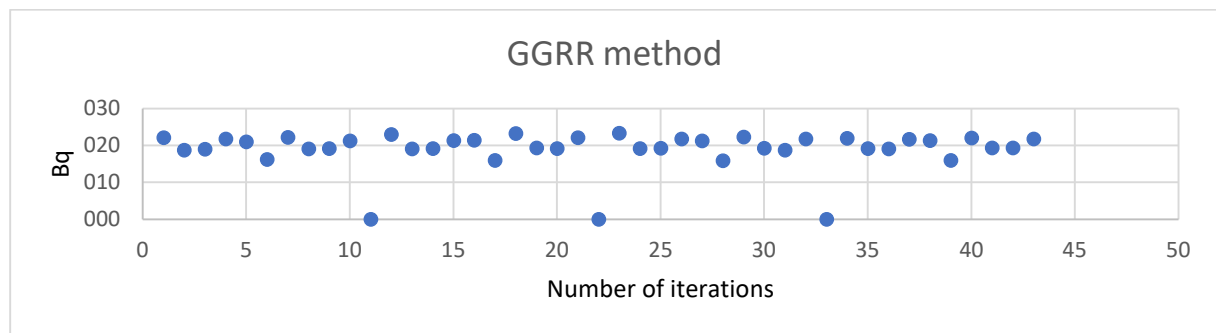
Gage R&R, which stands for gage repeatability and reproducibility, is a statistical tool that measures the amount of variation in the measurement system arising from the measurement device and the people taking the measurement. In this case the experiment has been carried out to confirm the repeatability and reproducibility of the profile measures. The method has been applied using 10 different ball studs and measuring them in 4 rounds of 40 measurements each. For this process 2 people were required for which one was measuring the ball studs meanwhile the other was observing the correctness of the procedure. In between each round the person who made the measurements changed with the person who oversaw the process. To also probe the

consistency between optical and equator measures, both have been also measured in each of the measurements. The results obtained are shown in figure 110 and 111

Figure 110. Value obtained to analyse the GRRR method

Teil	Beschreibung	Winkel Kinn	Winkel Kinn (Anzeige)	Winkel Stirn	Winkel Stirn (Anzeige)	BqmF	BqV	Im	Mm	PV	FPS	FPK	Bemerkung
6	Optischer Sensor Kreisabschnitt	127,27	-37,27	12,3	77,7	22,15	27,84	891	0,31	19,90	6,53	5,74	1
7	Optischer Sensor Kreisabschnitt	127,09	-37,09	13,71	76,29	18,79	23,78	1053	0,31	13,90	5,70	3,16	2
8	Optischer Sensor Kreisabschnitt	126,74	-36,74	12,3	77,7	19,04	24,72	1065	0,31	12,60	5,77	2,35	3
9	Optischer Sensor Kreisabschnitt	126,56	-36,56	12,3	77,7	21,80	32,08	977	0,32	12,50	3,38	5,19	4
10	Optischer Sensor Kreisabschnitt	127,27	-37,27	12,13	77,87	20,97	25,58	1024	0,30	10,20	3,09	2,28	5
11	Optischer Sensor Kreisabschnitt	127,09	-37,09	13,01	76,99	16,21	19,73	951	0,31	9,80	3,27	2,20	6
12	Optischer Sensor Kreisabschnitt	127,27	-37,27	12,48	77,52	22,18	27,90	892	0,32	21,50	7,07	6,47	1
13	Optischer Sensor Kreisabschnitt	127,09	-37,09	13,54	76,46	19,13	23,59	1040	0,32	26,70	7,87	2,95	2
14	Optischer Sensor Kreisabschnitt	126,74	-36,74	12,3	77,7	19,15	24,12	1060	0,31	9,90	4,07	3,16	3
15	Optischer Sensor Kreisabschnitt	126,56	-36,56	12,13	77,87	21,23	29,92	982	0,33	10,80	2,27	5,13	4
16	Optischer Sensor Kreisabschnitt	127,27	-37,27	12,48	77,52	22,97	26,19	866	0,30	15,00	5,17	4,19	1
17	Optischer Sensor Kreisabschnitt	127,27	-37,27	13,71	76,29	19,11	23,73	1039	0,30	22,60	6,96	2,44	2
18	Optischer Sensor Kreisabschnitt	126,74	-36,74	12,3	77,7	19,16	24,33	1059	0,30	11,80	5,09	3,22	3
19	Optischer Sensor Kreisabschnitt	126,56	-36,56	12,3	77,7	21,35	30,10	982	0,31	10,60	2,30	4,49	4
20	Optischer Sensor Kreisabschnitt	127,27	-37,27	12,13	77,87	21,40	25,19	1008	0,28	8,90	1,82	3,99	5
21	Optischer Sensor Kreisabschnitt	127,09	-37,09	12,83	77,17	16,00	20,03	962	0,30	11,00	3,47	2,15	6
22	Optischer Sensor Kreisabschnitt	127,44	-37,44	12,3	77,7	23,26	27,25	862	0,30	17,60	5,90	4,89	1
23	Optischer Sensor Kreisabschnitt	127,27	-37,27	13,71	76,29	19,35	23,76	1032	0,31	24,00	7,51	2,70	2
24	Optischer Sensor Kreisabschnitt	126,74	-36,74	12,3	77,7	19,16	24,10	1059	0,30	11,70	4,72	3,68	3
25	Optischer Sensor Kreisabschnitt	127,27	-37,27	12,3	77,7	22,16	29,92	789	0,11	100,10	34,12	71,26	4
26	Optischer Sensor Kreisabschnitt	127,62	-37,62	12,48	77,52	23,32	28,34	845	0,30	15,60	3,51	10,44	1
27	Optischer Sensor Kreisabschnitt	127,09	-37,09	13,54	76,46	19,20	23,30	1035	0,30	26,00	7,07	2,73	2
28	Optischer Sensor Kreisabschnitt	126,74	-36,74	12,48	77,52	19,24	24,81	1054	0,29	12,80	6,08	3,38	3
29	Optischer Sensor Kreisabschnitt	126,56	-36,56	12,3	77,7	21,82	32,34	976	0,30	12,30	3,03	5,06	4
30	Optischer Sensor Kreisabschnitt	127,27	-37,27	12,13	77,87	21,30	24,59	1012	0,28	8,70	1,83	1,49	5
31	Optischer Sensor Kreisabschnitt	127,09	-37,09	12,83	77,17	15,85	20,01	971	0,29	10,80	2,78	3,93	6
32	Optischer Sensor Kreisabschnitt	127,27	-37,27	12,48	77,52	22,32	28,52	876	0,28	16,20	6,03	5,15	1
33	Optischer Sensor Kreisabschnitt	127,09	-37,09	13,71	76,29	19,26	23,23	1038	0,29	25,00	8,25	4,07	2
34	Optischer Sensor Kreisabschnitt	126,74	-36,74	12,3	77,7	18,72	24,44	1071	0,30	14,30	5,81	3,47	3
35	Optischer Sensor Kreisabschnitt	126,91	-36,91	12,3	77,7	21,82	32,35	981	0,28	17,00	5,02	12,97	4
36	Optischer Sensor Kreisabschnitt	127,27	-37,27	12,48	77,52	21,94	26,31	890	0,29	17,30	6,21	4,57	1
37	Optischer Sensor Kreisabschnitt	127,09	-37,09	13,54	76,46	19,14	23,54	1037	0,30	26,50	7,23	2,26	2
38	Optischer Sensor Kreisabschnitt	126,74	-36,74	12,3	77,7	19,09	24,67	1059	0,30	12,60	5,79	2,79	3
39	Optischer Sensor Kreisabschnitt	126,74	-36,74	12,3	77,7	21,66	31,45	977	0,32	14,90	3,04	5,88	4
40	Optischer Sensor Kreisabschnitt	127,09	-37,09	12,13	77,87	21,32	25,61	1012	0,29	7,70	2,36	1,69	5
41	Optischer Sensor Kreisabschnitt	127,09	-37,09	12,83	77,17	15,99	19,80	962	0,30	11,00	3,59	3,33	6
42	Optischer Sensor Kreisabschnitt	127,27	-37,27	12,48	77,52	22,03	26,85	892	0,29	17,90	5,23	3,88	1
43	Optischer Sensor Kreisabschnitt	127,09	-37,09	13,54	76,46	19,35	24,03	1031	0,31	23,90	7,22	2,34	2
44	Optischer Sensor Kreisabschnitt	126,74	-36,74	12,3	77,7	19,33	25,03	1048	0,30	12,70	5,94	3,35	3
45	Optischer Sensor Kreisabschnitt	126,56	-36,56	12,3	77,7	21,80	32,27	976	0,32	13,80	4,13	5,93	4

Figure 951. GRRR method



As it can be seen on Figure 111, the Bq values for the GRRR remain constant around the value 20. The results obtained have been also shared with the client who also interpreted them. The feedback given by the client was very positive after their own check.

10. SUMMARY OF RESULTS OBTAINED AND CUSTOMER COMMENTS FOR FUTURE OBJECTIVES

The values obtained in the measurements have been a success. The sensor has been shown to have the ability to measure with exceptional consistency. The ball stud support module worked properly and allowed the measurement of the ball studs on the OptoShaft TT. The new axis of rotation of the sensor works correctly and allows determining a roughness value much more accurately than the one previously calculated. The machine is correctly adjusted and the Bq, I and M values are positive for measurements. The motors have been adjusted to the optimum speed and ranges for measurement and run consistently. The analyses carried out have helped to determine the number of measurements to obtain the most precise roughness possible in the least amount of time. The values obtained in the ball stud machine have been shown to be more accurate than in other measurement methods such as the touch meter. The resolution of software problems and the improvement of the user interface have improved the consistency of the machine. The machine can measure any type of ball stud without problems following the software instructions. The problems derived from the formation of the design of the profile in the optical measurement have been solved.

A disadvantage that cannot be solved is the detection of point defects in the ball studs. As 0.9 mm lines are analysed around the perimeter, the sensor may not detect this point defect. However, these kinds of defects are usually seen directly by an operator, in addition, the vast majority of ball studs analysed come directly from production, so they do not have these types of defects.

In order to continue optimizing the efficiency of measurement and analysis, it has been suggested in this project to visualize the analysis of the measurements through Python programming. This suggestion has been considered in a positive way by the Optosurf computer team and the suggestion to the client of the improvement will be studied.

In general terms, the client is very satisfied with the measurements made, as they have informed Optosurf, as well as in their internal reports. These favourable results confirm the sale of another two ball stud machines to the same company. In addition, competing companies of the client have taken an interest in Optosurf's technology.

11. REFERENCES

- ¹ <http://www.optosurf.de/>
- ² DIN 4760: Gestaltabweichungen
- ³ ISO 14406 Geometrical Product Specifications (GPS) – Extraction, 2003.
- ⁴ <https://www.asphericon.com/>
- ⁵ DIN EN ISO 4287: Benennungen, Definitionen und Kenngrößen der Oberflächenbeschaffenheit
- ⁶ <https://www.evaporatedcoatings.com/long-wave-pass-short-wave-pass-optical-filters/>
- ⁷ See Note 6
- ⁸ DIN EN ISO 11562: Meßtechnische Eigenschaften von phasenkorrekten Filtern
- ⁹ Constantine, D. et al. (2018). Experimental Analysis of the effect of vibration phenomena on workpiece topography due to cutter runout in end-milling process. *Machines*, Vol. 6, art. no. 27, doi: 10.3390/machines6030027
- ¹⁰ Constantine, D. et al. (2018). Experimental Analysis of the effect of vibration phenomena on workpiece topography due to cutter runout in end-milling process. *Machines*, Vol. 6, art. no. 27, doi: 10.3390/machines6030027.
- ¹¹ Exploring Surface Texture. H.Dagnall M.A. 1986
- ¹² Ver nota anterior
- ¹³ Oberflächenbeurteilung. Rauheitsmessung. Dipl.-Ing. Pat.-Ing. S. Jung
- ¹⁴ ISO 13565-2:1996 Geometrical Product Specifications (GPS)
- ¹⁵ See Note 14
- ¹⁶ See Note 14
- ¹⁷ Ver nota 1
- ¹⁸ See Note 1
- ¹⁹ See Note 1
- ²⁰ See Note 1
- ²¹ VDA 2009: Winkelaufgelöste Streulichtmesstechnik. Definition, Kenngrößen und Anwendung
- ²² Deutsches Institut für Normung e. V., DIN 4760, Beuth Verlag GmbH, 1982.
- ²³ See Note 1
- ²⁴ See Note 1
- ²⁵ See Note 1
- ²⁶ See Note 1
- ²⁷ See Note 1
- ²⁸ <https://www.awomansview.com/resources/young-on-your-way/hip-replacement-surgery/>
- ²⁹ <https://www.ford-trucks.com/>
- ³⁰ <https://www.tirereview.com/understanding-checking-and-replacing-ball-joints-for-vehicle-safety/>
- ³¹ <https://www.fordparts.com>
- ³² Micro-alloyed steels for non-heat-treated ball studs and pins SCT_2005_Hasler
- ³³ See Note 32
- ³⁴ <https://www.afdex.com/>
- ³⁵ https://press.zf.com/press/de/media/media_2252.html
- ³⁶ A.-E. Jiménez, M.-D. Bermúdez, in *Tribology for Engineers*, 2011
- ³⁷ See Note 35
- ³⁸ See Note 35
- ³⁹ See Note 35
- ⁴⁰ See Note 1
- ⁴¹ See Note 1
- ⁴² See Note 1
- ⁴³ See Note 1

```

import matplotlib.pyplot as plt
import pylab as p
import numpy as np
import pandas as pd

def OpFile(Stelle):
    fname="C:/Users/ignacio/PycharmProjects/probe/kugel zapfen 09.02.2021/" +
"Auswertung KZ" + str(Stelle) + " pro 5 grad.xlsx"
    M=pd.read_excel(fname,header=None)
    ME=np.array(M)

    return ME

def Max(WerteAr):
    N=len(WerteAr[0])
    L=int(np.size(WerteAr)/N)
    Max1=np.zeros(N)
    Max2=np.zeros(N)

    for i in range(N):
        SortAr=np.zeros(L)
        for j in range(L):
            SortAr[j]=WerteAr[j,i]
        SortAr.sort()
        Max1[i]=SortAr[-1]
        Max2[i]=SortAr[-2]

    return Max1, Max2

Stelle=3
InitM=OpFile(Stelle)

N=len(InitM[1]) - 1

Bahnen=31
X=np.zeros(N)
W=np.zeros(N)
WerteM=np.zeros((Bahnen,N))

ZZ=3
for i in range(Bahnen):
    for j in range(N):
        WerteM[i,j] = InitM[ZZ,j+1]
    ZZ=ZZ+2

for j in range(N):
    X[j] = InitM[1,j+1]
    if j<N/2:
        W[j] = -40 + j*0.4
    else:
        W[j] = 87 - (j-N/2+1)*0.4
    W[j]=round(W[j],0)

WerteK=np.zeros((6,N))

```



```

for i in range(6):
    WerteK[i]=WerteM[i*6]

Max1M,Max2M=Max(WerteM)
Max1K,Max2K=Max(WerteK)

BqmM=0
BqmK=0
j=0
for i in range(N-10):
    if W[i]<=70:
        BqmM=BqmM+Max1M[i]
        BqmK=BqmK+Max1K[i]
        j=j+1
BqmM=BqmM/j
BqmK=BqmK/j

fig = plt.figure(figsize=(35,20),dpi=50, facecolor='w', edgecolor='k')
ax = fig.add_subplot(111)
plt.title('KZ ' + str(Stelle) + ', Bqm für 5° = ' + str(round(BqmM,2)) + ', Bqm
für 30° = ' + str(round(BqmK,2)), loc='center', pad=None, fontsize=26)
line1,=plt.plot(X,Max1M,color='blue',linewidth=3, linestyle='--')
line2,=plt.plot(X,Max2M,color='red',linewidth=3, linestyle='--')
line3,=plt.plot(X,Max1K,color='darkorange',linewidth=2)
line4,=plt.plot(X,Max2K,color='forestgreen',linewidth=2)
plt.axis([-130,130,0,30])
ax.set_xticklabels(W[:,25])
plt.grid(b=True, which='both', color='black',linestyle='--')
plt.xlabel('Winkel, °', fontsize=20)
plt.ylabel('Bq', fontsize=20)
plt.legend((line1, line2, line3, line4), ('1. Maximum für 5°', '2. Maximum für
5°', '1. Maximum für 30°', '2. Maximum für 30°'), loc='lower right',
fontsize=16)
ax.tick_params(axis="x", labels=14)
ax.tick_params(axis="y", labels=14)
ax.set_xticks(np.arange(-130, 130, 10))
plt.show()

```